UNIVERSITY OF CALIFORNIA
RIVERSIDE

Characterization of HNF4a Isoforms in Mice and Their Role in Glycemia, Lipid Metabolism, and Aging

A Dissertation submitted in partial satisfaction
of the requirements for the degree of

Doctor of Philosophy

in

Biochemistry and Molecular Biology

by

Sarah Hasan Radi

December 2021

Dissertation Committee:
Dr. Frances Sladek, Chairperson
Dr. Djurdjica Coss
Dr. Nicole zur Nieden

The Dissertation of Sarah Hasan Radi is approved:

_____

_____

_____

Committee Chairperson

University of California, Riverside

ACKNOWLEDGEMENTS

To begin, I would like to thank Dr. Frances Sladek for all of her support over the years and her consistent mentorship throughout my projects. She believed in my scientific abilities and help mold me into the scientist I have become today. Moreover, all of the Sladek lab members past and present have not only taught me all of the lab techniques used in this thesis, but they also helped execute many of the experiments alongside me. Particularly, Dr. Poonam Deol, who helped in many of the animal harvests over the years and who has been a friend in lab over the years.

Many people in the biochemistry department have also been great help over the years, including the majority of the staff I have had the pleasure of working with. Most notably, Dr. Dawn Loyola who always listened to my griefs and gave wonderful advice and solutions to problems over the years. Additionally, Dr. Stephanie Dingwall who I have had the pleasure of working with many times as her teaching assistant and who has become one of my closest friends. She always supported me and helped me not only become a better teacher, but also a better scientist.

My parents have put up with so much over the years and have always supported my want for education. They not only endured the long nights waiting for me to return from lab, but also listened to me as I worked through the scientific reasoning behind my project out loud and gave me great input. My brother, Saif, also endured my ramblings about westerns and troubleshooting my experiments over the years, and always encouraged me to remain positive and patient.

Lastly, my amazing husband Omran, has not only physically helped me with my experiments, but has been my partner in crime with regards to my project. He listened to my hypotheses and experimental design and gave fantastic input on many aspects of my project. He also spent every late night in lab by my side and kept me sane throughout my doctorate journey, I would not have been able to get through it without him and my family's support and continued encouragement over the years.

DEDICATION

This thesis is dedicated to my parents, my brother, and my husband; I could not do it without your support.

ABSTRACT OF THE DISSERTATION

Characterization of HNF4a Isoforms in Mice and Their Role in Glycemia, Lipid Metabolism, and Aging

by

Sarah Hasan Radi

Doctor of Philosophy, Graduate Program in Biochemistry and Molecular Biology
University of California, Riverside, December 2021
Dr. Frances Sladek, Chairperson

Hepatocyte Nuclear Factor 4α (HNF4α), a master regulator of liver-specific gene expression, is regulated by two promoters (P1 and P2) which drive expression of two groups of HNF4α isoforms. HNF4α is a known regulator of gluconeogenesis and is mutated in maturity onset diabetes of the young one (MODY1). Moreover, HNF4α is heavily involved in regulating both lipid and glucose metabolism in the liver. Conventionally, it was thought that P1-HNF4α, but not P2-HNF4α, is expressed in the normal adult liver, while P1-HNF4α is downregulated and P2-HNF4α is upregulated in fetal liver as well as in liver cancer. This dissertation explores a previously undescribed role for P2-HNF4α in the normal adult mouse liver – one involved in the diurnal variations of lipid and carbohydrate metabolism. More specifically, P1-HNF4α appears to be a major driver of gluconeogenesis while P2-HNF4α is a driver of ketogenesis. We utilize P1-HNF4α-expressing (α1HMZ) and P2-HNF4α-expressing exon swap mice (α7HMZ) to determine the physiological function of the HNF4α isoforms in the switch between

gluconeogenesis and ketogenesis, and to characterize the impact of sex on those functions. Additionally, we use AICAR treatment to explore the effect of AMP-Activated Protein Kinase (AMPK) activation in these mice, as AMPK, an energy-sensing kinase, has been shown to phosphorylate P1-HNF4α in vitro. Finally, given the fact metabolism in general can heavily affect the aging process and more specifically that ketone bodies serve as a source of fuel for the brain, and have been implicated in prevention of neurological diseases, such as dementia, we explore the effect of differential HNF4α expression in aging mice.

The compelling data showing HNF4α isoforms are involved in the switch between gluconeogenesis and ketogenesis, a basic metabolic process that occurs on a daily basis, illuminate not only the molecular mechanism underlying the switch but also how that mechanism is impacted by sex. These studies have the potential to impact our understanding of numerous metabolic diseases, including diabetes, obesity, fatty liver disease and cancer.

TABLE OF CONTENTS

LIST OF FIGURES

LIST OF TABLES

CHAPTER 1: INTRODUCTION:
HNF4α isoforms: the fraternal twin master regulators of liver function

Liver

Whether referred to as “the seat of the soul” as the ancient Babylonians believed, “the seat of our darkest emotions” as Plato postulated, a term of endearment in Urdu, or the literal translation of “courage” in the Zulu language, one thing is clear, almost every culture past and present recognizes the importance and uniqueness of the liver.

The liver is the largest internal and main metabolic organ in the body. It is comprised of four lobes: the right lobe, the left lobe, the caudate lobe, and the quadrate lobe. The right lobe is about six times larger than the left lobe and is referred to as the large lobe. All evidence points to homogeneous function between the lobes of the liver which each have similar morphology. Liver tissue is composed of hepatocytes, sinusoidal endothelial cells, stellate cells and Kupffer cells. Interestingly, there is emerging evidence that different hepatocytes may carry out slightly different functions and express different genes. This suggests that hepatocytes within the liver may execute different processes (Özkan et al., 2020).

Due to large metabolic demands of the body and the consistent essential functions of the liver, the tissue is extremely well vascularized and uses 25% of the cardiac output although it makes up about 2.5% of the total body weight (Lautt & Greenway, 1987; Myers & Hickam, 1948). That being said, oxygen is not maintained at a constant pressure throughout the tissue and will differ based on the proximity to the portal triad, which includes the portal vein, hepatic artery, and bile duct. The liver is divided into three zones

with zone one receiving the most oxygen and having the highest respiratory enzyme activity, including beta-oxidation and gluconeogenesis. On the other end, closest to the central vein, zone three is the least oxygenated with the high activity of glycolysis, lipogenesis, and ketogenesis (Özkan et al., 2020) (Figure 1.1A, C). It is thought that zone two plays an important role in liver homeostasis and regeneration (Wei et al. 2021). While it is assumed that all hepatocytes are capable of the same functions, the liver is able to compartmentalize and focus certain functions via this oxygen gradient.

The liver is mainly composed of hepatocytes, the active non-connective epithelial cells in the liver driving all of its functions. Hepatocytes make up 70% of the cells in the liver by number and 80% by volume. Sinusoidal endothelial cells are highly specialized endothelial cells which line the smallest blood vessels in the liver. Stellate cells reside in the space of Disse in the liver between sinusoidal endothelial cells and the surface of hepatocytes and they function to maintain the basement membrane and store vitamin A. Kupffer cells are specialized macrophages of the sinusoid of the liver and take part in the breakdown of red blood cells (Figure 1.1B). The liver also surrounds the gallbladder, the site of bile storage; the liver is the organ that synthesizes bile from bilirubin, bile salts, and cholesterol to aid in fat digestion.

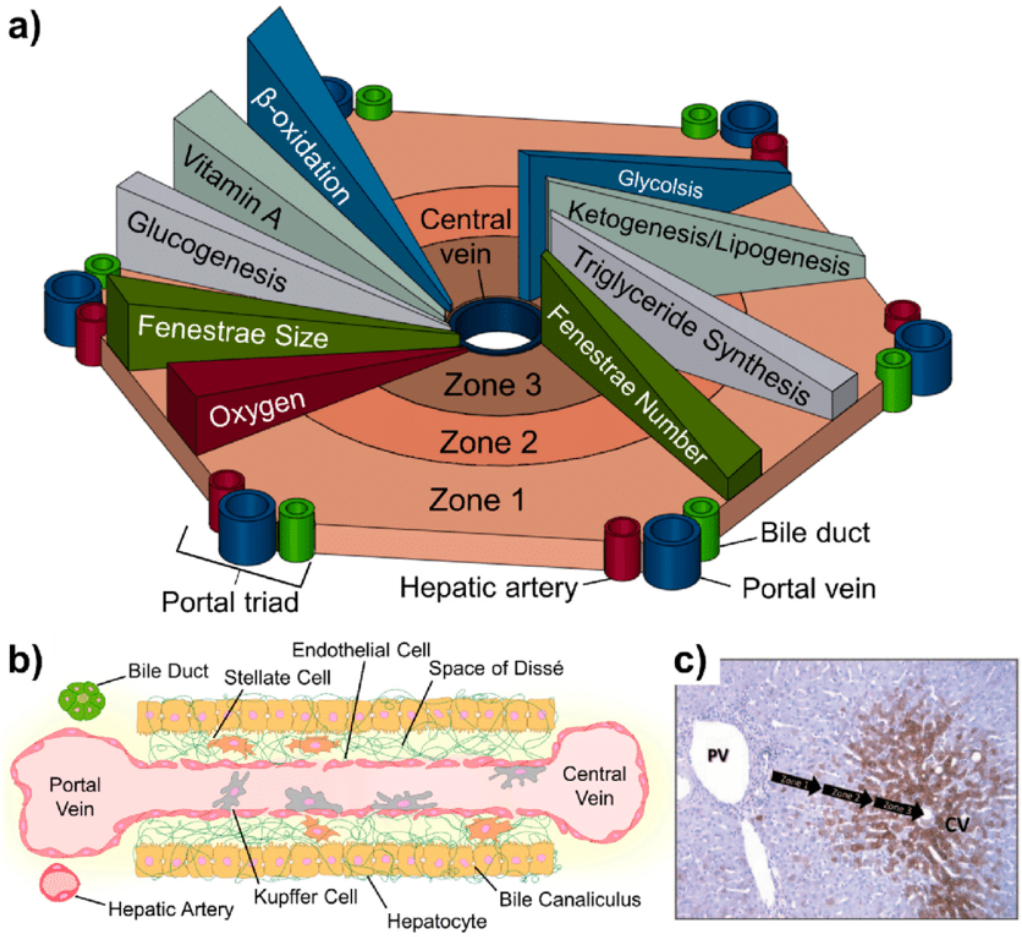

Figure 1. 1 Oxygen gradation in the liver creating zones of differential gene expression.

(a) Biochemical pathways, gradients and endothelial properties alternation across the zones of liver lobule. (b) Composition of the liver sinusoid. (c) Variation of CYP3A4 expression across the lobule. Metabolic activity (brown) increases from the portal vein to the central vein. Taken from Özkan et al 2020

The liver is heavily intertwined with almost all bodily functions providing energy, including during periods of starvation, maintaining homeostasis between meals, and storing excess lipids and carbohydrates postprandially. Post-prandial nutrients and other chemical compounds, such as glucose and amino acids, make their way from the intestine directly to the liver through the hepatic portal system. The liver absorbs, packages, detoxifies, metabolizes, and distributes these various elements to maintain homeostatic levels throughout the blood and other tissues.

Gluconeogenesis vs Ketogenesis:

The liver is the main organ responsible for maintaining glucose homeostasis between meals through a process referred to as gluconeogenesis. That being said, the kidneys have also been shown to carry out gluconeogenesis in the proximal tubules and account for approximately 40% of gluconeogenesis during times of hypoglycemia. The kidneys initiate the pathway primarily from lactate, while the liver is able to initiate *de novo* glucose synthesis from lactate, pyruvate, oxaloacetate, and glucogenic amino acids, depending on the availability of these compounds and the other needs of the body. Once produced, new glucose is transported through the blood to supply the brain, the muscles, and other organs with energy (Alsahli & Gerich, 2017).

During high levels of activity, muscles will consume oxygen more quickly than it can be delivered by red blood cells, creating an oxygen debt. When this occurs, the electron transport chain will shut down as it is lacking its ultimate electron acceptor, oxygen, inhibiting the mitochondria from the utilization of pyruvate. The myocytes begin utilizing the excess pyruvate in lactate fermentation, which recycles nicotinamide adenine

dinucleotide (NAD^+), a necessary cofactor, so glycolysis can continue producing energy. As lactate builds up in the myocytes it is exported through the blood to the liver where it is then converted to pyruvate and then to glucose through gluconeogenesis. The glucose is exported from the liver via the GLUT2 receptor and recirculated to the hypoxic muscles, creating what is known as the Cori cycle. This relieves the lactic acid burden on the muscles and allows them to remain active in a more anaerobic/high stress environment for longer periods of time.

Gluconeogenesis is an expensive process requiring adenosine triphosphate (ATP) investment and thus is heavily regulated by insulin, glucagon, and transcription factors. Specifically, gluconeogenesis has three bypass steps to overcome irreversible steps in glycolysis, requiring four enzymes to accomplish this task. The first bypass step utilizes two enzymes -- pyruvate carboxylase (*Pc*) which converts pyruvate to oxaloacetate followed by phosphoenolpyruvate carboxykinase (*Pck1*) to convert oxaloacetate to phosphoenolpyruvate. The second bypass converts fructose-1,6-bisphosphate to fructose-6-phosphate using fructose-1,6-bisphosphatase (*Fbp1*). Lastly, glucose-6-phosphatase (*G6pc1*) is used to convert glucose-6 phosphate to glucose. The rest of the pathway is shared with glycolysis with all reactions being reversible and driven by Le Châtelier's principle, which states that concentration of reactants and products will drive the direction of a reaction when the free energy change is close to zero. With the exception of the first bypass, which occurs in the mitochondria, and the last bypass occurring in the endoplasmic reticulum, gluconeogenesis occurs in the cytosol.

Gluconeogenesis in the liver is dependent on the availability of oxaloacetate. This metabolite is essential in the initial bypass of gluconeogenesis and is kept at exceptionally low levels in hepatocytes. If gluconeogenesis continues to run, oxaloacetate levels will run out, this will shut down gluconeogenesis and the tricarboxylic acid (TCA) cycle in the hepatocytes. This causes the liver to switch to fat utilization to supply the body with energy. This will occur in times of starvation or prolonged fasting. Fatty acids will be broken down via beta-oxidation in the mitochondria and produce acetyl-CoA. The acetyl-CoA is unable to enter the tricarboxylic acid cycle as it is missing the oxaloacetate necessary to condense with to begin the cycle. The acetyl-CoA is then utilized in ketogenesis (Figure 1.2).

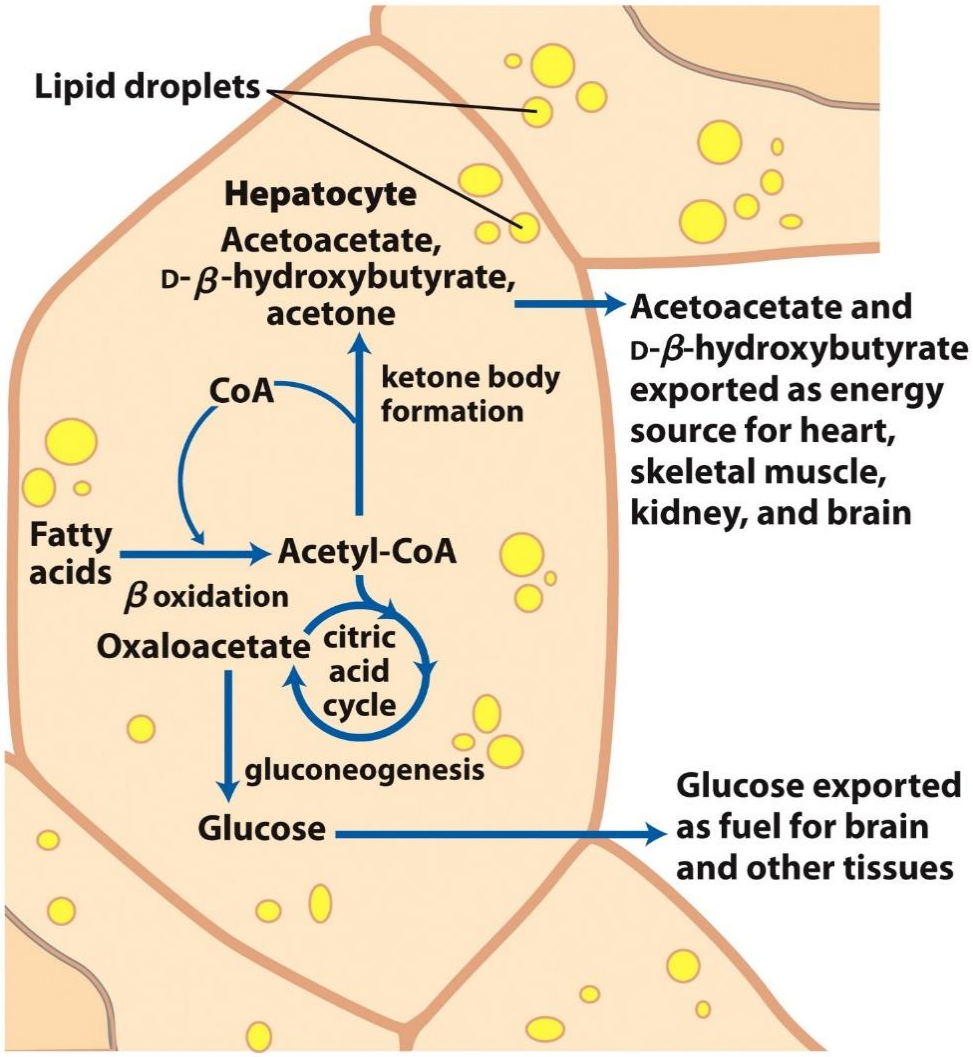

Figure 1. 2 Switch between gluconeogenesis and ketogenesis

Taken from Lehninger, 2008 Figure 17.20

Through ketogenesis the liver converts acetyl-CoA into beta-hydroxybutyrate, which is then sent into the bloodstream to be utilized by other organs such as the muscle and brain. At the destined organs, the beta-hydroxybutyrate is converted back into acetyl-CoA and utilized to supply the tissue with energy via the TCA cycle and electron transport chain. The resultant ketone bodies are then used to supply the rest of the body with energy. This is most crucial for the ability of the brain to continue to function during periods of low nutrition as the brain does not store nor utilize most forms of fat. During states of hypoglycemia, up to two-thirds of the energy needs of the brain can be met with ketone bodies. Similar to gluconeogenesis, ketogenesis is also tightly controlled by insulin, glucagon, and transcription factors. The major steps of ketogenesis are: thiolase (*Acat1*) which converts acetyl-CoA to acetoacetyl-CoA; the committed enzyme: β-hydroxy-β-methylglutaryl-CoA synthase (*Hmgcs2*) which converts acetoacetyl-CoA to β-hydroxy-β-methylglutaryl-CoA; β-hydroxy-β-methylglutaryl-CoA lyase (*Hmgcl*) which converts β-hydroxy-β-methylglutaryl-CoA to acetoacetate; and finally, β-hydroxybutyrate dehydrogenase (*Bdh1*) which converts acetoacetate to β-hydroxybutyrate, the main ketone body which increases in response to fasting (Figure 1.3). Ketogenesis occurs primarily in the mitochondria of hepatocytes. Moreover, the liver lacks the enzyme necessary for ketolysis, β-ketoacyl-CoA transferase (*Hadhb*) so it does not utilize the ketone bodies it produces.

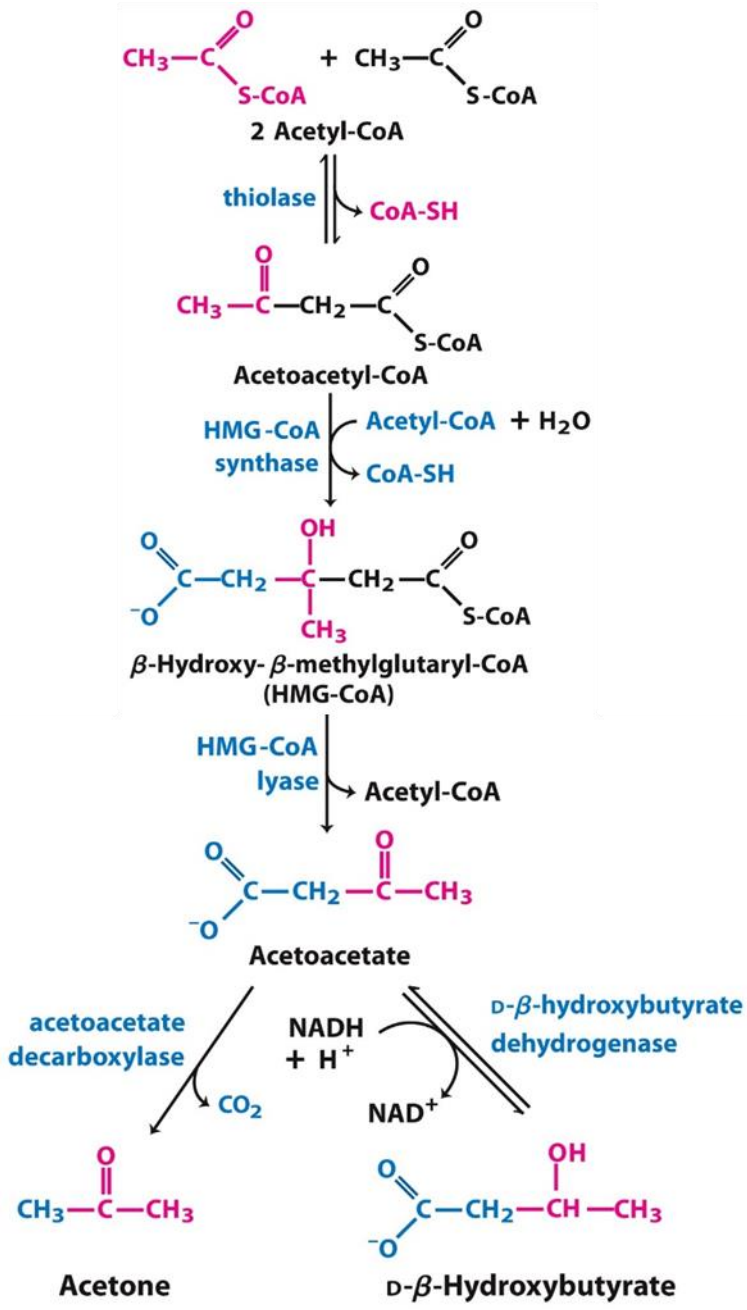

Figure 1. 3 Metabolites and enzymes involved in ketogenesis.

Taken from Lehninger, 2008 Figure 17.18

Fatty Acid and Cholesterol Synthesis:

In addition to the gluconeogenic and ketogenic pathways, the liver is the main site for fatty acid synthesis and distribution. The liver absorbs dietary fat and cholesterol delivered via chylomicrons, which the largest of the lipoprotein particles produced in the intestines and function to deliver lipids to the tissues. These are then processed in the liver and exported to supply other tissues with lipids. Additionally, the liver packages and exports synthesized triglycerides and cholesterol in very low-density lipoproteins to supply other tissues. High density lipoproteins are sent to gather excess cholesterol from tissues and are imported to the liver where the excess cholesterol is processed and recycled. Furthermore, the liver is essential for *de novo* fatty acid synthesis from excess short chain fatty acids, carbohydrates, or proteins. Like most metabolic processes fatty acid synthesis is tightly regulated by hormones like insulin, glucagon, and transcription factors. The liver can then store the synthesized fat in fat droplets, the excess of which causes non-alcoholic fatty liver disease (NAFLD). NAFLD can present in two main forms, non-alcoholic fatty liver or non-alcoholic steatohepatitis, the former does not present with excess inflammation or liver damage, while the latter is characterized by excess inflammation and can result in permanent scarring of the liver tissue (cirrhosis). Obesity and type two diabetes are the main risk factors that cause NAFLD, which is increasing in incidence in the United States (Kumar et al., 2020). Although more rare, non-alcoholic steatohepatitis can lead to more severe diseases such as cirrhosis and liver cancer which can result in liver failure.

Cholesterol synthesis also takes place in the liver which is necessary for cholesterol-based hormone synthesis such as testosterone, estrogen, and cortisol.

Cholesterol can either be absorbed from the diet in the intestines and sent to the liver or synthesized *de novo*. Exogenous cholesterol is mainly absorbed from meats, eggs, and dairy products. Nonetheless, *de novo* synthesis is sufficient for human cholesterol needs as people with dietary restrictions such as vegetarianism and veganism can produce sufficient amounts of cholesterol. Cholesterol *de novo* synthesis begins with acetyl-CoA which is converted to β-hydroxy-β-methylglutaryl-CoA and then to mevalonate using the committed enzyme β-hydroxy-β-methylglutaryl-CoA reductase (*Hmgcr*) in the endoplasmic reticulum of hepatocytes. This is an important regulated step as β-hydroxy-β-methylglutaryl-CoA can be used in multiple pathways. Through several enzymatic steps, mevalonate is converted to squalene, and then to cholesterol which has three six-membered rings and one five-membered ring. The liver must keep the appropriate balance of acetyl-CoA, glucose, to β-hydroxy-β-methylglutaryl-CoA, ketones, and fatty acids to provide the rest of the organs when needed.

A depiction of the intersection of these pathways is shown in Figure 1.4. The liver is constantly working to maintain homeostasis of metabolites throughout the body and as such it is essential to maintain strong enzymatic regulation through various forms of hormonal regulation, feedback inhibition, and transcription regulation.

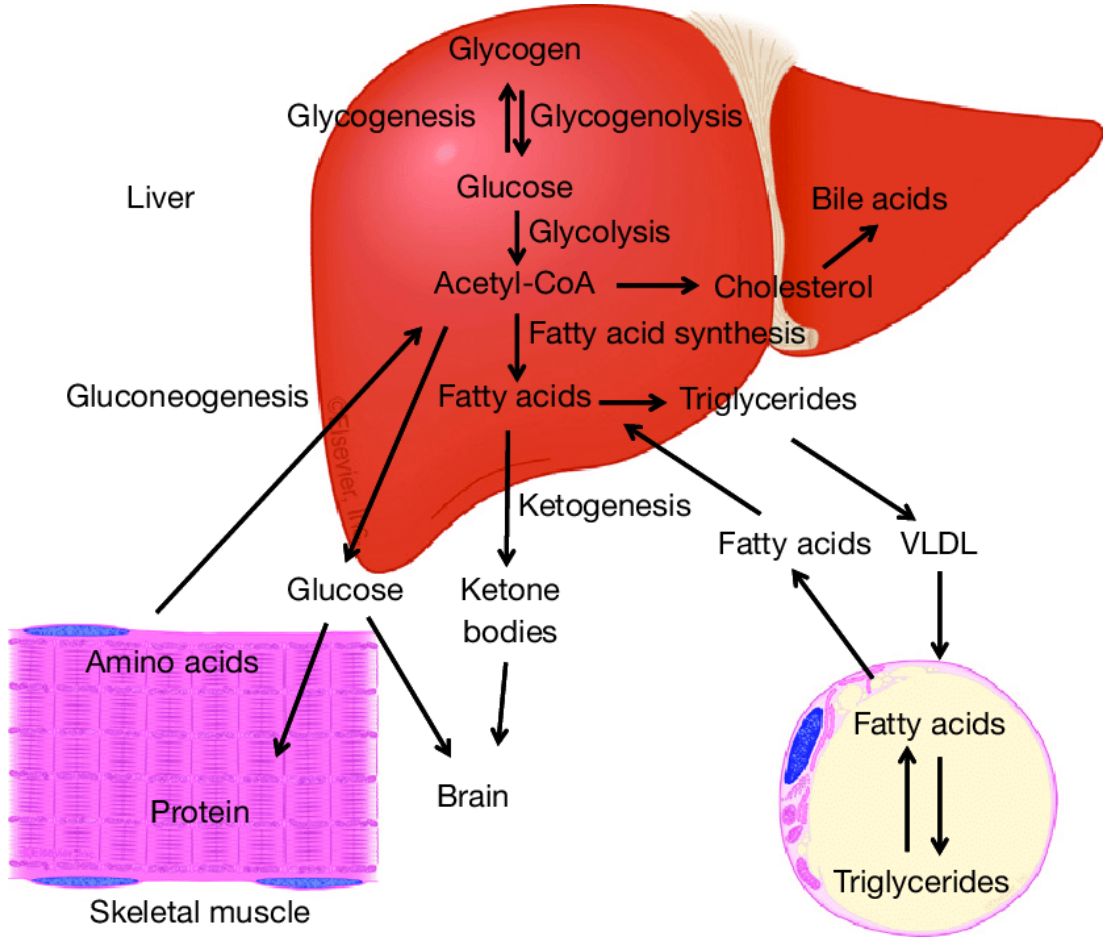

Figure 1. 4 Metabolic pathways executed by the liver.

Taken from Chinag JY 2014

P1- vs. P2-HNF4α

The liver is the site of many different metabolic processes and all of which are highly regulated through transcription factors. HNF4α has been implicated in the regulation of glucose and lipid metabolism and has been shown to be involved in the development of fatty liver disease, inflammatory bowel disease, hepatocellular, colorectal, renal, and gastric carcinomas. Moreover, HNF4α is mutated in Maturity Onset Diabetes of the Young 1 (MODY1) a hereditary form of type 2 diabetes (Miura et al., 2006; Sladek et al., 1998).

According to our RNA sequencing data, HNF4α is the most abundant nuclear receptor in the liver (Deans et al. 2021). HNF4α is one of the most highly conserved members of the nuclear receptor superfamily and is found in every animal organism. It typically binds DNA as a homodimer and is considered the master regulator of liver-specific gene expression (Bolotin & Sladek, 2009; Yusuf et al., 2012). HNF4α was first isolated from rat liver homogenate in 1990 and since then has been the subject of numerous studies investigating its structure, ligand, and function. Through crystallographic studies, a mixture of tightly bound fatty acids were found in the ligand binding domain of bacterially expressed HNF4α (Wisely et al., 2002), however the identity of the fatty acids and whether they bind in a native physiological environment needed to be investigated. Wildtype rat HNF4α2 was expressed in mammalian COS-7 cells and gas chromatography/mass spectrometry (GC/MS) was used to identify linoleic acid (9, 12, octadecadienoic acid, C18:2, $\Delta^{9, 12}$) bound to HNF4α (Yuan et al., 2009). Typically, ligand binding to nuclear receptors causes a conformational change and a resultant recruitment of coactivators or corepressors. However, the binding of linoleic acid (LA) only moderately

affected the transcription of HNF4α target genes, and that effect could have been due to a decreased level of HNF4α protein in the presence of LA (Yuan et al., 2009). HNF4α appears to have high endogenous transcriptional activity in its ligand-free state but its expression is also increased in the fasted state presumably due to the fact that insulin decreases the expression of HNF4α (Xie et al., 2009).

The human HNF4A gene is driven by two highly conserved promoters, denoted P1 and P2. These drive the expression of twelve different HNF4α isoforms. P1 activation will express HNF4α1, HNF4α2, HNF4α3, HNF4α4, HNF4α5, and HNF4α6; while P2 activation will express HNF4α7, HNF4α8, HNF4α9, HNF4α10, HNF4α11, and HNF4α12. The specific differences between the isoforms can be seen in Figure 1.5A (Ko et al., 2019). The P1/P2 promoter structure and various HNF4α isoforms are highly conserved from rodents to man.

Early studies investigating HNF4α did not explore different isoforms and the majority of the studies in the adult liver solely focused on the role of the predominant P1-HNF4α. Even though the P2-isoform was discovered in 1998, it took many years before any functional differences were observed in the isoforms. More recently, the scientific community has taken an interest in exploring the differences between P1- and P2-HNF4α in all of the tissues where they are endogenously expressed, conveniently the small differences in size can be visualized using a standard western blot (Figure 1.5B).

The most well characterized isoforms in the liver are HNF4α1/2 and HNF4α7/8, which differ at the N-terminal domain which is a site known to interact with coactivators (Ruse et al., 2002; Torres-Padilla et al., 2002; Wärnmark et al., 2003). HNF4α1/2 have the

1A exon incorporated at their N-terminal domain which includes an activation function 1 (AF-1) domain. The difference between HNF4α1 and HNF4α2 is that the latter has a ten amino acid insert in the F-domain. HNF4α7/8 have the 1D exon incorporated at their N-terminal domain, and like HNF4α1 and HNF4α2, HNF4α8 has the insert in the F-domain compared to HNF4α7. The insert increases the transcriptional activity of HNF4α (Ruse et al., 2002). The remaining domains in the isoforms, the ligand binding domain, DNA binding domain and the F domain are identical. The DNA-binding domain has a zinc-finger motif and is followed by a hinge region. The ligand binding domain is not only responsible for binding ligands but is also involved in the homodimerization and heterodimerization of HNF4α and contains a transactivation AF-2 domain (Ko et al., 2019). The N-terminal domain is responsible for transcriptional activation while the F-domain at the C-terminus is responsible for transcription repression (Ruse et al., 2002).

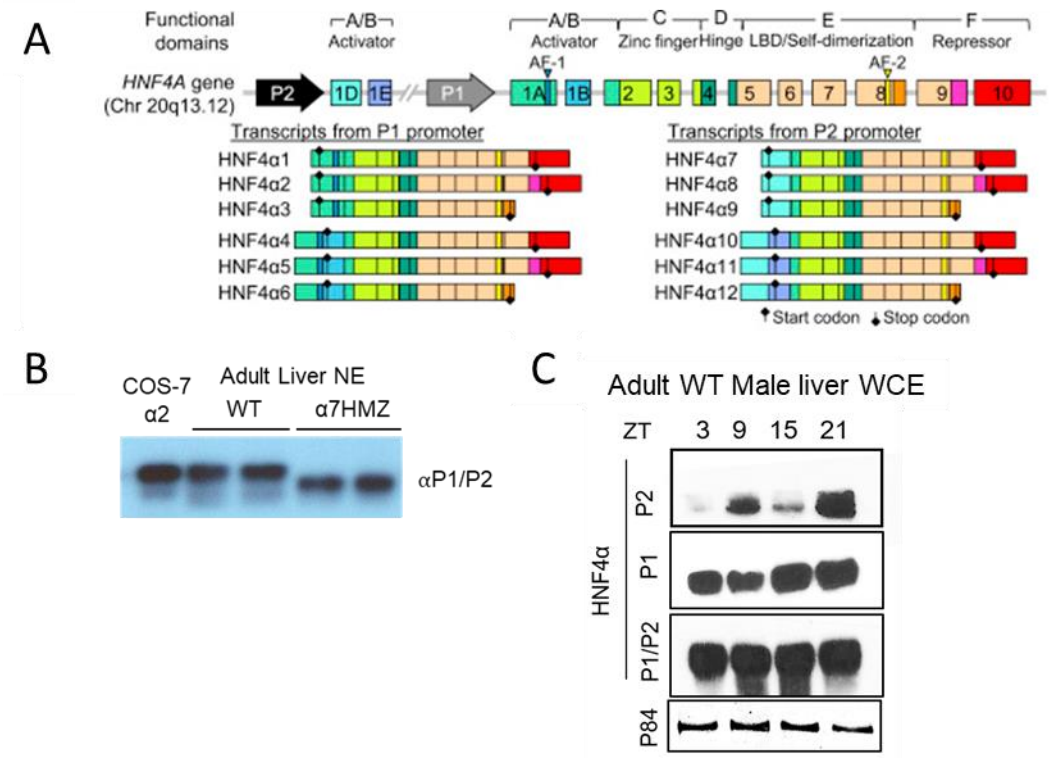

Figure 1. 5 Depiction of the two promoters of the Hnf4a gene and the isoforms resulting from their respective activation.

A) Schematic showing the gene structure of human HNF4A and its 12 transcripts, generated by alternative usage of P1 or P2 promoters, and alternative splicing at N and C termini. Taken from Ko et al. 2019. B) Immunoblot (IB) comparison of HNF4A isoforms from Cos7 cells (P1-HNF4α), WT male mouse liver (mainly P1-HNF4α) and α7HMZ male mouse liver (P2-HNF4α); C) IB of HNF4α1 (P1) and HNF4α7 (P2) protein in adult male liver at the indicated Zeitgeber times (ZT). (B, C taken from Deans et al. 2021).

HNF4α is expressed in a few different tissues in the body, and it plays distinct roles in each. Different tissues also express different isoforms. Both P1- and P2-driven HNF4α isoforms are expressed in both the fetal and adult liver, though there seems to be a circadian aspect to the expression of P2-driven isoform expression in the adult liver (Figure 1.5D) (Deans et al. 2021). P1-HNF4α is the predominant form expressed in the proximal tubules of the kidneys, though its role has yet to be elucidated; it is speculated that it could play a role in gluconeogenesis in that tissue (Curthoys & Moe, 2014; Legouis et al., 2020). P2-HNF4α is the predominant form in the pancreas where it plays a role in insulin secretion from β-cells (Miura et al., 2006). P2-HNF4α is also the predominant form in the stomach, though P1-HNF4α seems to be found there as well and they seem to function in differentiation of the epithelial cells as well as the development of gastric cancer (Moore et al., 2016). Both P1- and P2-driven HNF4α are expressed throughout the small intestines and the colon and contribute to cellular differentiation and proliferation, respectively (Chellappa et al., 2016). Upon initial examination, it was thought that P2-HNF4α was not expressed in the adult liver and this was due to a strong repression of the P2- promoter by expression of P1-HNF4α (Briançon et al., 2004).

P1-HNF4α was initially cloned from crude rat liver extracts as a protein that binds sites necessary for the transcription of transthyretin (Ttr), a carrier protein for vitamin A and thyroid hormone in the serum, and for apolipoprotein CIII (Apoc3), a major lipoprotein comprising chylomicrons and very low-density lipoproteins (Sladek et al., 1990). A few years later, HNF4α was found to help activate the main gluconeogenic gene *Pck1* by binding to AF1 elements in the promoter, along with COUP-TF. P2-HNF4α was cloned in

1998 from an embryonic cell line and shown to be expressed in the stomach (Nakhei et al., 1998).

To examine the differential effects of the HNF4α isoforms in vivo, we and others have utilized an exon swap mouse model developed in the Pasteur Institute (Briançon & Weiss, 2006). A whole-body HNF4α knockout is embryonic lethal and a liver-specific knockout causes death around six weeks of age in mice due to dyslipidemia, high serum bile acid levels and ureagenesis defects (Hayhurst et al., 2001; Inoue et al., 2002). Therefore, the exon-swap model allowed the examination of a single group of HNF4α isoforms, either P1- or P2-HNF4α, throughout the tissues that express HNF4α. This was accomplished by replacing the first exon in the P1-driven HNF4α with the first exon from the P2-driven HNF4α sequence and vice versa (Figure 1.6A) (Briançon & Weiss, 2006). The mice with the second copy of the P2-driven HNF4α at the P1 promoter will only produce P2-driven HNF4α regardless of which promoter is activated and these are referred to as α7HMZ mice. The mice with a second copy of the P1-driven HNF4α exon at the P2 promoter will only produce P1-driven HNF4α and are referred to as α1HMZ mice (Figure 1.6B). Both the α1HMZ and α7HMZ mice are viable and fertile. The α7HMZ mice did have significantly lower levels of cholesterol, triglycerides, and free-fatty acids compared to wildtype and α1HMZ mice, and had significantly higher levels of ketone bodies compared to the other two groups (Briançon & Weiss, 2006).

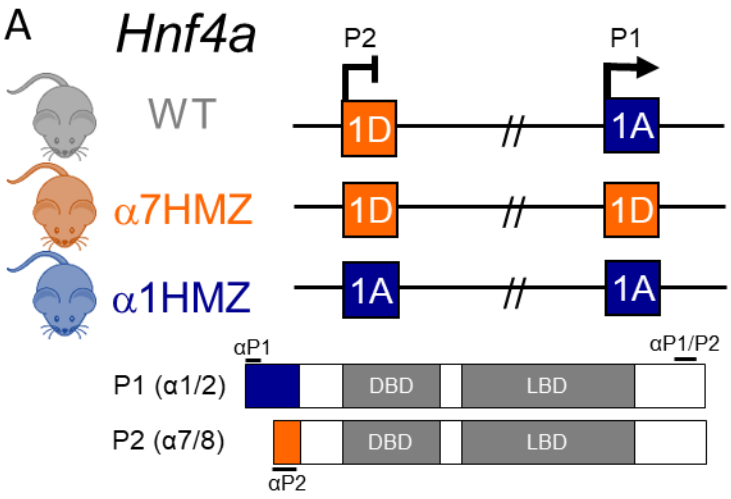

B

Wildtype mice	Embryonic Liver	Adult Liver	Kidney	Pancreas	Intestine	Stomach
P1-HNF4α	+	+	+	-	+	-
P2-HNF4α	+	+	-	+	+	+

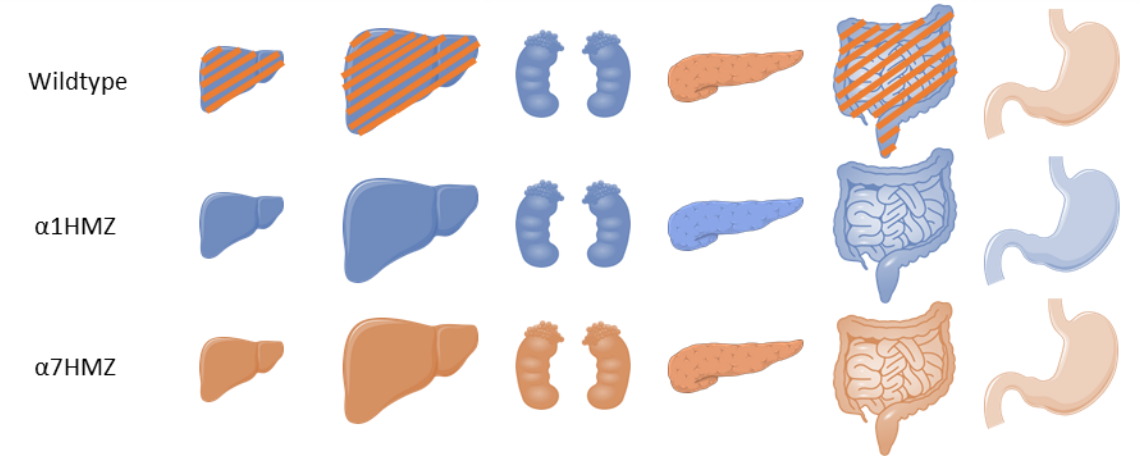

Figure 1. 6 HNF4α1 and HNF4α7

A) *Hnf4a* locus in wildtype (WT) and exon swap mice (α7HMZ and α1HMZ); HNF4A protein structure with isoform-specific antibodies. DBD, DNA binding domain; LBD, ligand binding domain. B) Depiction of the HNF4a isoforms expressed in different tissues in WT, α1HMZ and α7HMZ mice. Stripes indicate both isoforms are present.

There are many other transcription factors that regulate genes involved in basic metabolism. For instance, the glucocorticoid receptor (NR3C1, GR) binds cortisol and other glucocorticoids and through interaction with *Pcg1a* it stimulates gluconeogenesis by activating the expression of glucose-6-phosphatase (G6P) and phosphoenolpyruvate carboxykinase (PEPCK) (Nicolaides et al., 2020). The estrogen receptor (NR3A1, ESR1) is activated by binding to estrogen and is also involved in regulating glucose metabolism. Estrogen stimulates the phosphorylation of energy sensing kinases Ak strain transforming kinase (AKT) and AMP-activated protein kinase (AMPK), this increases insulin sensitivity in skeletal muscles and increases glucose uptake through GLUT4 glucose transporters (Barros & Gustafsson, 2011). Moreover, the peroxisome proliferator activated receptor (PPAR) genes (NR1C1, NR1C2, NR1C3) are another group of proteins that are involved in glucose and lipid metabolism. PPARdelta in the liver has been shown to increase insulin sensitivity in diabetic mouse models and improves hyperglycemia by decreasing hepatic glucose production (Han et al., 2017). Both GR and the PPAR genes have been shown to interact with HNF4α and play an important role in glucose homeostasis in the liver (Bailly et al., 2009; Peeters & Baes, 2010).

HNF4α Isoform differences in Colorectal Cancer

P1-HNF4α was first discovered in rat liver, and subsequently found in the kidney and intestines (Sladek et al., 1990; Xanthopoulos et al., 1991). P2-HNF4α was isolated from F9 embryonic carcinoma cells and was found to be expressed at low levels in the liver, pancreas, and intestines, and at higher levels in the stomach; though P1-HNF4α was also found to be present in all of these tissues except the pancreas (Nakhei et al., 1998).

Later studies confirmed the expression of P2-HNF4α in the stomach, pancreas, intestines, fetal liver, and in hepatocellular carcinoma (Fekry et al., 2018). P1-HNF4α has notably stronger transactivation activity compared to P2-HNF4α, as it contains the AF-1 domain in its N-terminal domain (Torres-Padilla et al., 2002).

One of the earliest studies exploring the difference between P1- and P2-HNF4α explored their differential phosphorylation by Src tyrosine kinase in human colon cancer (Chellappa et al., 2012). Src was shown to phosphorylate P1-HNF4α as well as a truncated form containing the N-terminal A/B and DNA-binding domains, yet it does not phosphorylate P2-HNF4α. Through site-directed mutagenesis of a tyrosine residue to the non-phosphorylatable phenylalanine, Y14F abolished the phosphorylation signal, making it the likely phosphorylation site in the N-terminal domain, and is a residue not present in the N-terminal domain of P2-HNF4α. Moreover, mass spectrometry identified another phosphorylated peptide from the ligand binding domain, and it was determined that Y277/Y279 was also phosphorylated by Src. Both sites were validated by site directed mutagenesis. Interestingly, Y14F mutants lacked a phosphorylation signal indicating that it is necessary for Y14 to be phosphorylated before the subsequent Y277/279 phosphorylation can take place. Y277 in the ligand binding domain is near a salt-bridge between E150 and K281, which is part of the protein that links the cofactor binding site to the dimer interface, while Y279 is in a hydrophobic region at the dimer interface. Therefore, it is speculated that phosphorylation in the ligand binding domain negatively impacts HNF4α dimerization and subsequent transactivation.

Through phosphomimetic mutants from tyrosine to glutamate, it was found that Y277E/Y279E double mutant completely abolished HNF4α transactivation, but only slightly reduced DNA binding activity. Interestingly, the double mutant was found to be exported to the cytosol, had greatly reduced protein stability through the proteasome, and reduced ability to recruit coactivators. Src activation in CaCo2 colorectal cancer cells that express both P1- and P2-HNF4α resulted in a specific phosphorylation and decrease of P1- and not P2-HNF4α. The phospho-Y14 of P1-HNF4α is able to bind the SH2 domain in Src thereby activating the kinase and causing a phosphorylation of the two tyrosines in the LBD. Though both P1- and P2-HNF4α have a proline-rich region in the F-domain that can bind to the SH3 domain of Src, that binding is not sufficient for phosphorylation. This all could explain the role of the oncogenic Src tyrosine kinase in colorectal cancer, which typically shows a decrease in P1-HNF4α and no change or a slight increase in P2-HNF4α. The role of the isoforms in colorectal cancer still needed to be elucidated. Tumors from 450 human patients with Stage III colon cancer were screened and stained using a P1-HNF4α antibody. This revealed four categories for the tumors: loss of P1 staining in approximately 12% of the tumors, predominantly cytoplasmic P1 staining in 18-24% of the tumors, both nuclear and cytoplasmic staining of P1 in approximately 47-49% of the tumors, and lastly only nuclear P1 staining in approximately 18-23% of the tumors. Moreover, a subset of the tumors were stained with anti-phospho-Src antibody (pTyr419). The tumors that had little or only cytoplasmic staining for P1-HNF4α had consistent staining of pSrc in the nucleus. Conversely, the tumors with appreciable P1-HNF4α staining had low pSrc staining. Moreover, the adjacent non-cancerous tissue with almost

exclusively nuclear P1-HNF4α staining had little to no pSrc staining. Taken together, these data support the notion that activation of Src may lead to the cytoplasmic localization and/or the complete loss of P1-HNF4α expression.

Vuong et al. 2015 explored the differential effects of the HNF4α isoforms on tumor growth in human colorectal cancer (Vuong et al., 2015). Using Tet-On-Inducible (using doxycycline) HCT116 cell lines that express either HNF4α2 or HNF4α8, these cells were injected in immunocompromised mice and allowed to develop for 8 days when the mice were fed a diet supplemented with doxycycline to induce HNF4α expression. The tumors with HNF4α2 were significantly smaller compared to the parental controls, which do not express any HNF4α, while those with HNF4α8 were not. Moreover, the HNF4α8 tumors showed higher invasive index using an *in vitro* invasion/migration assay, suggesting that while HNF4α2 is actively tumor suppressive in colorectal cancer, HNF4α8 is at least permissive of the cancer state. RNA sequencing was performed on these cell lines. Though the isoforms have identical DNA and ligand binding domains, only approximately 40% of the upregulated genes were common between the HNF4α2 and HNF4α8 cell lines, with approximately 200 differentially expressed genes. Gene ontology analysis showed both HNF4α2 and HNF4α8 upregulated genes in drug metabolism, oxidative stress, negative regulation of phosphorylation, glycoprotein metabolism and wound healing. Moreover, HNF4α2 specifically upregulated cell death and cellular response to extracellular stimulus, while HNF4α8 upregulated genes involved in cell adhesion, many of which actually increased cell proliferation. HNF4α8 also upregulated antiapoptotic genes. Additionally,

HNF4α2 upregulated genes involved in growth inhibition, while HNF4α8 upregulated genes involved in growth promotion.

To further explore the mechanism by which the HNF4α isoforms regulate genes in a differential fashion, ChIP sequencing was performed. There were many more ChIP peaks in the HNF4α2 line compared to the HNF4α8 line, though there were approximately 2200 common peaks between the groups. When compared to the RNA sequencing data, there were 101 upregulated genes in the HNF4α2 group that had unique ChIP peaks, with another 80 that had an overlap in ChIP peaks from both HNF4α2 and HNF4α8, and finally 67 genes that did not have an HNF4α peaks suggesting an indirect mechanism for upregulation. With regards to HNF4α8 upregulated genes, one gene was solely occupied by HNF4α8, 109 genes had peaks for both isoforms, and 94 had peaks for HNF4α2.

To examine the difference in proliferation activation between the isoforms, the role of TCF factors in the Wnt/β-catenin pathway was investigated. Through ChIP sequencing, and co-expression of TCF4 with or without the HNF4α isoforms, HNF4α8 was seen to preferentially recruit TCF4 compared to HNF4α2, and those genes were involved in cellular signaling, including Wnt signaling. Taken together, these results help explain the contradictory notion that HNF4α is both a tumor suppressor and at least somewhat oncogenic; the isoforms perform distinct roles in the HCT116 cells by interacting with different co-regulators.

HNF4α has been implicated not only in colon cancer, but also in inflammatory bowel disease (IBD) and colitis. Indeed, HNF4α is considered to be an IBD susceptibility gene (Ahn et al., 2008; Barrett et al., 2009; Oshima et al., 2007). Using genetically

engineered exon swap mice expressing either P1-HNF4α or P2-HNF4α throughout the tissues where HNF4α is endogenously expressed, the differential role of the isoforms in these inflammatory diseases and their role in colon cancer was investigated (Chellappa et al., 2016). To begin, wildtype colons were examined to elucidate the expression of HNF4α isoforms in the crypts. Using isoform specific monoclonal antibodies, P1-HNF4α was seen in the top one-third, differentiation compartment and colocalized with NKCC1 staining, while P2-HNF4α was seen in the bottom two-thirds, proliferative compartment and colocalized with Ki67 staining. Following five days of dextran sodium sulfate (DSS) treatment to induce colitis, HNF4α levels decreased and recovered when the treatment stopped. Interestingly, P1-HNF4α was seen near the bottom of the crypts post-treatment, which is consistent with a loss of proliferation in the crypts following DSS treatment. Moreover, in a colitis-associated colon cancer model, following a single injection of azoxymethane and multiple DSS treatments, P1-HNF4α was specifically reduced while P2-HNF4α seems not to be affected. phosphoSrc was also observed in the tumors.

This study utilized exon swap mice which exclusively express either P1-HNF4α or P2-HNF4α in tissues where HNF4α is endogenously expressed. The exon swap results in only P1-HNF4α being expressed throughout the crypts in the α1HMZ mice, and P2-HNF4α in the α7HMZ mice. After induction of colitis-associated colon cancer, the α1HMZ mice had significantly fewer and smaller tumors compared to the wildtype controls. Conversely, the α7HMZ mice had significantly greater tumor number and size compared to the wildtype (Chellappa et al., 2016).

There were also differences in mortality rate following DSS treatment, with the α7HMZ mice exhibiting a 73% mortality rate, a significant decrease in body weight and colon length, and more inflammation and damage to the colonic crypts (Chellappa et al., 2016). In contrast to the wildtype where there was a decrease in both isoforms and subsequent increase in P1-HNF4α during recovery, in α7HMZ mice there was a marked increase in HNF4α protein during treatment followed by a decrease during recovery. Conversely, the α1HMZ mice were less susceptible to the DSS-induced colitis compared to the wildtype mice.

Expression profiling of the exon swap mice revealed that the α1HMZ mice had an increase in genes involved in wound healing, immunity, and metabolic pathways such as lipid, amino acid, and cholesterol metabolism; while the α7HMZ mice had an increase in cell cycle and DNA repair genes and a decrease in cell adhesion, motility and ion transport genes (Chellappa et al., 2016). These findings were corroborated using rapid immunoprecipitation mass spectrometry of endogenous proteins (RIME) analysis. RIME analysis allows for the study of protein complexes, especially βand transcription factor complexes. α7HMZ colons showed an interaction between HNF4α and CUL4 and PCM1 which are important in cell proliferation and are overexpressed in difference cancers. RIME analysis also showed unique protein interactions with HNF4α in the exon swap mice, indicating that although the DNA and ligand binding domains of the isoforms are identical, the differential N-terminus of the HNF4α isoforms plays a role in determining which protein-protein interactions HNF4α can partake.

Experimental induction of colitis showed that RELMβ activated the innate immune system in response to loss of epithelial barrier function and increased exposure to gut microbiota. Therefore, mice lacking the *Retnlb* gene are known to be resistant to experimental colitis (Hogan et al., 2006). Thus, the likely cause of the extra sensitivity to DSS treatment is the marked increase in RELMβ in the α7HMZ mice compared to wildtype. RELMβ knockout /α7HMZ mice were created to validate this hypothesis. Although the histological score of the crypts was somewhat improved it was not significant, however the body weight and survival were restored post treatment in the knockout mice.

Isoform differences in the liver

For years, with regards to the liver, P2-HNF4α was thought to be expressed only in liver cancer and fetal liver. Hepatocellular carcinoma is one of the most common cancers in the world and is on the rise as NAFLD is rising in parallel with obesity and metabolic syndromes (Cholankeril et al., 2017; Massarweh & El-Serag, 2017; Seydel et al., 2016; Wong et al., 2014). Hepatocellular carcinoma is usually associated with liver inflammation and cirrhosis. Additionally, it is markedly more common in males compared to females. Many studies have shown that HNF4α levels are suppressed in hepatocellular carcinoma tissues in humans compared to non-cancerous tissues (Lazarevich & Fleishman, 2008; Tanaka et al., 2006; Yin et al., 2008). A study found that expression of HNF4α correlated negatively with hepatocellular carcinoma formation; though they did not specify isoform they are likely examining P1-HNF4α levels (Ning et al., 2010). Using a diethylnitrosamine rat model, the group observed that as the hepatocellular carcinoma progressed, HNF4α

levels diminished (Ning et al., 2010). Moreover, after examining human tissue samples using microarray analysis, HNF4α levels were significantly decreased in cirrhotic and hepatocellular carcinoma tissues. Interestingly, there was enhanced epithelial-to-mesenchymal transition in the tissues that had decreased HNF4α, an essential part of the metastatic process in many cancers (Roche, 2018). Upon HNF4α delivery, the epithelial cell marker E-cadherin reduction and mesenchymal marker vimentin increase were both blocked indicating HNF4α is able to inhibit the epithelial-to-mesenchymal transition. HNF4α has also been shown to be inhibited by cyclin D1 (Sladek et al. 2012), an essential driver of cell proliferation. Similarly, HNF4α seems to inhibit the expression of cyclin D1, as a liver-specific HNF4α knockout results in elevated levels of cyclin D1 (Bonzo et al., 2012). This further solidifies the tumor suppressive action of P1-HNF4α.

P2-HNF4α has long been known to be highly expressed in the fetal liver. During embryonic days 15 and 19 in mice it is even higher than the P1-HNF4α isoform level (Dean et al., 2010). Originally, P2-HNF4α expression in the adult liver was only observed during hepatocellular carcinoma and was indicative of a worse prognosis for those patients. Conversely, the expression of P1-HNF4α in hepatocellular carcinoma usually indicates a favorable prognosis as it can slow down progression and increase differentiation (Cai et al., 2017). Though hepatocellular carcinoma is more prevalent in males, there is an increase in incidence in females (*Cancer Facts & Figures 2021*, n.d.). A 2019 study examined how HNF4α deficiency in the liver causes a favorable environment for hepatocellular carcinoma development irrespective of sex (Fekry et al., 2019). They used a tamoxifen-inducible Albumin/CRE system to knock out HNF4α in male and female mouse livers. These mice

quickly accumulated fat in their livers post knockout induction and had hypoglycemia following a 4-hour fast, though the fed glycemia was normal. Additionally, both females and males had higher levels of cyclin D1 in the liver which is known to be inhibited by P1-HNF4α, and Apolipoprotein C2 was reduced in the knockout, which is consistent as it is a known target gene of P1-HNF4α. When combined with a high fat diet, both male and female knockout mice had 100% incidence of hepatocellular carcinoma at 38 weeks of age compared to none of the wildtype mice developing hepatocellular carcinoma though they did exhibit inflammation, fibrosis, and steatosis. This shows that P1-HNF4α knockout and high fat diet is sufficient to induce hepatocellular carcinoma in both sexes, unlike the diethylnitrosamine model which has a higher incidence of cancer in males. Normally, it has been theorized that the reason females are more resistant to hepatocellular carcinoma is because the circulating estrogen inhibits Interleukin-6 (*Il6*), which is essential for the pathogenesis of hepatocellular carcinoma as it induced epithelial-to-mesenchymal transition, the inhibition of which has been shown to prevent the cancer (Naugler et al., 2007). The HNF4α knockout model in addition to a high fat diet induced *Il6* in both males and females which is likely why there was a 100% incidence for both sexes. This study did not examine the effects of P2-HNF4α in the development of hepatocellular carcinoma, though other studies note its upregulation during the disease (Cai et al., 2017; Fekry et al., 2018).

Over the years a handful of studies have seen P2-HNF4α mRNA and protein to be expressed in the healthy adult liver, but most did not address it or explore that finding (Ko et al., 2019; Nakhei et al., 1998). A couple of recent studies have not only demonstrated

the expression of P2-HNF4α in the adult liver, but they explore its potential role in metabolism.

Using mainly a primary hepatocyte model, with some experiments in mice, a group investigated the role of P2-HNF4α reactivation in the adult liver (Da Li et al., 2020). Fasting upregulated the H19 non-coding RNA, which is elevated in type 2 diabetes, which subsequently increased HNF4α, PGC1α, PEPCK, and G6PC mRNA, and surprisingly increased TET3 mRNA. TET3 overexpression in hepatocytes led to an increase in *Pck1*, *G6pc*, and glucose production, while a knockdown in the presence of glucagon did not result in an increase in these genes. These results were mimicked in H19 knockout mice, and the knockdown showed TET3 was necessary for hepatic glucose production. H19 elevation along with *Tet3* elevation was seen in human livers of type-2 diabetes patients indicating this mechanism is likely conserved between humans and mice.

Most interesting, conditions that increased *Tet3* lead to an increase in specifically P2-HNF4α. In primary hepatocytes, glucagon caused an increase in P2- but not P1-HNF4α, and increased expression of gluconeogenic markers *Pck1* and *G6pc* and abolished glucagon-induced glucose production. Mice injected with an adenoviral vector to deliver P2-HNF4α specific siRNA, had decreased fasting glucose, fasting insulin, *Pck1* and *G6pc* levels, and pyruvate tolerance test (a test specific to gluconeogenic glucose production). Moreover, upon TET3 overexpression in H19 knockout hepatocytes and P2-HNF4α knock down, there was an abolition of the TET3-induced glucose production seen before. These results were repeated and confirmed in primary human hepatocytes as well.

TET3 is known to demethylate DNA and activate transcription, this group speculated that it was demethylating the P2-promoter increasing P2-specific transcription of HNF4α. Using chromatin immunoprecipitation (ChIP) followed by quantitative-polymerase chain reaction (qPCR), the P2-promoter was preferentially bound by TET3 upon glucagon stimulation, specifically leading to an increase in 5-hydroxymethylcytosine, a byproduct of an early step in DNA demethylation. It is speculated that FOXA2 could play a role in the P2-promoter activation as it was found to preferentially bind to the P2-promoter via ChIP sequencing from human liver tissue. Upon FOXA2 knockdown in primary mouse hepatocytes, TET3 was no longer found to associate with the P2-promoter following glucagon stimulation, indicating FOXA2 is essential for this interaction to occur.

P2-HNF4α has been found to increase in the liver of fasted mice, and the group hypothesized it was a more potent gluconeogenesis activator. Using a luciferase assay, they found that P2-HNF4α had significantly more transactivation activity in the presence of increasing amounts of PGC1α using a fragment of the *Pck1* promoter. PGC1α has been established to be required for P1-HNF4α activation of *Pck1* and *G6pc* as PGC1α lacks the ability to bind DNA itself (Rhee et al., 2003; Yoon et al., 2001). Lastly, the group investigated the relevance of TET3 or P2-HNF4α inhibition in stabilization of glucose levels in both high fat diet and genetic mouse models of type 2 diabetes. As expected, both knock down of TET3 and P2-HNF4α lead to decreased hepatic gluconeogenesis, PCK1, and G6PC, along with enhanced glucose tolerance and insulin sensitivity.

Another study from my lab found that P2-HNF4α was discovered to be expressed in the normal adult liver in a circadian fashion, specifically at zeitgeber time (ZT) 9 and

ZT 21 (Deans et al. 2021). Moreover, they used transcriptomic and metabolomic studies to explore the differences in wildtype and P2-HNF4α only expressing exon swap, α7HMZ, mice.

RNA sequencing of adult male wildtype and α7HMZ mice revealed approximately 1600 differentially expressed genes. Kegg pathway analysis revealed wildtype mice had enriched cell adhesion, drug and linoleic acid metabolism, and steroid hormone biosynthesis genes; while α7HMZ mice had enriched ribosomal, oxidative phosphorylation and RNA transport and processing genes. Moreover, using Gene Ontology enrichment analysis, α7HMZ mice had non-alcoholic fatty liver disease, viral carcinogenesis, alcoholism, and neurological diseases enriched.

Comparison of the differentially expressed genes to fetal livers showed wildtype mice had an overlap of approximately only 10% with fetal livers, while α7HMZ had an overlap of approximately 50%. Yet, *Mki67* and *Pcna*, proliferation genes, were not upregulated in the adult α7HMZ livers as one would expect in a fetal phenotype. Moreover, when compared to a hepatoma cell line, there was not a significant overlap in either wildtype or α7HMZ mouse differentially expressed genes. This indicates that though P2-HNF4α has a distinct function in the adult liver compared to P1-HNF4α, that function is not related to fetal gene expression nor cancer.

The RNA sequencing was performed at three different times of the day, ZT 3.5, 6.5, and 13.5, as nuclear receptors are known to play a role in circadian regulation. The α7HMZ mice had significantly less alternation between the time points compared to wildtype, suggesting they had reduced sensitivity to the circadian clock. The nuclear

receptor CAR (*Nr1i3*), along with other genes essential in circadian clock regulation, were downregulated in α7HMZ mice at all three time points. Additionally, α7HMZ males had a down regulation of the androgen receptor (*Ar*) and a slight upregulation of the estrogen receptor (*Esr1*) suggesting a feminization of the α7HMZ liver.

HNF4α has been known to regulate phase I and II enzymes in the liver, and between the wildtype and α7HMZ mice, there were differences in many cytochrome P450 genes (*Cyp* genes, phase I), and glucuronosyltransferases (*Ugt*, Phase II). Metabolomics showed a significant decrease in UDP glucuronic acid in α7HMZ mice, which needs glucose for its production, therefore this could be linked to glucose metabolism differences in these mice.

ChIP sequencing was performed on these mice and revealed 572 unique peaks in the wildtype mice, and 1067 peaks in the α7HMZ mice, though the common peaks were more likely to be in the promoter region of genes. Moreover, there were approximately 22% of the wildtype and α7HMZ differentially expressed genes that had ChIP peaks within 50 kilobases of a transcription start site. Because most of the genes did not have ChIP peaks nearby, RIME analysis was done at ZT 3.5 and 13.5 on the wildtype and α7HMZ livers. There were 167 wildtype- and 108 α7HMZ-specific protein interactions at ZT3.5, 357 wildtype- and 256 α7HMZ-specific protein interactions at ZT 13.5, and 96 proteins binding both groups at both time points, 141 at ZT 3.5, and 401 at ZT 13.5. Taken together, these data indicate that not only do the isoforms bind DNA differently, this is likely facilitated by unique interactions between the isoforms.

As there was dysregulation in the *Clock* machinery in the α7HMZ mice, livers were harvested from wildtype male mice to check for expression of P2-HNF4α protein at different times of the day. P2-HNF4α was indeed found at ZT9 and ZT21 in wildtype livers and its level was exacerbated in *Clock* knockout livers. Moreover, the clock in the liver is closely linked to metabolism as the liver is the main metabolic organ, metabolomic analysis of primary metabolites and complex lipids was performed on both wildtype and α7HMZ mice at ZT 3.5. 100 out of the 359 metabolites were downregulated in α7HMZ livers, and metabolite set enrichment analysis showed an increase in carbohydrate metabolism and protein biosynthesis in wildtype mice. Conversely, genes and metabolites involved in ketone body formation were enriched in the α7HMZ mice.

Although the paper examining the role of TET3 in type 2 diabetes determined that P2-HNF4α is likely a stronger activator of gluconeogenesis than P1-HNF4α (Da Li et al., 2020), this study with exon swap mice shows that P2-HNF4α expression is involved in an upregulation of ketogenesis and a downregulation of gluconeogenesis (Deans et al. 2021). This discrepancy is likely due to differences in models used in the studies as well as the fact that the switch between gluconeogenesis and ketogenesis is heavily temporal. The TET3 study used mainly a primary hepatocyte model and used C57Bl6/J mice for their mouse model, while the latter study used mainly a mouse model and used either a mixed 129/Sv background, or C57Bl6/N mice. Moreover, the exon swap mice used have the difference in HNF4α expression throughout their lives, while the mice used in the TET3 study had HNF4α knock down during adulthood. Taken together these studies indicate that P2-HNF4α is present in the adult liver, it is increased in response to fasting, and thus is

involved in fasting induced metabolic processes. The exact function within the adult liver and the mechanism as to how it performs this function still needs to be elucidated.

HNF4α is the master regulator of liver specific gene expression, but also plays important roles in the gut. HNF4α has been implicated in glucose and lipid metabolism and cancer. Mutation of the HNF4α gene results in MODY1, a rare form of type-2 diabetes. The HNF4α gene is driven by two promoters which give rise to P1- and P2-driven isoforms. It was initially thought that P1-HNF4α was the only form in the adult liver and was tumor suppressive. In liver cancer, P2-HNF4α was upregulated and thought to be permissive of proliferation. It was recently discovered that P2-HNF4α is expressed in the normal adult liver and the following chapter attempts to understand the differential role the isoforms play.

REFERENCES

Ahn, S.-H., Shah, Y. M., Inoue, J., Morimura, K., Kim, I., Yim, S., Lambert, G., Kurotani, R., Nagashima, K., Gonzalez, F. J., & Inoue, Y. (2008). Hepatocyte nuclear factor 4alpha in the intestinal epithelial cells protects against inflammatory bowel disease. *Inflammatory Bowel Diseases*, *14*(7), 908–920.

Alsahli, M., & Gerich, J. E. (2017). Renal glucose metabolism in normal physiological conditions and in diabetes. *Diabetes Research and Clinical Practice*, *133*, 1–9.

Bailly, A., Briançon, N., & Weiss, M. C. (2009). Characterization of glucocorticoid receptor and hepatocyte nuclear factor 4alpha (HNF4alpha) binding to the hnf4alpha gene in the liver. *Biochimie*, *91*(9), 1095–1103.

Barrett, J. C., Lee, J. C., Lees, C. W., Prescott, N. J., Anderson, C. A., Phillips, A., Wesley, E., Parnell, K., Zhang, H., Drummond, H., & Others. (2009). UK IBD Genetics Consortium Genome-wide association study of ulcerative colitis identifies three new susceptibility loci, including the HNF4A region. *Nature Genetics*, *41*, 1330–1334.

Barros, R. P. A., & Gustafsson, J.-Å. (2011). Estrogen receptors and the metabolic network. *Cell Metabolism*, *14*(3), 289–299.

Bolotin, E., Schnabl, J. & Sladek, F. (2009). HNF4A (Homo sapiens). *Transcription Factor Encyclopedia,*. http://www.cicreg.ca/tfe

Bonzo, J. A., Ferry, C. H., Matsubara, T., Kim, J.-H., & Gonzalez, F. J. (2012). Suppression of hepatocyte proliferation by hepatocyte nuclear factor 4α in adult mice. *The Journal of Biological Chemistry*, *287*(10), 7345–7356.

Briançon, N., Bailly, A., Clotman, F., Jacquemin, P., Lemaigre, F. P., & Weiss, M. C. (2004). Expression of the alpha7 isoform of hepatocyte nuclear factor (HNF) 4 is activated by HNF6/OC-2 and HNF1 and repressed by HNF4alpha1 in the liver. *The Journal of Biological Chemistry*, *279*(32), 33398–33408.

Briançon, N., & Weiss, M. C. (2006). In vivo role of the HNF4alpha AF-1 activation domain revealed by exon swapping. *The EMBO Journal*, *25*(6), 1253–1262.

Cai, S.-H., Lu, S.-X., Liu, L.-L., Zhang, C. Z., & Yun, J.-P. (2017). Increased expression of hepatocyte nuclear factor 4 alpha transcribed by promoter 2 indicates a poor prognosis in hepatocellular carcinoma. *Therapeutic Advances in Gastroenterology*, *10*(10), 761–771.

Cancer Facts & Figures 2021. (n.d.). Retrieved November 16, 2021, from

https://www.cancer.org/research/cancer-facts-statistics/all-cancer-facts-figures/cancer-facts-figures-2021.html

Chellappa, K., Deol, P., Evans, J. R., Vuong, L. M., Chen, G., Briançon, N., Bolotin, E., Lytle, C., Nair, M. G., & Sladek, F. M. (2016). Opposing roles of nuclear receptor HNF4α isoforms in colitis and colitis-associated colon cancer. *eLife*, *5*. https://doi.org/10.7554/eLife.10903

Chellappa, K., Robertson, G. R., & Sladek, F. M. (2012). HNF4α: a new biomarker in colon cancer? *Biomarkers in Medicine*, *6*(3), 297–300.

Chiang, J. Y. L. (2014). Liver Physiology: MetaboLism and Detoxification. In Pathophysiology of Human DIseases (pp. 1770–1782). unknown.

Cholankeril, G., Patel, R., Khurana, S., & Satapathy, S. K. (2017). Hepatocellular carcinoma in non-alcoholic steatohepatitis: Current knowledge and implications for management. *World Journal of Hepatology*, *9*(11), 533–543.

Curthoys, N. P., & Moe, O. W. (2014). Proximal tubule function and response to acidosis. *Clinical Journal of the American Society of Nephrology: CJASN*, *9*(9), 1627–1638.

Da Li, Cao, T., Sun, X., Jin, S., Di Xie, Huang, X., Yang, X., Carmichael, G. G., Taylor, H. S., Diano, S., & Huang, Y. (2020). Hepatic TET3 contributes to type-2 diabetes by inducing the HNF4α fetal isoform. *Nature Communications*, *11*(1), 342.

Deans, J. R., Deol, P., Titova, N., Radi, S. H., Vuong, L. M., Evans, J. R., Pan, S., Fahrmann, J., Yang, J., Hammock, B. D., Fiehn, O., Fekry, B., Eckel-Mahan, K., Sladek, F. M. (2021). Alternative HNF4α isoform regulates the sex-specific diurnal balance between carbohydrate and lipid metabolism in the liver. bioRxiv 2021.02.28.433261; doi: https://doi.org/10.1101/2021.02.28.433261(2021)

Dean, S., Tang, J. I., Seckl, J. R., & Nyirenda, M. J. (2010). Developmental and tissue-specific regulation of hepatocyte nuclear factor 4-alpha (HNF4-alpha) isoforms in rodents. *Gene Expression*, *14*(6), 337–344.

Fekry, B., Ribas-Latre, A., Baumgartner, C., Deans, J. R., Kwok, C., Patel, P., Fu, L., Berdeaux, R., Sun, K., Kolonin, M. G., Wang, S. H., Yoo, S.-H., Sladek, F. M., & Eckel-Mahan, K. (2018). Incompatibility of the circadian protein BMAL1 and HNF4α in hepatocellular carcinoma. *Nature Communications*, *9*(1), 4349.

Fekry, B., Ribas-Latre, A., Baumgartner, C., Mohamed, A. M. T., Kolonin, M. G., Sladek, F. M., Younes, M., & Eckel-Mahan, K. L. (2019). HNF4α-Deficient Fatty Liver Provides a Permissive Environment for Sex-Independent Hepatocellular Carcinoma. *Cancer Research*, *79*(22), 5860–5873.

Han, L., Shen, W.-J., Bittner, S., Kraemer, F. B., & Azhar, S. (2017). PPARs: regulators of metabolism and as therapeutic targets in cardiovascular disease. Part II: PPAR-β/δ and PPAR-γ. *Future Cardiology*, *13*(3), 279–296.

Hayhurst, G. P., Lee, Y. H., Lambert, G., Ward, J. M., & Gonzalez, F. J. (2001). Hepatocyte nuclear factor 4alpha (nuclear receptor 2A1) is essential for maintenance of hepatic gene expression and lipid homeostasis. *Molecular and Cellular Biology*, *21*(4), 1393–1403.

Hogan, S. P., Seidu, L., Blanchard, C., Groschwitz, K., Mishra, A., Karow, M. L., Ahrens, R., Artis, D., Murphy, A. J., Valenzuela, D. M., Yancopoulos, G. D., & Rothenberg, M. E. (2006). Resistin-like molecule β regulates innate colonic function: Barrier integrity and inflammation susceptibility. *The Journal of Allergy and Clinical Immunology*, *118*(1), 257–268.

Inoue, Y., Hayhurst, G. P., Inoue, J., Mori, M., & Gonzalez, F. J. (2002). Defective ureagenesis in mice carrying a liver-specific disruption of hepatocyte nuclear factor 4alpha (HNF4alpha). HNF4alpha regulates ornithine transcarbamylase in vivo. *The Journal of Biological Chemistry*, *277*(28), 25257–25265.

Ko, H. L., Zhuo, Z., & Ren, E. C. (2019). HNF4α Combinatorial Isoform Heterodimers Activate Distinct Gene Targets that Differ from Their Corresponding Homodimers. *Cell Reports*, *26*(10), 2549–2557.e3.

Kumar, R., Priyadarshi, R. N., & Anand, U. (2020). Non-alcoholic Fatty Liver Disease: Growing Burden, Adverse Outcomes and Associations. *Journal of Clinical and Translational Hepatology*, *8*(1), 76–86.

Lautt, W. W., & Greenway, C. V. (1987). Conceptual review of the hepatic vascular bed. *Hepatology* , *7*(5), 952–963.

Lazarevich, N. L., & Fleishman, D. I. (2008). Tissue-specific transcription factors in progression of epithelial tumors. *Biochemistry. Biokhimiia*, *73*(5), 573–591.

Legouis, D., Faivre, A., Cippà, P. E., & de Seigneux, S. (2020). Renal gluconeogenesis: an underestimated role of the kidney in systemic glucose metabolism. *Nephrology, Dialysis, Transplantation: Official Publication of the European Dialysis and Transplant Association - European Renal Association*. https://doi.org/10.1093/ndt/gfaa302

Massarweh, N. N., & El-Serag, H. B. (2017). Epidemiology of Hepatocellular Carcinoma and Intrahepatic Cholangiocarcinoma. *Cancer Control: Journal of the Moffitt Cancer Center*, *24*(3), 1073274817729245.

Miura, A., Yamagata, K., Kakei, M., Hatakeyama, H., Takahashi, N., Fukui, K., Nammo,

T., Yoneda, K., Inoue, Y., Sladek, F. M., Magnuson, M. A., Kasai, H., Miyagawa, J., Gonzalez, F. J., & Shimomura, I. (2006). Hepatocyte nuclear factor-4alpha is essential for glucose-stimulated insulin secretion by pancreatic beta-cells. *The Journal of Biological Chemistry*, *281*(8), 5246–5257.

Moore, B. D., Khurana, S. S., Huh, W. J., & Mills, J. C. (2016). Hepatocyte nuclear factor 4α is required for cell differentiation and homeostasis in the adult mouse gastric epithelium. *American Journal of Physiology. Gastrointestinal and Liver Physiology*, *311*(2), G267–G275.

Myers, J. D., & Hickam, J. B. (1948). AN ESTIMATION OF THE HEPATIC BLOOD FLOW AND SPLANCHNIC OXYGEN CONSUMPTION IN HEART FAILURE. *The Journal of Clinical Investigation*, *27*(5), 620–627.

Nakhei, H., Lingott, A., Lemm, I., & Ryffel, G. U. (1998). An alternative splice variant of the tissue specific transcription factor HNF4alpha predominates in undifferentiated murine cell types. *Nucleic Acids Research*, *26*(2), 497–504.

Naugler, W. E., Sakurai, T., Kim, S., Maeda, S., Kim, K., Elsharkawy, A. M., & Karin, M. (2007). Gender disparity in liver cancer due to sex differences in MyD88-dependent IL-6 production. *Science*, *317*(5834), 121–124.

Nicolaides, N. C., Chrousos, G., & Kino, T. (2020). Glucocorticoid Receptor. In K. R. Feingold, B. Anawalt, A. Boyce, G. Chrousos, W. W. de Herder, K. Dhatariya, K. Dungan, J. M. Hershman, J. Hofland, S. Kalra, G. Kaltsas, C. Koch, P. Kopp, M. Korbonits, C. S. Kovacs, W. Kuohung, B. Laferrère, M. Levy, E. A. McGee, … D. P. Wilson (Eds.), *Endotext*. MDText.com, Inc.

Ning, B.-F., Ding, J., Yin, C., Zhong, W., Wu, K., Zeng, X., Yang, W., Chen, Y.-X., Zhang, J.-P., Zhang, X., Wang, H.-Y., & Xie, W.-F. (2010). Hepatocyte nuclear factor 4 alpha suppresses the development of hepatocellular carcinoma. *Cancer Research*, *70*(19), 7640–7651.

Oshima, T., Kawasaki, T., Ohashi, R., Hasegawa, G., Jiang, S., Umezu, H., Aoyagi, Y., Iwanari, H., Tanaka, T., Hamakubo, T., Kodama, T., & Naito, M. (2007). Downregulated P1 promoter-driven hepatocyte nuclear factor-4alpha expression in human colorectal carcinoma is a new prognostic factor against liver metastasis. *Pathology International*, *57*(2), 82–90.

Özkan, A., Stolley, D., Cressman, E. N. K., McMillin, M., DeMorrow, S., Yankeelov, T. E., & Rylander, M. N. (2020). The Influence of Chronic Liver Diseases on Hepatic Vasculature: A Liver-on-a-chip Review. *Micromachines*, *11*(5). https://doi.org/10.3390/mi11050487

Peeters, A., & Baes, M. (2010). Role of PPARα in Hepatic Carbohydrate Metabolism.

PPAR Research, *2010*. https://doi.org/10.1155/2010/572405

Rhee, J., Inoue, Y., Yoon, J. C., Puigserver, P., Fan, M., Gonzalez, F. J., & Spiegelman, B. M. (2003). Regulation of hepatic fasting response by PPARgamma coactivator-1alpha (PGC-1): requirement for hepatocyte nuclear factor 4alpha in gluconeogenesis. *Proceedings of the National Academy of Sciences of the United States of America*, *100*(7), 4012–4017.

Roche, J. (2018). The Epithelial-to-Mesenchymal Transition in Cancer. *Cancers*, *10*(2). https://doi.org/10.3390/cancers10020052

Ruse, M. D., Jr, Privalsky, M. L., & Sladek, F. M. (2002). Competitive cofactor recruitment by orphan receptor hepatocyte nuclear factor 4alpha1: modulation by the F domain. *Molecular and Cellular Biology*, *22*(6), 1626–1638.

Seydel, G. S., Kucukoglu, O., Altinbas, A., Demir, O. O., Yilmaz, S., Akkiz, H., Otan, E., Sowa, J.-P., & Canbay, A. (2016). Economic growth leads to increase of obesity and associated hepatocellular carcinoma in developing countries. *Annals of Hepatology*, *15*(5), 662–672.

Sladek, F. M. (2012). The yin and yang of proliferation and differentiation: cyclin D1 inhibits differentiation factors ChREBP and HNF4α [Review of *The yin and yang of proliferation and differentiation: cyclin D1 inhibits differentiation factors ChREBP and HNF4α*]. *Cell Cycle* , *11*(17), 3156–3157.

Sladek, F. M., Dallas-Yang, Q., & Nepomuceno, L. (1998). MODY1 mutation Q268X in hepatocyte nuclear factor 4alpha allows for dimerization in solution but causes abnormal subcellular localization. *Diabetes*, *47*(6), 985–990.

Sladek, F. M., Zhong, W. M., Lai, E., & Darnell, J. E., Jr. (1990). Liver-enriched transcription factor HNF-4 is a novel member of the steroid hormone receptor superfamily. *Genes & Development*, *4*(12B), 2353–2365.

Tanaka, T., Jiang, S., Hotta, H., Takano, K., Iwanari, H., Sumi, K., Daigo, K., Ohashi, R., Sugai, M., Ikegame, C., Umezu, H., Hirayama, Y., Midorikawa, Y., Hippo, Y., Watanabe, A., Uchiyama, Y., Hasegawa, G., Reid, P., Aburatani, H., … Kodama, T. (2006). Dysregulated expression of P1 and P2 promoter-driven hepatocyte nuclear factor-4alpha in the pathogenesis of human cancer. *The Journal of Pathology*, *208*(5), 662–672.

Torres-Padilla, M. E., Sladek, F. M., & Weiss, M. C. (2002). Developmentally regulated N-terminal variants of the nuclear receptor hepatocyte nuclear factor 4alpha mediate multiple interactions through coactivator and corepressor-histone deacetylase complexes. *The Journal of Biological Chemistry*, *277*(47), 44677–44687.

Vuong, L. M., Chellappa, K., Dhahbi, J. M., Deans, J. R., Fang, B., Bolotin, E., Titova, N. V., Hoverter, N. P., Spindler, S. R., Waterman, M. L., & Sladek, F. M. (2015). Differential Effects of Hepatocyte Nuclear Factor 4α Isoforms on Tumor Growth and T-Cell Factor 4/AP-1 Interactions in Human Colorectal Cancer Cells. *Molecular and Cellular Biology*, *35*(20), 3471–3490.

Wärnmark, A., Treuter, E., Wright, A. P. H., & Gustafsson, J.-A. (2003). Activation functions 1 and 2 of nuclear receptors: molecular strategies for transcriptional activation. *Molecular Endocrinology* , *17*(10), 1901–1909.

Wei, Y., Wang, Y. G., Jia, Y., Li, L., Yoon, J., Zhang, S., Wang, Z., Zhang, Y., Zhu, M., Sharma, T., Lin, Y.-H., Hsieh, M.-H., Albrecht, J. H., Le, P. T., Rosen, C. J., Wang, T., & Zhu, H. (2021). Liver homeostasis is maintained by midlobular zone 2 hepatocytes. Science, 371(6532). https://doi.org/10.1126/science.abb1625

Wisely, G. B., Miller, A. B., Davis, R. G., Thornquest, A. D., Jr, Johnson, R., Spitzer, T., Sefler, A., Shearer, B., Moore, J. T., Miller, A. B., Willson, T. M., & Williams, S. P. (2002). Hepatocyte nuclear factor 4 is a transcription factor that constitutively binds fatty acids. *Structure* , *10*(9), 1225–1234.

Wong, R. J., Cheung, R., & Ahmed, A. (2014). Nonalcoholic steatohepatitis is the most rapidly growing indication for liver transplantation in patients with hepatocellular carcinoma in the U.S. *Hepatology* , *59*(6), 2188–2195.

Xanthopoulos, K. G., Prezioso, V. R., Chen, W. S., Sladek, F. M., Cortese, R., & Darnell, J. E., Jr. (1991). The different tissue transcription patterns of genes for HNF-1, C/EBP, HNF-3, and HNF-4, protein factors that govern liver-specific transcription. *Proceedings of the National Academy of Sciences of the United States of America*, *88*(9), 3807–3811.

Xie, X., Liao, H., Dang, H., Pang, W., Guan, Y., Wang, X., Shyy, J. Y.-J., Zhu, Y., & Sladek, F. M. (2009). Down-regulation of hepatic HNF4alpha gene expression during hyperinsulinemia via SREBPs. *Molecular Endocrinology* , *23*(4), 434–443.

Yin, C., Lin, Y., Zhang, X., Chen, Y.-X., Zeng, X., Yue, H.-Y., Hou, J.-L., Deng, X., Zhang, J.-P., Han, Z.-G., & Xie, W.-F. (2008). Differentiation therapy of hepatocellular carcinoma in mice with recombinant adenovirus carrying hepatocyte nuclear factor-4alpha gene. *Hepatology* , *48*(5), 1528–1539.

Yoon, J. C., Puigserver, P., Chen, G., Donovan, J., Wu, Z., Rhee, J., Adelmant, G., Stafford, J., Kahn, C. R., Granner, D. K., Newgard, C. B., & Spiegelman, B. M. (2001). Control of hepatic gluconeogenesis through the transcriptional coactivator PGC-1. *Nature*, *413*(6852), 131–138.

Yuan, X., Ta, T. C., Lin, M., Evans, J. R., Dong, Y., Bolotin, E., Sherman, M. A.,

Forman, B. M., & Sladek, F. M. (2009). Identification of an endogenous ligand bound to a native orphan nuclear receptor. *PloS One*, *4*(5), e5609.

Yusuf, D., Butland, S. L., Swanson, M. I., Bolotin, E., Ticoll, A., Cheung, W. A., Zhang, X. Y. C., Dickman, C. T. D., Fulton, D. L., Lim, J. S., Schnabl, J. M., Ramos, O. H. P., Vasseur-Cognet, M., de Leeuw, C. N., Simpson, E. M., Ryffel, G. U., Lam, E. W.-F., Kist, R., Wilson, M. S. C., … Wasserman, W. W. (2012). The transcription factor encyclopedia. *Genome Biology*, *13*(3), R24.

CHAPTER 2: HNF4α Isoforms Regulate Carbohydrate and Lipid Metabolism in a Sex Specific Fashion; Potential role for AMPK?

ABSTRACT

Using previous RNA-seq data, it was determined that HNF4α exon-swap mice expressing P2-HNF4α (α7HMZ) significantly upregulate lipid metabolism and ketogenesis genes in response to a fast in comparison to exon-swap mice expressing P1-HNF4α (α1HMZ) which upregulate glucose metabolism and gluconeogenesis genes (Deans et al. 2021). Here, we show that the α7HMZ mice also have elevated ketone bodies in both the fed and fasted states, and do not survive a prolonged fast as well as WT or α1HMZ mice. AMP-activated protein kinase (AMPK) is known to be activated in response to a fast and has been shown to phosphorylate and decrease HNF4α levels. Using an acute AICAR injection, an AMPK activator, we show that all of the genotypes have decreased glucose, while the α7HMZ mice have significantly elevated ketone bodies compared to the other groups, though not necessarily in response to AICAR. Most interestingly, both exon swap mice develop seizures soon after the AICAR injection; more so in females compared to males. We propose this is due to an electrolyte imbalance and that HNF4α in the kidneys may play a role in this response. Some of the differential effects in the exon-swap mice may be due to AMPK preferentially phosphorylating P1-HNF4α and not phosphorylating P2-HNF4α. We show that acute AICAR treatment decreases P1-HNF4α in the α1HMZ mice. These data help elucidate the differential roles of the HNF4α isoforms in the liver.

INTRODUCTION

Intermittent Fasting:

During an intermittent fast, food is restricted anywhere from 12 hours to days. Intermittent fasting has gained popularity in recent years, although it has been practiced annually by Muslims during the holy month of Ramadan for centuries. During this month, food and drink is restricted from dawn until sunset (Lessan & Ali, 2019). Due to Ramadan and the growing popularity of 16 to 24-hr intermittent fasting, many scientists have examined the effects of these fasts on different aspects of metabolism (Cherif et al., 2016; Maughan et al., 2010; V & Zargar, 2017). Intermittent fasting seems to be effective in treating obesity and type-2 diabetes (Grajower & Horne, 2019; V & Zargar, 2017; Zubrzycki et al., 2018). Obesity increases the risk for type-2 diabetes and, moreover, is accompanied by an increase in metabolic syndrome which increases the risk of heart disease, diabetes and stroke.

Intermittent fasting can take many forms, including alternating fasted and *ad libitum* feeding days, periodic fasting or fasting one or two days a week, and time-restricted feeding which involves only eating during a defined time period, usually three to 12 hours a day (Zubrzycki et al., 2018). All of these induce a metabolic shift from lipid storage to lipid mobilization, which is typically triggered 12 to 36 hours after the last meal which corresponds to the time when glycogen stores in the liver become depleted. Although many studies differ in the methods for the intermittent fast, most show a decrease in body weight (Zubrzycki et al., 2018). Interestingly, they also show that intermittent fasting compared to

continuous energy restriction does not result in a decrease in metabolic rate which is usually associated with weight gain.

Intermittent fasting has also been shown to lower the risk of cardiovascular disease by lowering plasma lipids, LDL cholesterol, and hypertension. Many studies have examined the effects of intermittent fasting on glycemia. Interestingly, even without weight loss, intermittent fasting resulted in a decrease in blood glucose levels, hemoglobin glycosylation (HbA1c), and insulin resistance (Zubrzycki et al., 2018).

Keto Diet

The "Keto Diet" was first invented in the 1920's after determining that the benefits of fasting on childhood epilepsy could be mimicked using a low-carbohydrate and high-fat diet to induce ketogenesis (Sampaio, 2016; Wheless, 2008). Moreover, the diet was found to be more sustainable than mere fasting. With the introduction of effective antiepileptic drugs, the use of the ketogenic diet diminished (Sampaio, 2016; Wheless, 2008). This was until it was featured on a popular television show in the 1990's as the treatment that cured a seizure-stricken child (Wheless, 2008). It was observed that the diet resulted in an increased fat burn and better serum lipid profile, leading to its adoption as a mainstream weight loss diet.

Recently, the ketogenic diet has gained popularity and has led to the rise of "Keto-Friendly" recipes, menu items, and even full restaurants. Many studies began looking at the effects of the ketogenic diet on obesity and diabetes. A non-randomized clinical trial examining the effect of diet on type-2 diabetes found that the low-carb, high-fat diet induced beta-hydroxybutyrate levels between 0.4 and 0.6 mmol/L which corresponded to

roughly 10-15% weight loss. Moreover, triglycerides, small dense low-density lipoprotein (LDL) particle count and HbA1c levels decreased while high density lipoprotein (HDL) increased (O'Neill & Raggi, 2020). Despite the beneficial health aspects of the ketogenic diet, there are some caveats. Like many other diet trends, the diet needs to be maintained to realize sustainable weight loss and can lead to a regain of weight upon the termination of the diet and reintroduction of carbohydrates. The ketogenic diet has been shown to significantly increase both HDL and LDL cholesterol levels, the latter of which is associated with an increased risk of coronary heart disease. Additionally, there are limitations to the study that demonstrated the benefits of the ketogenic diet on type-2 diabetes: it was a non-randomized study and required extra resources to those on the ketogenic diet, such as extra equipment to measure vitals including a ketone meter, digital scale, blood pressure machine, and access to health coaches and medical providers on a web-based application (O'Neill & Raggi, 2020).

In the general population, most people who are adopting the ketogenic diet are not monitoring their ketone levels and, especially for those with type-2 diabetes, can quickly reach detrimental blood ketone levels leading to ketoacidosis. Ketoacidosis leads to the decrease in blood pH which decreases the efficacy of oxygen delivery by hemoglobin molecules and can lead to organ damage. A case-study notes that although non-diabetic ketoacidosis is rare, a lactating woman who adopted the ketogenic diet was admitted to the hospital with a blood pH of 7.2 and ketone levels of 7.1 mmol/L, she was given glucose as well as low levels of insulin to control and reverse her ketosis (von Geijer & Ekelund, 2015).

Metabolic sexual dimorphism

One of the main factors that influence metabolism is sex. It has been long observed that males and females differ with respect to their fat storage and mobility, and thus their predisposition to obesity, coronary heart disease, and type-2 diabetes. Animal studies that aimed to control for non-biological factors, found that the sexes differ in their propensity to developing obesity and this difference could be directly due to the sex hormones. Female mice gained less weight on a high-fat diet compared to males, and this was reverted by ovariectomy (Palmer & Clegg, 2015). It is thought that estrogens decrease obesity by decreasing appetite and increasing energy expenditure (Palmer & Clegg, 2015).

The fat distribution between males and females differs greatly. Males tend to store visceral fat leading to accumulation of fat in the midsection and an "apple body shape" or android pattern of adipose accumulation. Females, conversely, tend to store fat subcutaneously, mainly in the hips, thighs and buttocks, resulting in a "pear body shape" or gynoid pattern of adipose accumulation (Palmer & Clegg, 2015). The differences in fat accumulation seem to be attributed to estrogen receptor distribution. Total body estrogen receptor α (ERα) knockout mice have increased adiposity and increased visceral fat compared to wildtype (Palmer & Clegg, 2015). Moreover, the ratio of ERα/ERβ plays a role in the determination of fat accumulation, a higher ratio like that in visceral fat limits fat accumulation.

Women and men have a documented difference in lipid mobilization and lipid metabolism in general. This could be due to differences not only in adipose distribution, but also in insulin sensitivity between the sexes. In response to a fast, women have

significantly higher levels of both plasma fatty acids and ketone bodies suggesting an increased mobilization of fatty acids from adipose tissue in females than in males (Mittendorfer, 2005). Additionally, females in a fed state have higher levels of circulating ketone bodies compared to males, also likely due to differences in sex hormones. The estrogen pathway has also been implicated in affecting certain metabolic pathways by activating AMP-activated protein kinase (Lipovka & Konhilas, 2014). This could also explain why women have more circulating lipids as their hormones may put them closer to a fasted state.

AMP-Activated Protein Kinase and HNF4α

Metabolism is an intricate process that is controlled hormonally, transcriptionally, and most rapidly post-transcriptionally. One of the major players in post-transcriptional modification in response to fasting is AMP-activated protein kinase (AMPK). AMPK is a promiscuous serine/threonine heterotrimeric kinase made up of the catalytic α subunit and the two regulatory β and γ subunits. Vertebrates have multiple isoforms for each subunit, in humans there are two α isoforms, α1 and α2, encoded by the *PRKAA1* and *PRKAA2* genes, respectively. The β1 and β2 isoforms are encoded by the *PRKAB1* and *PRKAB2* genes, and the γ1, γ2, and γ3 subunits are encoded by the *PRKAG1*, *PRKAG2*, and *PRKAG3* genes, respectively. These isoforms can combine to create twelve distinct AMPK complexes, though functional differences between the complexes have yet to be elucidated (Herzig & Shaw, 2018). AMPK senses low energy levels by binding adenine nucleotides (AMP/ATP) in the γ subunits and based on that ratio will be activated when AMP levels

are elevated. In addition to fasting and a low glucose state, AMP levels will be elevated in a low oxygen state and during mitochondrial dysfunction.

AMPK is an important target for type-2 diabetes treatment. The most prescribed diabetes medication in the United States is Metformin. This compound enters the mitochondria and inhibits the electron transport chain. This results in a decrease in ATP production and thus an increase in the AMP:ATP ratio in the cell. This decrease in the AMP:ATP ratio triggers the cells to uptake glucose and results in decreased glucose levels, making Metformin an effective drug to treat diabetes. Another AMPK activator that is prominently used in experimental rodent models is the AMP analog AICAR, 5′-aminoimidazol-4-carboxoxamide 1-β-d-ribofuranoside. AICAR activates AMPK much like Metformin although AICAR directly binds AMPK and activates it.

Upon activation, AMPK phosphorylates many target proteins to upregulate catabolic and downregulate anabolic pathways. One of the direct targets of AMPK is HNF4α (Hong et al., 2003). HNF4α is mutated in maturity onset diabetes of the young 1 (MODY1) which is a rare form of type-2 diabetes. MODY1 mutations decrease the ability of the pancreas to effectively release insulin in response to glucose levels (Sladek et al., 1998). Because AMPK and HNF4α are found on the same pathways, the possibility of a direct interaction was explored. Using an *in vitro* phosphorylation assay, it was found that P1-HNF4α was phosphorylated on Serine-304 in the ligand binding domain. Additionally, an N-terminal phosphorylation was found, although this site was not further explored

(Hong et al., 2003). This site is noteworthy as it is in the differential region between the P1- and P2-HNF4α isoforms (Figure 2.1).

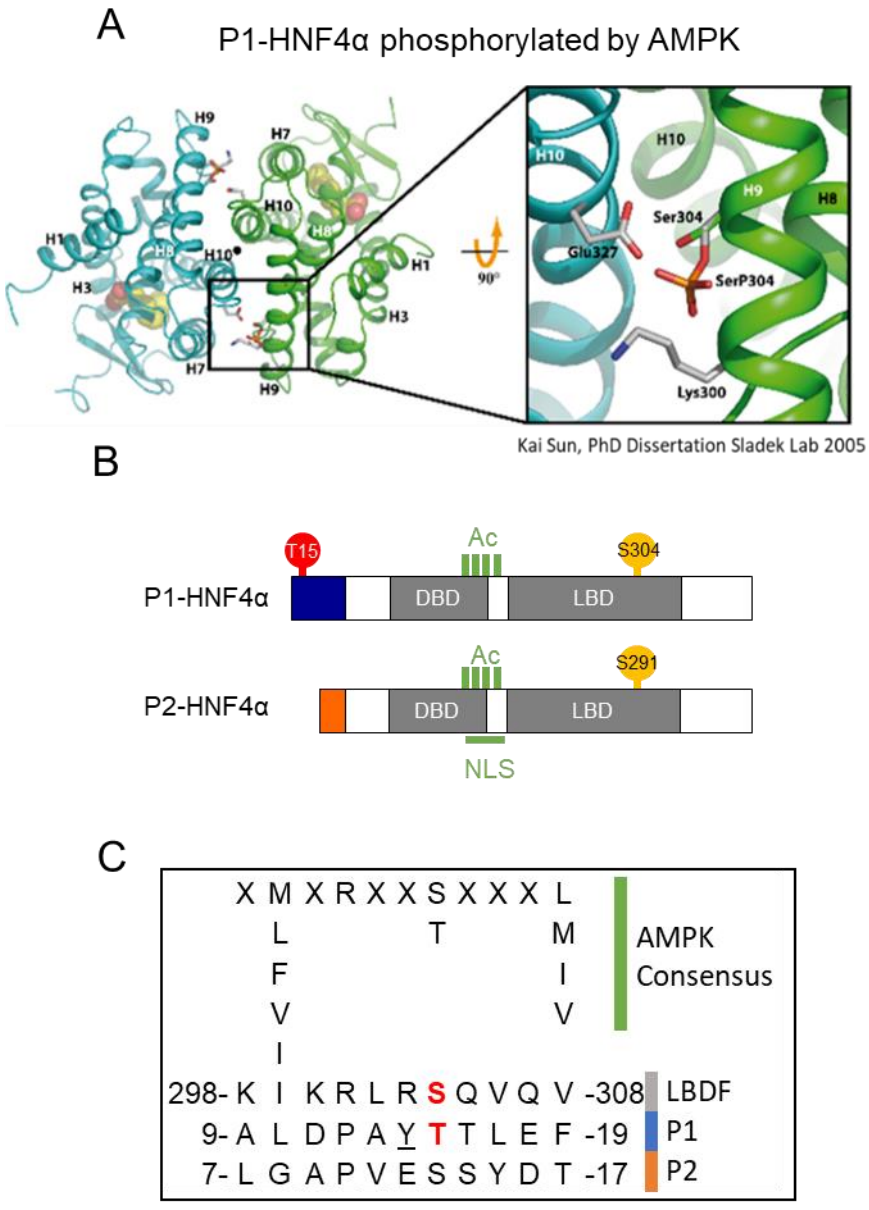

Figure 2. 1 P1- but not P2-HNF4α has been shown to be phosphorylated by AMPK.

A) Ribbon diagram of the ligand binding domain of HNF4α showing the effect of phosphorylation of S304. B) depiction of the isoforms of HNF4α and the location of S304 along with T15 in the NTD of P1-HNF4α along with the Acetylation (Ac) sites overlapping with the Nuclear Localization Signal (NLS). C) AMPK consensus site. The N-terminal domain (NTD) of HNF4α1 is phosphorylated in vitro by AMPK. HNF4α7 NTD is a poorer target and has not been examined. Y14 is underlined.

MATERIALS AND METHODS

Animal Model

Adult male and female wildtype (WT), α1HMZ, and α7HMZ mice in either a 192/Sv and C57BL6 mixed background (Briançon & Weiss, 2006) or a pure C57BL6/N background (backcrossed 10+ generations) were kept in either a non-barrier or specific pathogen free (SPF) barrier facility. Mice were fed a standard lab chow (LabDiet, #5001, St. Louis, MO). All mice were fed ad libitum, unless fasted or being entrained, and kept in 12-hr light/dark conditions and euthanized by CO_2 asphyxiation followed by tissue harvest at the indicated time points. Care and treatment of the animals were in strict accordance with guidelines from the Institutional Animal Care and Use Committee at the University of California, Riverside.

Prolonged Fast

WT, α1HMZ, and α7HMZ ~20-week-old male mice maintained in a non-barrier facility, were placed on Sani-Chip (woodchip) bedding and food was removed at T=0. Mice were kept in original housing arrangement and were not singly housed. Afterwards glucose was measured with a One Touch® Ultra®2 meter and either One Touch® Ultra® Blue Test Strips or GenUltimate! Test Strips (Cat#100-50) using blood from a tail vein nick. Body weight was measured at the same time as the blood glucose. The mice were harvested and blood was collected via the inferior vena cava. Blood was allowed to coagulate on ice for 30 min and the samples were spun at 10,000 x g for 5 min at 4°C. Serum was removed and stored at 20°C. Ketone bodies were measured using the Cayman Chemical β-Hydroxybutyrate (Ketone Body) Colorimetric Assay Kit (Cat#700190). Subsequent

experiments were done on female WT (3-4 month) mice maintained in SPF barrier facility. Ketone bodies were measured using blood from a tail vein nick and the Precision Xtra® Blood Glucose & Ketone Monitoring System with Abbott Blood β Ketone Test Strips.

Altered Feeding

Male and female mice were housed in a non-barrier facility on Sani-Chip bedding. At zeitgeber time (ZT) 0 (8 AM), food was removed from the cage, and at ZT12 (8 PM) fresh food was added to the cage. This was repeated daily (7 days a week) for two weeks. After two weeks, food was removed at ZT0 and at different time points, glucose and ketone bodies were measured via tail bleeds and a glucose or ketone body meter as described above. At ZT14, food was returned to the cage. Mice were allowed to recover for at least two weeks before repeating any measurements.

Glucose Tolerance and Insulin Tolerance Tests

For the glucose tolerance test (GTT), WT, α1HMZ, and α7HMZ male and female mice (three to seven months old) housed in a non-barrier facility were weighed and singly housed on Sani-Chip bedding and fasted for 5 hours starting at 8 AM on the morning of the experiment (ZT0). At 1 PM (ZT5) blood glucose levels were measured using the One Touch® Ultra®2 meter and One Touch® Ultra® Blue Test Strips. After the T=0 reading, mice were administered 1.0 g/kg D-glucose using a 10% glucose solution (Sigma Aldrich, Cat# G8270) via intraperitoneal (IP) injection using a 31-gauge insulin syringe. Glucose levels were measured at 15-, 30-, 60-, and 120-minutes post injection using blood from a tail vein nick at the tip of the tail. For the insulin tolerance test (ITT), the mice were treated exactly the same as the GTT but were injected with 1 U/kg of Humulin (Eli Lilly) and

glucose levels were measured at the same time points as above. A syringe of 10% glucose was kept on-hand in case mice became hypoglycemic (below 40 mg/dL) and was administered at 1.0 g/kg via IP injection.

Liver RNAseq and Serum metabolomics analysis

WT and α7HMZ males from mixed background mice, 16 to 20 weeks old, were harvested at 10:30am (ZT3.5), 1:30pm (ZT 6.5), or 8:30pm (ZT 13.5). Mice harvested at ZT3.5 were either fed or fasted for 12 hours overnight (from 10:30pm (ZT15.5) to 10:30am (ZT3.5). There was an N of three per group. RNAseq and metabolomics were performed as previously described in Deans et al. 2021.

AICAR Time Course

WT, α1HMZ, and α7HMZ male and female mice housed in an SPF barrier facility were weighed and individually housed in cages with Sani-Chip bedding. Mice were fasted for two hours before treatment with AICAR. 50 mg/mL AICAR solution was prepared in 0.9% saline. The AICAR solution was warmed to 37^0 C and agitated for one hour. Baseline glucose and ketone body levels were measured from tail bleeds as described above. Mice were injected with 10% of their body weight of AICAR solution for a final dose of 500mg/kg (Bumpus et al. 2011) (Halseth et al. 2002). Glucose and ketone bodies were measured at different time intervals as indicated in the figures. At the end of the experiment, mice were housed with original cage-mates and were given hydrogels, and food directly on the bedding.

Western Blot Analysis

Protein extracts were separated by 10% sodium dodecyl sulfate-polyacrylamide gel electrophoresis (SDS-PAGE) and transferred to polyvinylidene difluoride (PVDF) membrane (Immobilon, Millipore) as previously described (Maeda et al., 2002). Signals were detected using the SuperSignal West Dura extended-duration substrate kit (Thermo Fisher Scientific). A Bradford assay (Bio-Rad) was used to measure the protein concentration. 8-10 μg nuclear extracts (NE) (Jiang et al., 1995) were loaded per lane. Coomassie staining of the blot verified equal loading of protein. The primary antibodies (Abs) were mouse monoclonal anti-HNF4α P1/P2 (R&D Systems, catalog no. PP-H1415-00), which recognize the C terminus of both the P1- and P2-HNF4α isoforms; monoclonal anti-HNF4α P1 and P2 (catalog no. PP-K9218-00 and PP-H6939-00, respectively, R&D Systems), which recognize the N terminus of HNF4α. The secondary Abs were horseradish peroxidase (HRP)-conjugated goat anti-mouse (GαM-HRP) Abs (Abcam).

Statistical Analysis

Data are presented as means ± standard error of means. One-way ANOVA with Tukey's post-hoc analysis (GraphPad Prism version 9, GraphPad Software, La Jolla, CA USA) was used to test for differences between groups. Student's *t*-test was used when comparing two conditions. Statistical significance for all data was set at $P \leq 0.05$.

RESULTS

Role of HNF4α isoforms in glucose/insulin pathway

Glucose and insulin tolerance tests (GTT and ITT, respectively) were performed on WT and HNF4α exon-swap mice. WT and α7HMZ males had lower glucose tolerance compared to females as evidenced by smaller area under the curve (AUC) (Figure 2.2A, B). When comparing the two genotypes, α7HMZ females had significantly more glucose tolerance compared to WT females (Figure 2.2C). Although the males of the different genotypes trended in a similar fashion, the difference was not significant (Figure 2.2D).

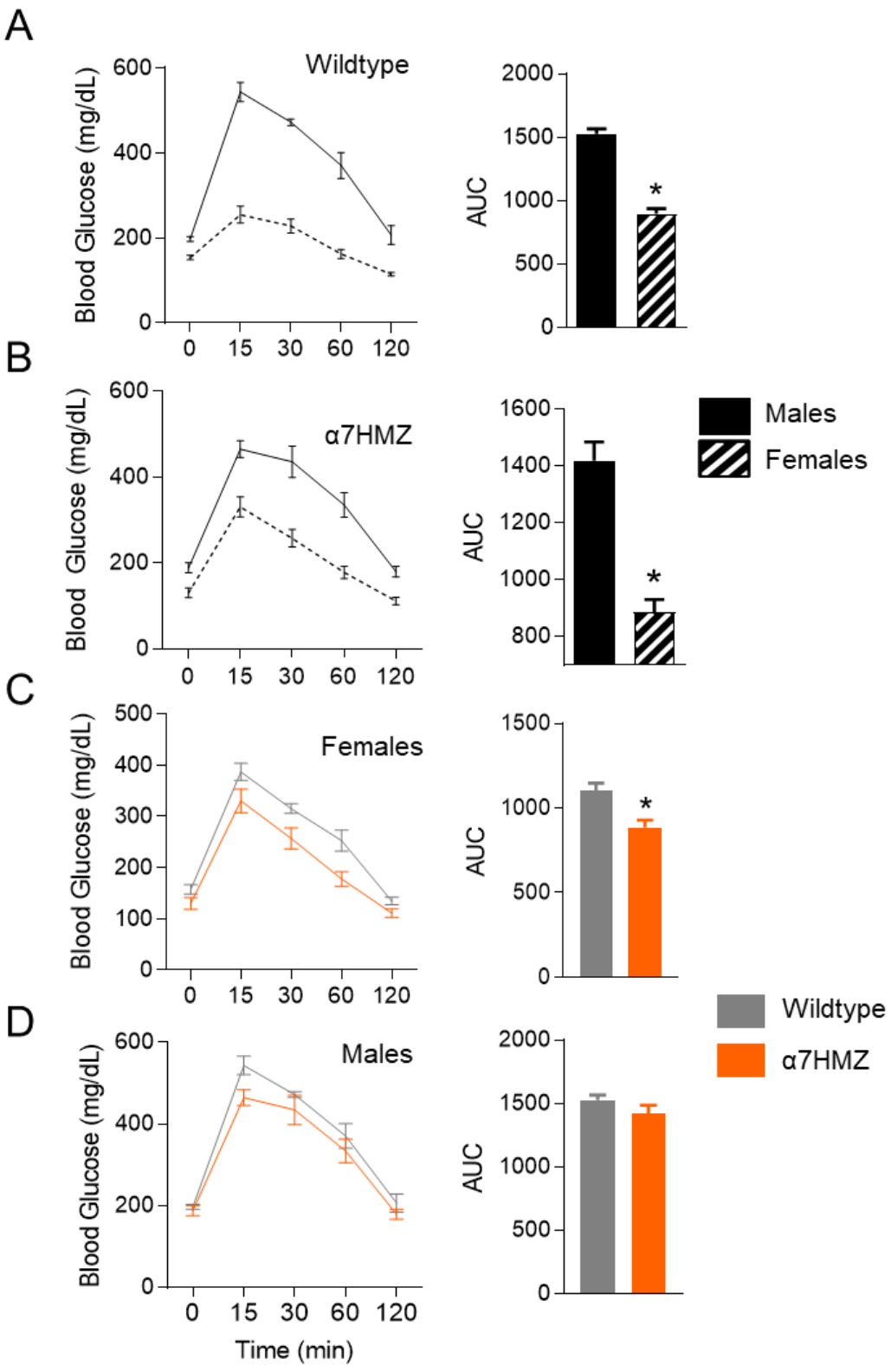
A
Wildtype
Blood Glucose (mg/dL)
600
400
200
0
0 15 30 60 120
AUC
2000
1500
1000
500
0
*
B
α7HMZ
Blood Glucose (mg/dL)
600
400
200
0
0 15 30 60 120
AUC
1600
1400
1200
1000
800
*
Males
Females
C
Females
Blood Glucose (mg/dL)
500
400
300
200
100
0
0 15 30 60 120
AUC
1500
1000
500
0
*
D
Males
Blood Glucose (mg/dL)
600
400
200
0
0 15 30 60 120
Time (min)
AUC
2000
1500
1000
500
0
Wildtype
α7HMZ

Figure 2. 2 Characterization of glucose tolerance in wildtype and α7HMZ male and female mice.

Glucose tolerance test (GTT) and Area Under the Curve (AUC) of A) Wildtype male (n=6, 6 months) and female (n=7, 3 months) mice. B) α7HMZ males (n=5, 7 months) and females (n=5, 7 months). C, D) Comparison of wildtype and α7HMZ mice. T=0 is blood glucose post 5-hr fast prior to glucose injection. * $p<0.05$ Student's T-Test.

While there was no difference in insulin sensitivity between males and females in WT mice (Figure 2.3A), the α7HMZ females were significantly more sensitive to insulin than the α7HMZ males (Figure 2.3B). When comparing the females of both genotypes, the α7HMZ females were significantly more insulin sensitive compared to the WT females (Figure 2.3C). In fact, four of the five α7HMZ females had to be removed from the experiment due to severely low glucose levels after the 30-minute time point. While the male mice trended in a similar fashion, there was no significant difference between the two genotypes (Figure 2.3 D).

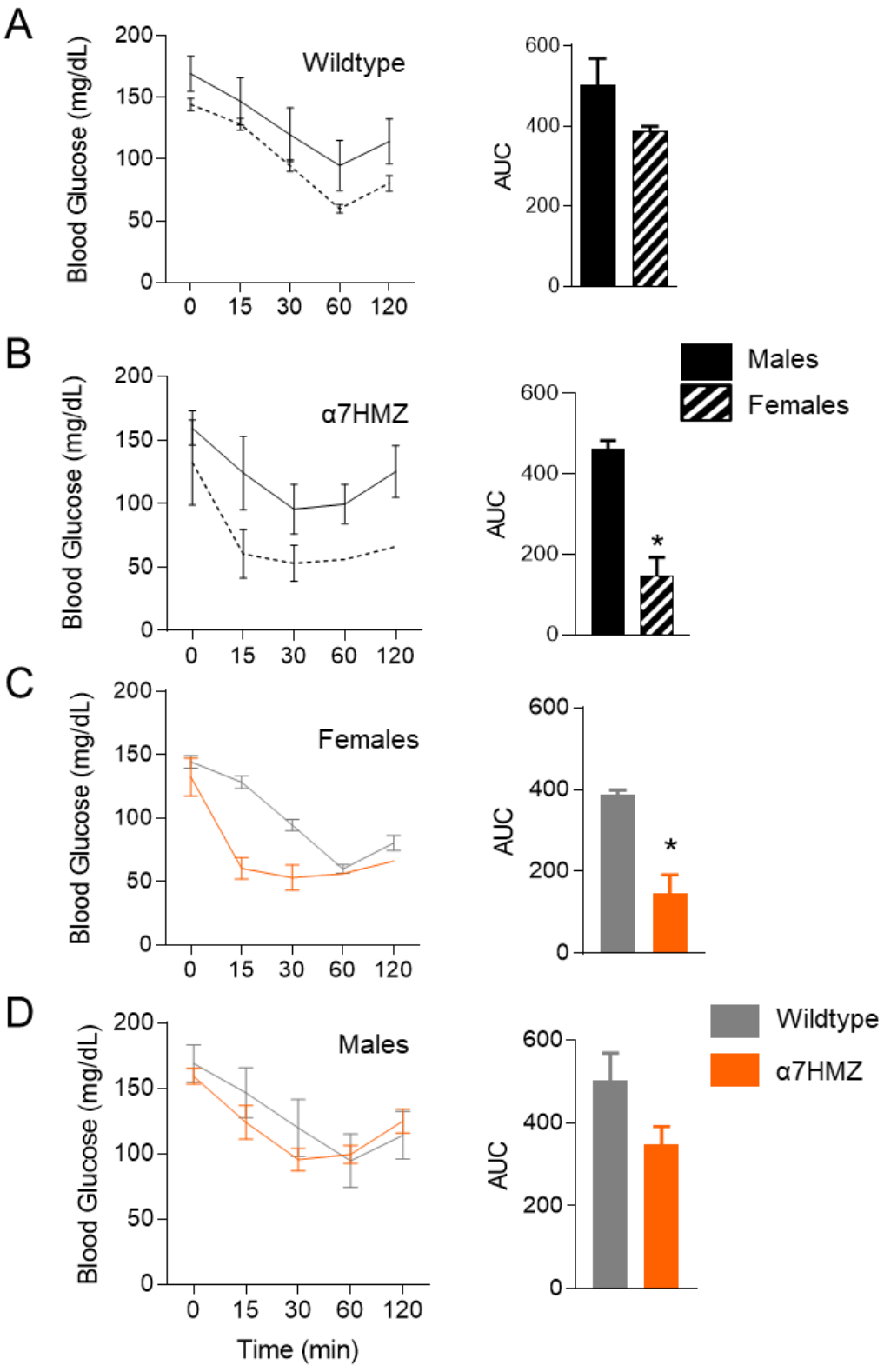
A
Blood Glucose (mg/dL)
200
150
100
50
0
Wildtype
0
15
30
60
120
AUC
600
400
200
0
B
Blood Glucose (mg/dL)
α7HMZ
Males
Females
AUC
*
C
Blood Glucose (mg/dL)
Females
AUC
*
D
Blood Glucose (mg/dL)
Males
Wildtype
α7HMZ
AUC
Time (min)

Figure 2. 3 Characterization of insulin tolerance of wildtype and α7HMZ male and female mice.

Insulin tolerance test (ITT) and Area Under the Curve (AUC) of A) WT male (n=6, 6 months) and female (n=8, 3 months) mice; B) α7HMZ males (n=5, 7 months) and females (n=5, 7 months); and C, D) Comparison of wildtype and α7HMZ mice. B,C) Female α7HMZ mice were removed for severe hypoglycemia, T=30 n=3, T=60 and 120 n=1. T=0, blood glucose post 5-hr fast prior to insulin injection. * $p<0.05$ Student's T-Test.

When the α1HMZ males were analyzed and compared to the other groups, there was no significant difference between the glucose tolerance in any of the genotypes (Figure 2.4A). Conversely, the α1HMZ males had significantly more insulin resistance compared to the α7HMZ males (Figure 2.4B). Comparing the body weight of the males and females from all three genotypes used in the GTT and ITT experiments, the WT females weighed significantly less than all other groups (Figure 2.5). That being said, they were the youngest mice tested which could account for that difference.

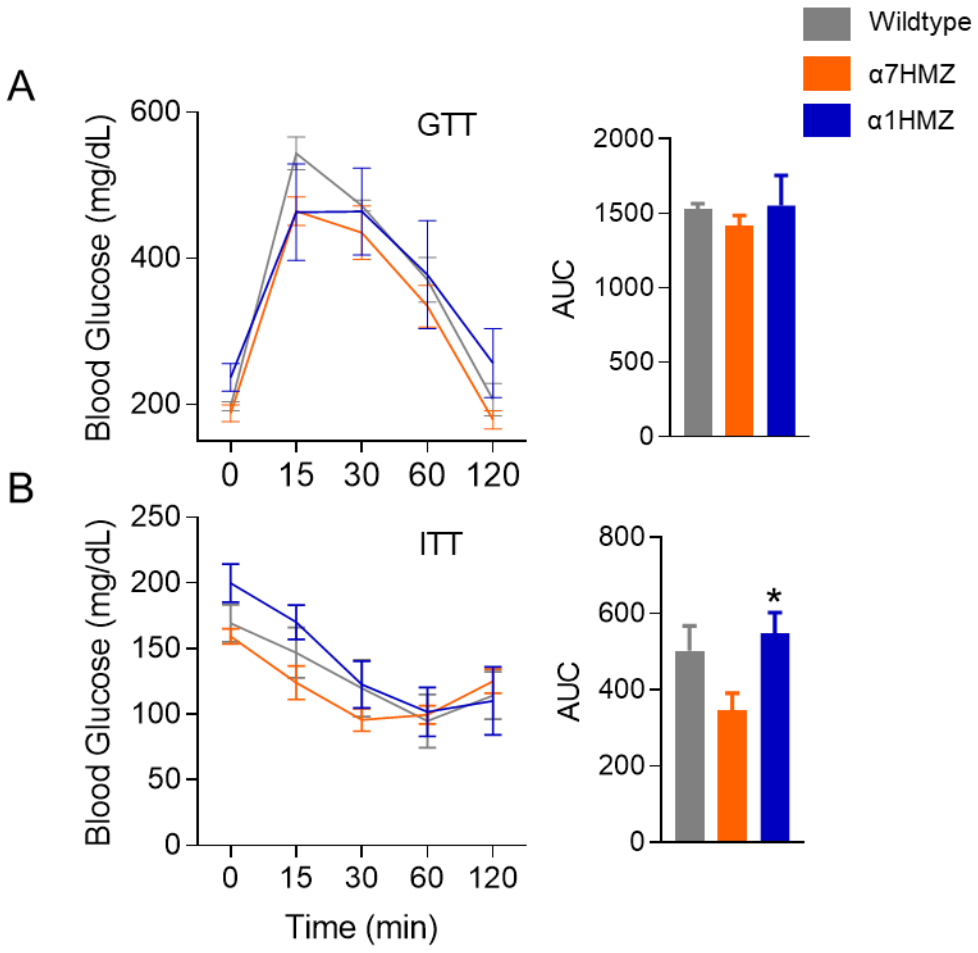

Figure 2. 4 α1HMZ male mice have more insulin tolerance compared to wildtype and α7HMZ male mice.

Wildtype male (n=6, 6 months), α7HMZ males (n=5, 7 months), and α1HMZ males (n= 4, 6 months) A) GTT and area under the curve. B) ITT and area under the curve. * $p<0.05$ Student's T-Test α1HMZ v α7HMZ.

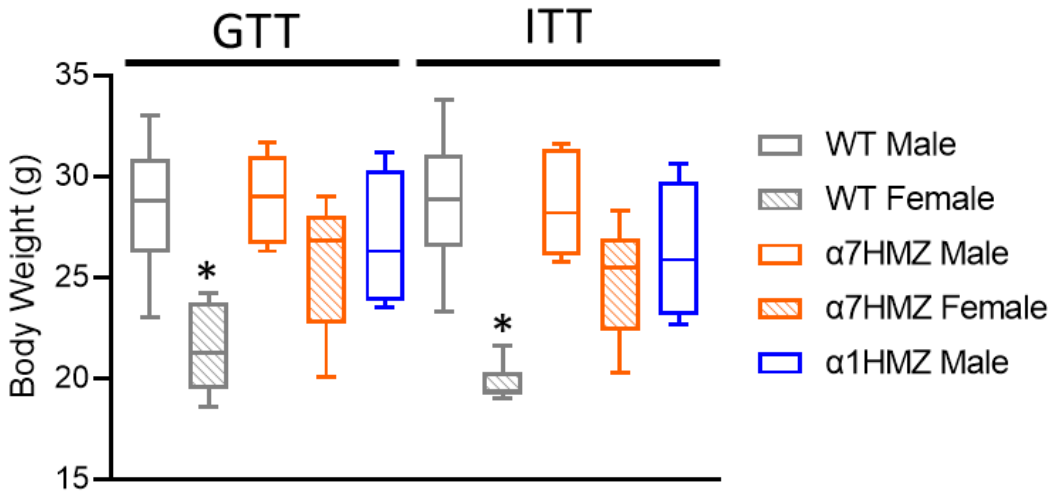

Figure 2. 5 Body weight comparison of mice used in GTT/ITT studies showing wildtype females have significantly lower body weight than other groups.

See figures 2.2-2.4 for n numbers and ages. Body weight taken post 5-hr fast. * $p<0.05$ vs all other groups in GTT or ITT, Student's T-test

Role of HNF4α isoforms in the fasting response

To further investigate the differences in the metabolic profiles of the mice revealed by the GTT and ITT assays, we utilized RNAseq to examine the expression profiles of WT and α7HMZ male mice in a fed and fasted state. RNAseq analysis of the livers of 16- to 20-week-old WT and α7HMZ male mice was used to examine the effect of different HNF4α isoforms on hepatic gene expression. Comparing the differential expressed genes (DEGs) between the fed and 12-hour fasted state at 10:30 AM (ZT3.5), the WT mice had 1746 DEGs unique to them, and the α7HMZ had 795 unique DEGs. There was a 1044-gene overlap between the genotypes in the fed versus fasted comparison (Figure 2.6A). The α7HMZ males had fewer DEGs compared to WT males between the fed and fasted state (Figure 2.6A), suggesting the α7HMZ mice are closer to a fasted state when they are normally fed as fewer genes change in response to the fast. Examining the key gluconeogenic gene, *Pck1*, the WT fasted livers had significantly higher expression of *Pck1* compared to the α7HMZ livers. Conversely, examining the key ketogenic gene, *Hmgcs2*, the α7HMZ livers have higher expression in both the fed and fasted state compared to the WT mice (Figure 2.6B). Using metabolic analysis, the α7HMZ males had significantly lower glucose, pyruvate, and citrate, and significantly higher β-hydroxybutyrate (βHB) serum levels compared to WT. Moreover, oxaloacetate levels trended down in α7HMZ mice, however they were not significant (Figure 2.6C). These results suggest that the α7HMZ male mice are in a more ketogenic state than the WT males. Looking at fatty acid metabolism genes, α7HMZ fasted mice, red arrow, had the highest expression in most of the fatty acid metabolism genes both in the fed and fasted state compared to WT (Figure

2.6D). This shows the α7HMZ mice favor fatty acid metabolism both normally and in a fasted state compared to WT mice.

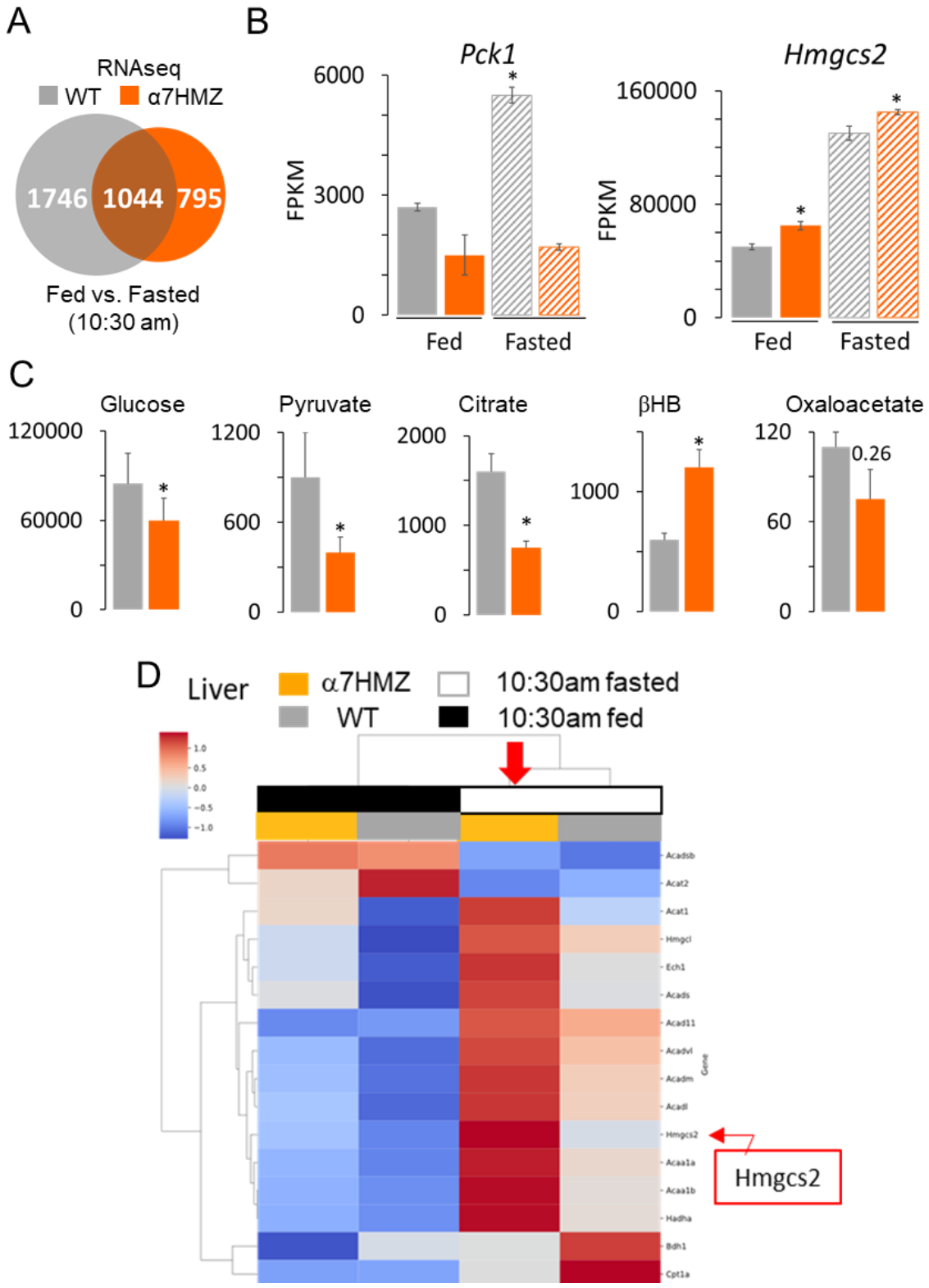
A
RNAseq
WT
α7HMZ
1746
1044
795
Fed vs. Fasted
(10:30 am)
B
Pck1
Hmgcs2
FPKM
6000
3000
0
160000
80000
0
Fed
Fasted
C
Glucose
Pyruvate
Citrate
βHB
Oxaloacetate
120000
60000
0
1200
600
2000
1000
1000
120
60
0.26
D
Liver
α7HMZ
WT
10:30am fasted
10:30am fed
Acadsb
Acat2
Acat1
Hmgcl
Ech1
Acads
Acad11
Acadvl
Acadm
Acadl
Hmgcs2
Acaa1a
Acaa1b
Hadha
Bdh1
Cpt1a
Gene
Hmgcs2

Figure 2. 6 α7HMZ adult male mice favor a ketogenic state compared to wildtype mice

Orange: α7HMZ (solid, fed; hatched, fasted). Grey: Wildtype (solid, fed; hatched, fasted). A, B) RNA sequencing (n=3). C) Liver metabolomics performed circa 10:30 am in fed mice (n=7), Y-axis is peak height, βHB = β-Hydroxybutyrate, * $p<0.05$ Student's T-test. Data from (Deans et al. 2021), D) significant differences in fat metabolism genes between wildtype and α7HMZ fasted (12 hours) male mice (n=3, 16-20 weeks). Gene catalyzing the committed step in ketone body synthesis is highlighted, Hmgcs2. Heat map created by J. Lomeli

Since α7HMZ mice had altered levels of expression of two key genes in the fed and fasted state compared to WT males, we hypothesized that α7HMZ mice were in a fasted-like state even in the fed condition and hence might survive a prolonged fast better than WT or α1HMZ mice. To address this, male mice of all three genotypes were subjected to a prolonged fast for 72 hours. During that time, glucose levels were monitored using tail vein bleeds. The glucose levels of all three genotypes cycled throughout the fast, with the α1HMZ having significantly higher glucose levels compared to the α7HMZ 48 hours into the fast. Additionally, the α1HMZ mice had higher glucose levels 12 hours after they were refed at 72 hours (Figure 2.7A). α1HMZ mice also had significantly higher blood glucose levels in a fed state compared to the other two genotypes (Figure 2.7B). Most notably, half of the α7HMZ mice died 60 hours into the fast. The mice from the other two genotypes survived the entire fast and completely recovered (Figure 2.7C). The surviving mice were harvested and blood was collected to examine serum βHB levels: the α7HMZ mice had significantly higher βHB levels compared to the other two genotypes (4.2 vs 2.5 to 3.0 mM for WT and α1HMZ) (Figure 2.7D).

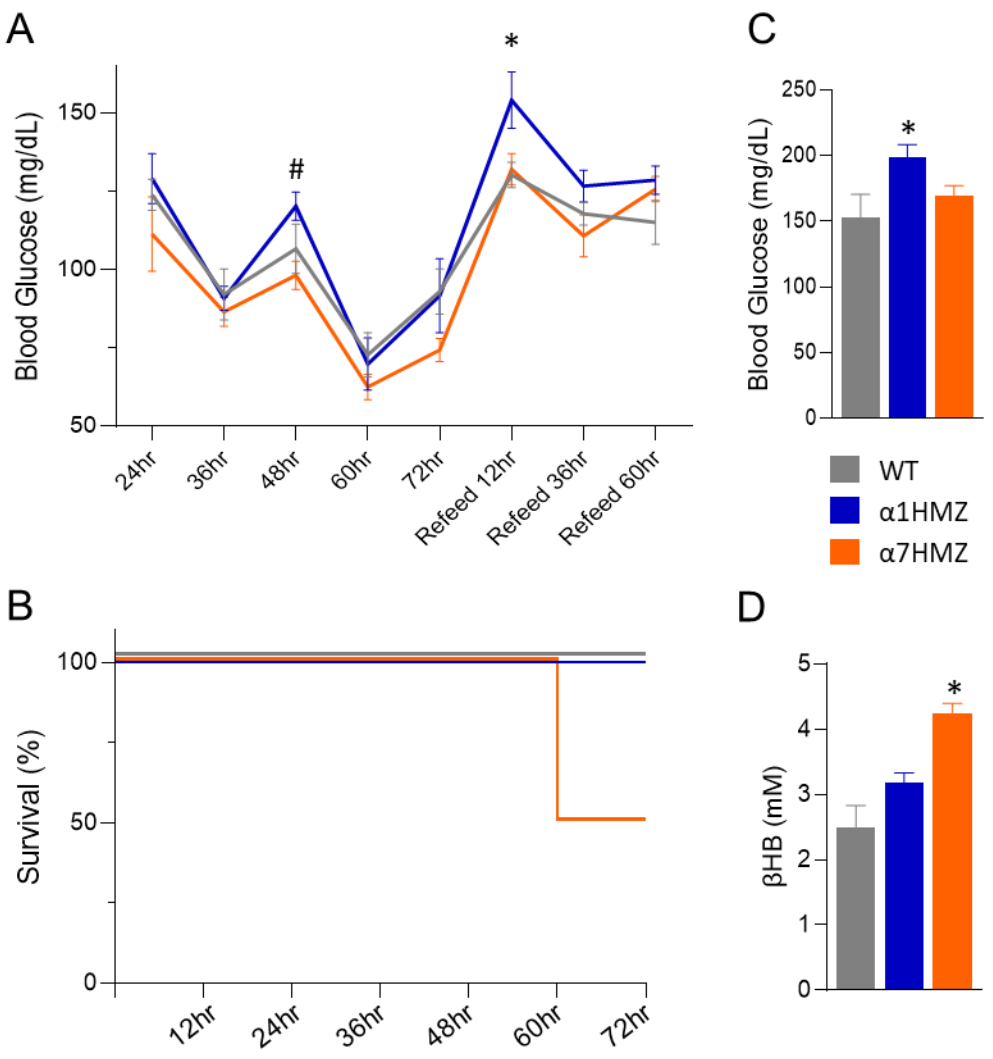

Figure 2. 7 Exposure of exon swap mice to Extreme fast

showing A) α1HMZ males with elevated glucose compared to wildtype and α7HMZ at 48-hr fast and 12-hr after re-feed (n=6-10) and B) α7HMZ males dying before the completion of the fast. C) Glucose levels in a fed state 7pm (n=4-6). * $p<0.05$ α7HMZ v. α1HMZ, # $p<0.05$ α1HMZ v. Wildtype, Student's T-test. D) Surviving α7HMZ males have higher βHB = β-hydroxybutyrate post 60-hr fast, serum levels (n=3-5) *$p<0.05$ α7HMZ vs both wildtype and α1HMZ, Student's T-test

Next, we examined the effects of time-restricted feeding on male and female mice of all three genotypes. To do so, we subjected the mice to intermittent fasting by removing their food from ZT0 to ZT12, restricting their feeding to ZT12 to ZT0 when they normally are active and feeding. To avoid any light-driven circadian effects, we analyzed the ketone body levels of the mice one hour before any light change occurred during the fed and fasted states. For the fed state, the mice were examined at ZT23 an hour before the lights came on and the food was removed. For the fasted state, the mice were examined at ZT11, an hour before the lights shut off and the mice were given food. As anticipated, the βHB levels of the mice were lower in the fed state compared to the fasted state (Figure 2.8A). Importantly at ZT11, the WT and α7HMZ females had significantly higher βHB levels compared to the α1HMZ females. Additionally, in the fed state, the α7HMZ females had significantly higher βHB compared to the α1HMZ (Figure 2.8A). The WT males also had significantly lower βHB levels in the fed state compared to the fasted state, while the α7HMZ males had significantly higher βHB levels in the fed state compared to the WT and α1HMZ (Figure 2.8B). Taken together, these results show that expression of P2-HNF4α in the α7HMZ (or WT) mice correlates with increased levels of circulating ketone bodies. They also show that the absence of P2-HNF4α in α1HMZ females and males inhibits the ability of those mice to increase their ketone body levels during a fast.

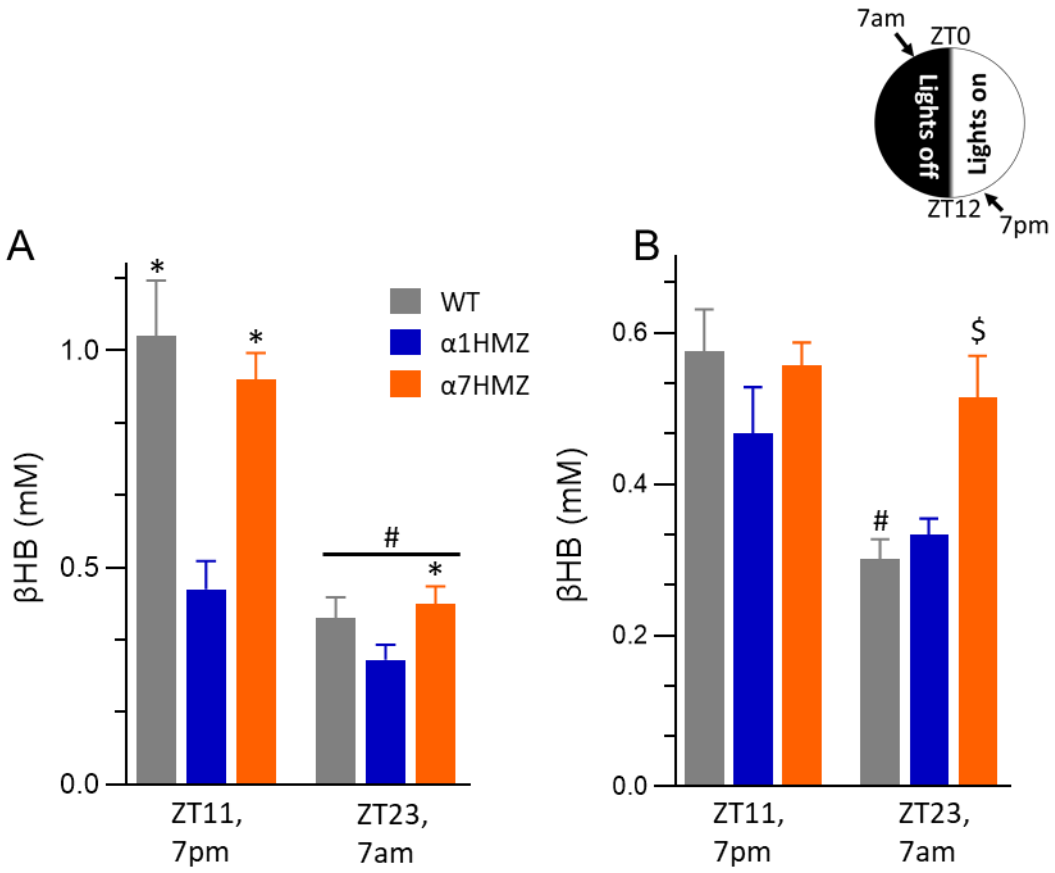

Figure 2. 8 P2-HNF4α is necessary in female mice to elevate ketone body in a response to a time-restricted diet.

Time-restricted feeding showing female (A) (not synchronized for estrous cycle) and male (B) blood βHB (β-hydroxybutyrate) levels from tail vein bleeds. # $p<0.05$ compared to ZT 11, * $p<0.05$ compared to α1HMZ of same time point, $ $p<0.05$ compared to other 2 groups of same time point (n=5-8), Student's T-test

To further explore the complementary nature of glucose and ketone body levels, we subjected WT females to prolonged fasts of 21 and 24 hours and tracked glucose and ketone body levels. As anticipated, as glucose levels became progressively lower, the βHB levels became progressively higher (Figure 2.9A). When the timing was adjusted slightly, it was evident that the levels of glucose recover slightly from the low at 21 hours into the fast (Figure 2.9B). The βHB levels were the opposite of the glucose levels, highest at 21 hours and decreasing somewhat at 27 hours as the glucose levels increased (Figure 2.9B). Males trended similarly to the females; however, they did not have the recovery in glucose and decrease in βHB levels at the 27-hour time point (Figure 2.9C).

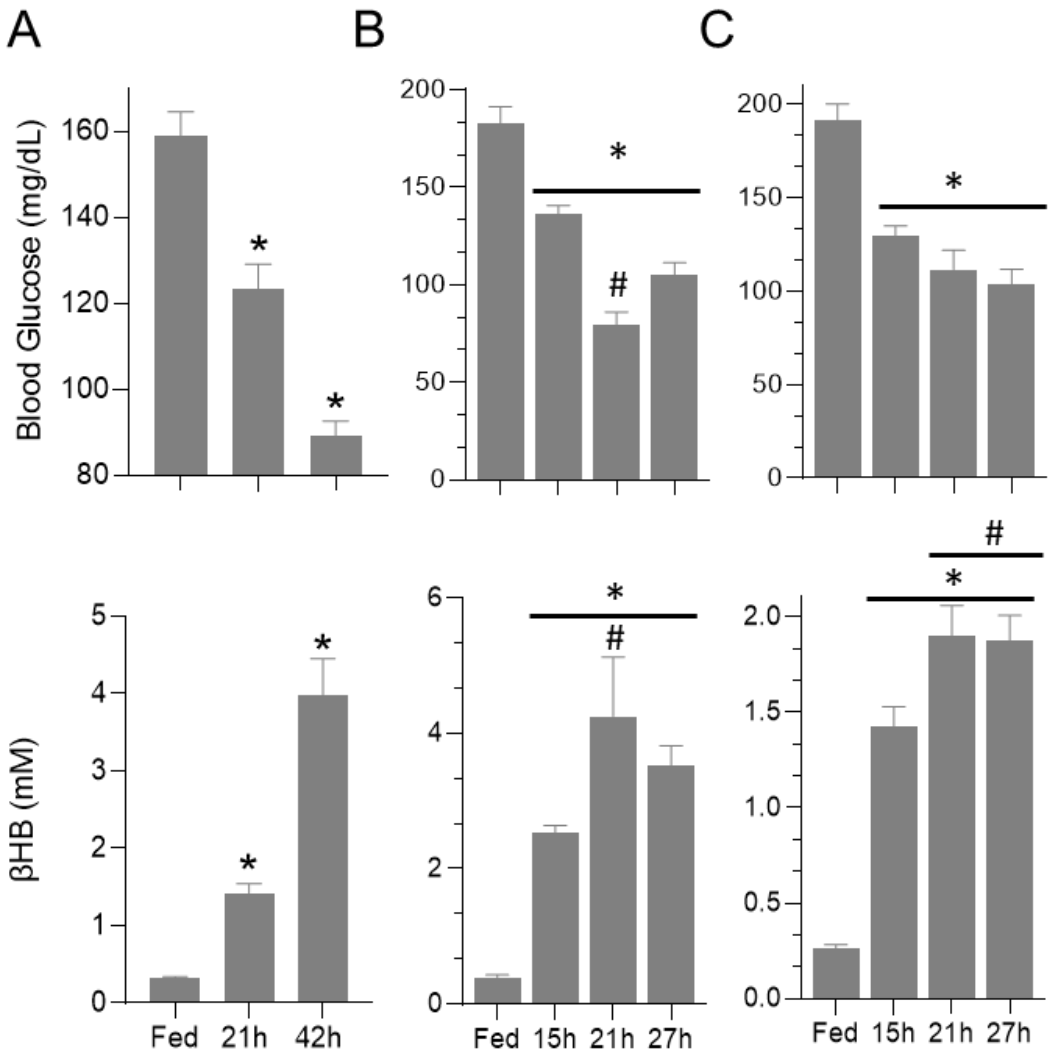

Figure 2. 9 As glucose levels drop, beta hydroxybutyrate levels increase during a fast.

A) Wildtype females (n=4, 3-4 months) fasted for 21 or 42 hours, blood glucose and βHB (β-hydroxybutyrate) levels were taken via tail vein bleed. * $p<0.05$ vs Fed, One-Way ANOVA B) Wildtype females (n=4-5, 3-4 months) fasted for 15 (ZT3), 21(ZT9) or 27 (ZT15) hours, blood glucose and βHB levels were taken via tail vein bleed. * $p<0.05$ vs Fed, # $p<0.05$ vs 15-hr fast, One-Way ANOVA C) Wildtype Males (n=4, 3-4 months) fasted for 15 (ZT3), 21(ZT9) or 27 (ZT15) hours, blood glucose and βHB levels were taken via tail vein bleed. * $p<0.05$ vs Fed, # $p<0.05$ vs 15-hr fast, One-Way ANOVA

Role of HNF4α isoforms in response to AMPK activator AICAR

Glucose metabolism is regulated by many pathways, most notably the AMPK pathway which is activated by fasting along with AICAR and Metformin. AMPK has been shown to phosphorylate HNF4α (Hong et al., 2003). Indeed, others have put HNF4α in two downstream pathways of AMPK which have opposing effects on gluconeogenesis (Figure 2.10) (Fulco & Sartorelli, 2008) and through other interactions could have differential effects on HNF4α. We hypothesize that the differential effects observed through AMPK and HNF4α could be explained by the different HNF4α isoforms playing distinct roles in the metabolic pathways (Figure 2.10).

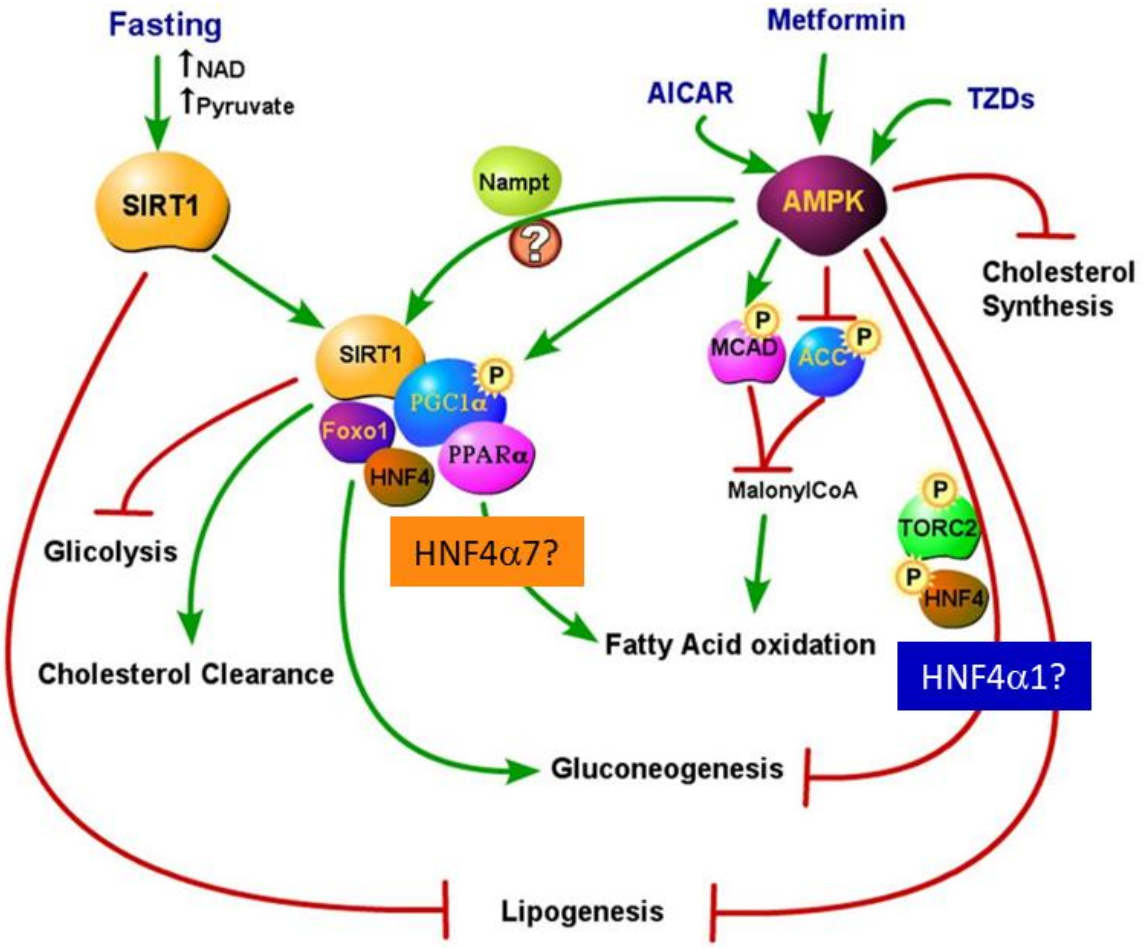

Figure 2. 10 AMP- Activated Protein Kinase (AMPK) regulation of glucose and lipid metabolism and the potential differential involvement of HNF4α isoforms

Image modified from Fulco et al. 2008.

In order to examine the role of HNF4α isoforms in the AMPK pathway, we treated exon swap mice with an IP injection of the synthetic activator of AMPK, AICAR. α7-Heterozygous (α7HTZ), α7HMZ, and α1HMZ male and female mice were treated with either a single IP injection of 500 mg/kg AICAR or 0.9% saline as a control and their glucose and βHB levels were monitored over 45 minutes. The α7HTZ mice express both isoforms of HNF4α in their livers throughout the day. Utilizing these mice allowed us to conduct the experiment at anytime in the day and ensured both isoforms would be present during the experiment. The AICAR treated α7HTZ males had significantly higher glucose levels compared to the α7HMZ males at 20 minutes post injection, although the overall area under the curve (AUC) was not significantly different for any of the genotypes (Figure 2.11A). The α7HMZ had significantly higher βHB levels at all time points compared to both the α7HTZ and the α1HMZ mice and the AUC was significantly higher in the α7HMZ compared to the other two groups (Figure 2.11B). The female α7HTZ had significantly higher glucose levels at 10- and 20-minutes post injection, compared to the α7HMZ, and the AUC was significantly higher than the other two genotypes (Figure 2.11C). The α7HMZ females had significantly higher βHB levels at 10-, 20- and 30- minutes compared to the α1HMZ, and at 30-minutes it was also significantly higher than the α7HTZ. The overall area under the curve was significantly higher in the α7HMZ compared to both other groups (Figure 2.11D). Overall, the AICAR injection did not have a differential effect on the exon swap mice, but did lower glucose in all of the conditions tested.

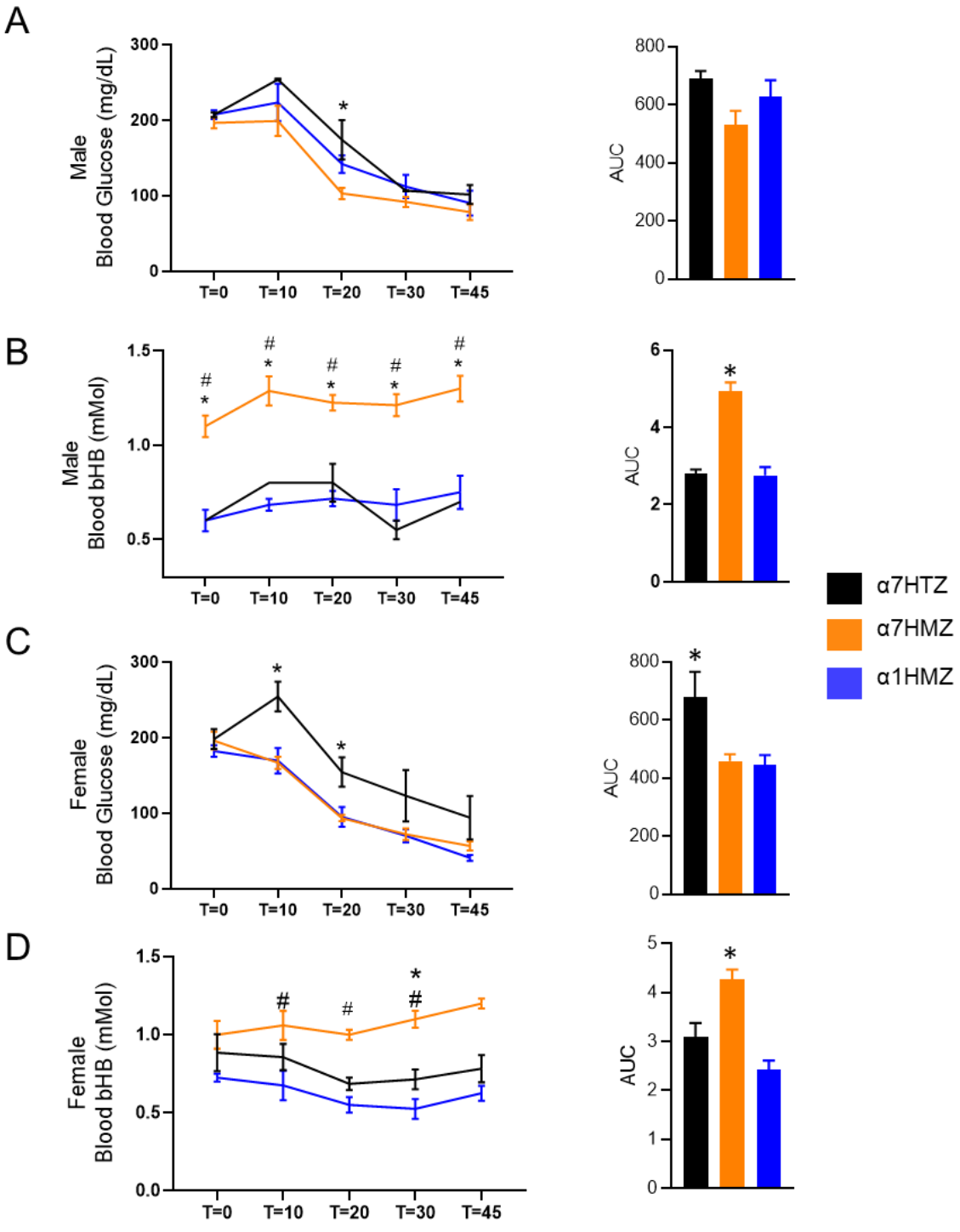
A
Male
Blood Glucose (mg/dL)
300
200
100
0
T=0
T=10
T=20
T=30
T=45
AUC
800
600
400
200
0
B
Male
Blood bHB (mMol)
1.5
1.0
0.5
AUC
6
4
2
0
C
Female
Blood Glucose (mg/dL)
AUC
D
Female
Blood bHB (mMol)
AUC
α7HTZ
α7HMZ
α1HMZ

Figure 2. 11 AICAR does not affect glucose and ketone bodies in heterozygous or homozygous exon swap, yet α7HMZ males and females have higher ketone bodies at all time points.

A, B) blood glucose and ketone body levels in HTZ (n=2), α1HMZ (n=6), and α7HMZ (n=8) males (3-4 months) after AICAR injection (T=0) following a 2-hour fast. Time in minutes post injection. Along with area under the curve (AUC) graphs. C,D) blood glucose and ketone body levels in HTZ (n=7), α1HMZ (n=4), and α7HMZ (n=5) females (3-4mos) after AICAR injection (T=0) following a 2-hour fast. Time in minutes post injection. Along with area under the curve (AUC) graphs. Experiments performed at ZT7*$p<0.05$ α7HMZ vs HTZ #$p<0.05$ α7HMZ v α1HMZ, Student's T-test

Unexpectedly, after the AICAR injection, the homozygous exon swap mice exhibited considerably worse survival than the α7HTZ mice. Half of the male α7HMZ mice died over the course of days 2 through 6 after AICAR injection, while approximately a third of the α1HMZ males died by day 2 with the remaining mice surviving (Figure 2.12A). The female homozygous exon swap mice also had diminished survival post AICAR injection: 40% of the α7HMZ females died, while 50% 0f the α1HMZ females died the day the day after the AICAR time course (Figure 2.12B). The α7HTZ males and females did not have any survivability issues post AICAR injection (Figure 2.12 A, B).

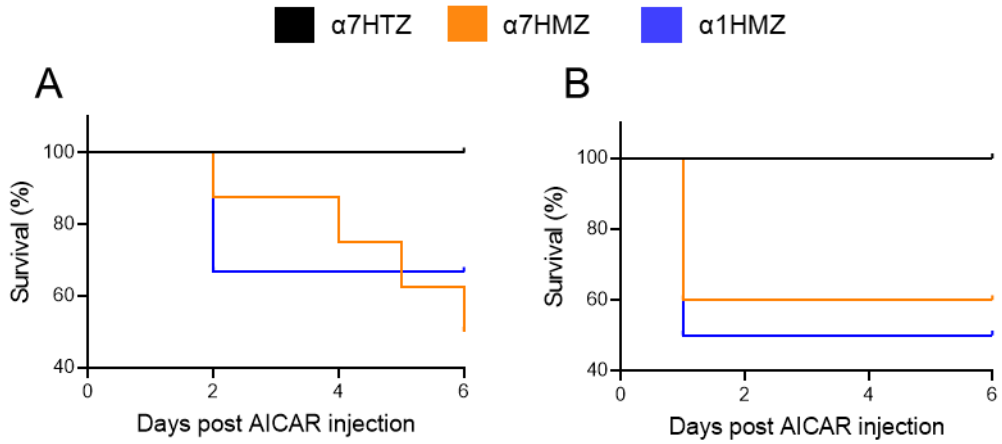

Figure 2. 12 Male and female mice expressing one isoform of HNF4α do not survive AICAR injection as well as HTZ mice.

A) Survival graph showing male (3-4 months) HTZ (n=2), α7HMZ (n=8) and α1HMZ (n=6) survival post AICAR injection. B) Survival graph showing female (3-4 months) HTZ (n=7), α7HMZ (n=5) and α1HMZ (n=4) survival post AICAR injection.

Unexpectedly, the homozygous exon swap mice also exhibited seizures in response to the AICAR injection. There were a large number of seizures among the α7HMZ and α1HMZ, males and females at approximately 30-minutes post AICAR injection. In contrast, none of the α7HTZ females (or males) seized. The α7HMZ mice seized more than the α1HMZ mice, and the females seized more than the males in both genotypes (Figure 2.13A). To determine whether the seizures were related to glucose or ketone body levels, we performed a correlation analysis using GraphPad Prism Trendline analysis. The number of seizures did not significantly correlate with low glucose levels ($p>0.05$). In contrast, the seizures did significantly correlate with elevated βHB levels in both males and females (Figure 2.13B).

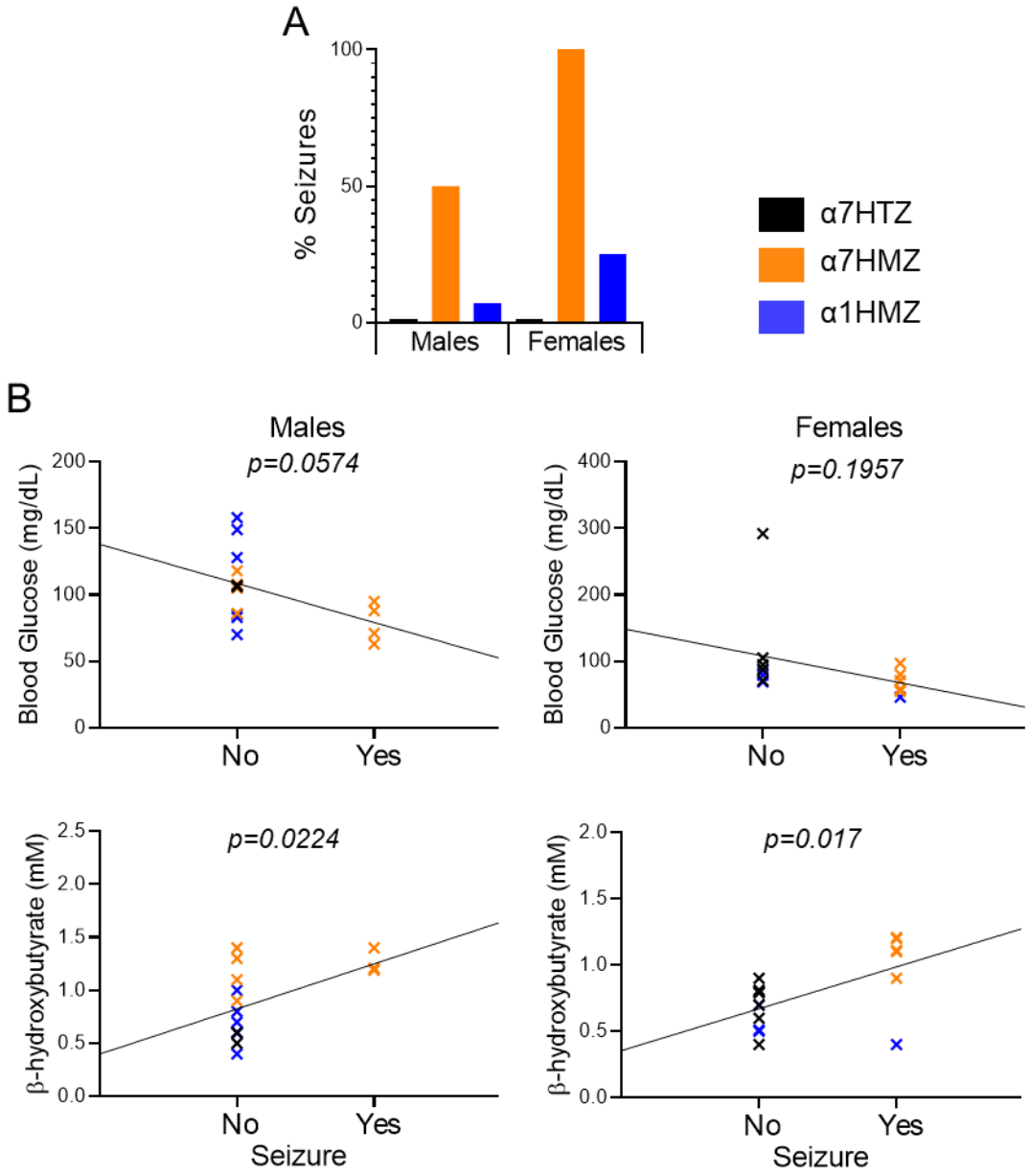

Figure 2. 13 Seizure frequency correlates with ketone bodies and trend with glucose in both male and female mice.

A) Frequency of seizures in male HTZ (n=2), α7HMZ (n=8), α1HMZ (n=14), and female HTZ (n=7), α7HMZ (n=5) and α1HMZ n=4) mice post AICAR injection. All mice seized around T=30 post injection. (B) graphs correlating presence of seizures and glucose level or ketone body level at time of seizure. Trendline and correlative p value analyzed using GraphPad Prism trendline analysis. p value indicates significance of non-zero slope.

The AICAR time course was repeated with α1HMZ males, but they were given either a glucose or saline gavage in addition to food at 60-minutes post AICAR injection. There were no significant differences between the glucose or βHB levels in the glucose and saline gavaged groups (Figure 2.14A, B). Interestingly, the glucose gavage did not ameliorate the diminished survival of the α1HMZ mice, but the saline gavage did (Figure 2.14C). The AICAR injection was repeated in the other groups that seized, but with a saline gavage at 20-minutes post AICAR injection, before the 30- minute time point when they usually began to seize. The seizures completely disappeared in the α7HMZ females. In contrast, the frequency of the seizures did not change significantly in the α7HMZ males or α1HMZ females, but both groups seized much later, the earliest being 55 minutes post AICAR injection and the latest observed being two hours post injection, compared to the groups that were not gavaged (Figure 2.14D).

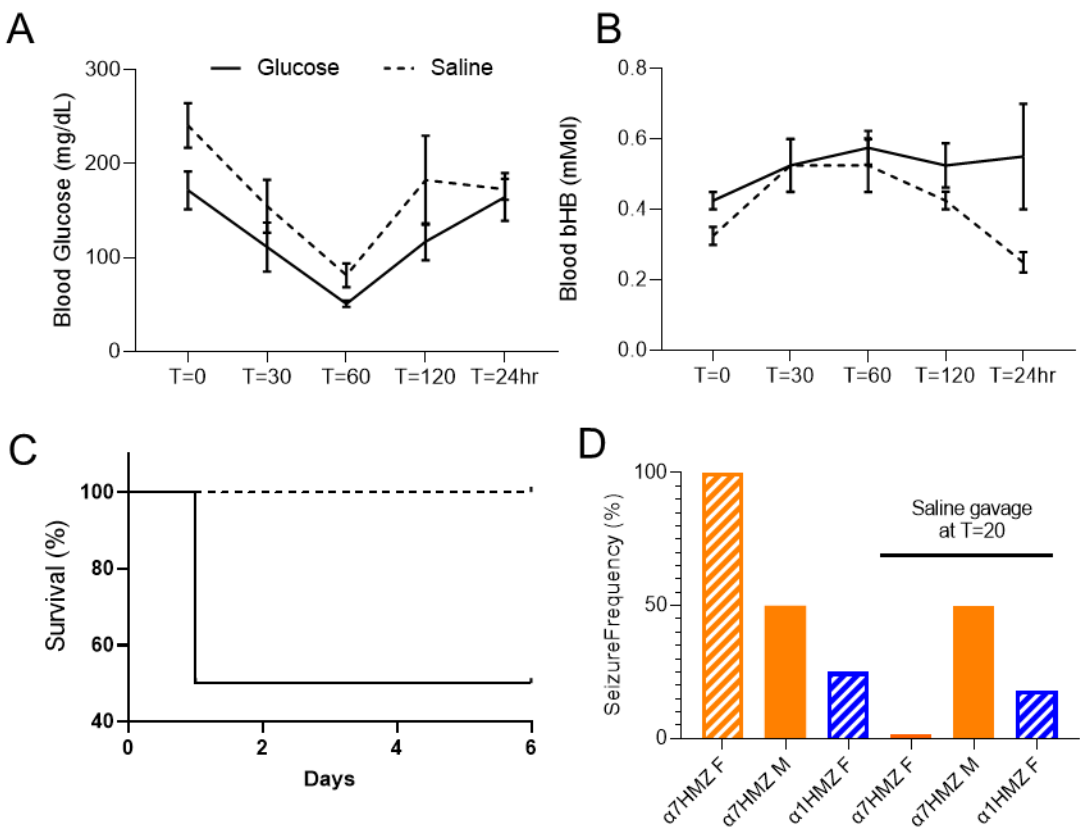

Figure 2. 14 Saline gavage diminishes seizure frequency in exon swap mice

A, B) blood glucose and ketone body levels in α1HMZ males (6 months) after AICAR injection (T=0) following a 2-hour fast. Time in minutes post injection. Mice gavaged with glucose (n=4) or saline (n=4) at T=60. C) Survival graph showing male α1HMZ mice survival post AICAR injection. D) Comparison of seizure percentage in mice with and without saline gavage, M=Male F= Female. Statistical analysis done using Student's T-test.

In order to look at the impact of the AICAR injection on HNF4α protein levels in the liver, α1HMZ males and females were treated with AICAR and harvested 20-minutes later. Liver nuclear extracts were loaded on an immunoblot and probed for HNF4α. Notably, the AICAR-treated males had significantly lower HNF4α protein levels than the saline control group. When normalized to protein loading, there was no significant difference in the levels of HNF4α in the AICAR- and saline-treated female livers (Figure 2.15).

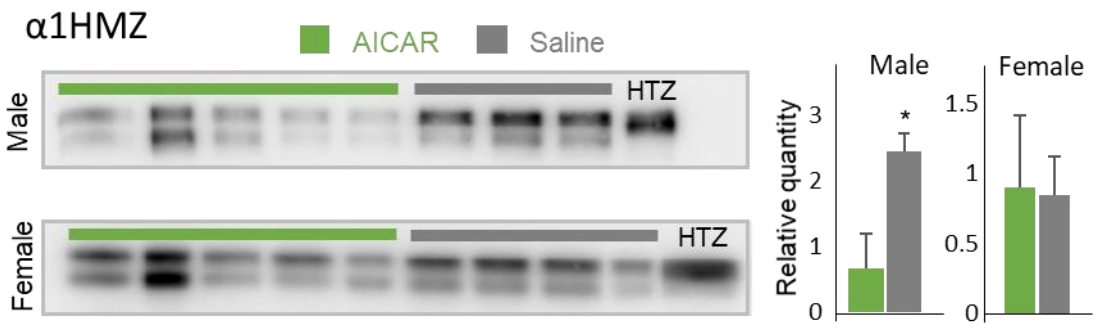

Figure 2. 15 AICAR decreases P1-HNF4α protein

10-month-old mice were treated with AICAR or saline alone as vehicle control via IP injection and harvested at T=20 minutes. 8ug of nuclear extract (NE) were loaded per well. Positive control is NE of α7HTZ male mouse, 11-months-old. Male mice have lower levels of HNF4α1 post AICAR treatment, while females do not. Relative quantity normalized to Coomassie.*$p<0.05$, Student's T-test.

DISCUSSION

The liver is well known to play a central role in carbohydrate and lipid metabolism and there are well established differences in metabolism between males and females. Furthermore, the nuclear receptor HNF4α was established early on as playing an important role in liver metabolism (Sladek, 1993; Sladek & Darnell, 1992) and associated with sex-specific gene expression in the liver (Holloway et al., 2008; Zhang et al., 2011). However, what has not been clear is the role of the different HNF4α isoforms in hepatic metabolism nor how they may intersect with sex. The results in this chapter indicate that the P1- and P2-driven HNF4α isoforms do indeed play differential roles in glucose and fat metabolism and that they intersect with sex in different ways.

Effect of HNF4α isoforms on glucose and insulin tolerance

To begin, we utilized glucose and insulin tolerance tests to characterize the differences between the metabolic profiles of males and females and elucidate any differences the HNF4α isoforms could play. To do so, we tested males and females of both WT and α7HMZ mice. Both the WT and α7HMZ mice have significantly lower glucose tolerance in the males compared to the females (Figure 2.2A, B). The difference between the genotypes is more interesting as there are only significant differences in the females. This was the first indication that the α7HMZ females do not favor glucose metabolism compared to WT. Additionally, the α1HMZ males are less insulin sensitive compared to the α7HMZ males (Figure 2.4). HNF4α has been shown to affect insulin secretion in the pancreas, where the predominant form is P2-HNF4α. That being said, when these mice were first examined there were no significant differences in insulin levels between the

genotypes (Briançon, 2005). The difference in insulin response could be due to differences in gene expression such as differences in the insulin receptor or other aspects of the insulin pathway although these will have to be further elucidated. When comparing the body weights of the mice there were no significant differences except in the WT females compared to all the other groups (Figure 2.5). This difference is likely due to the females being three months of age while the other mice are around six months of age. When aged mice, over 18 months of age, were compared there were no significant differences in weight (data shown in chapter 4).

RNAseq and metabolomics analysis of WT and α7HMZ mice

The RNAseq analysis allowed us to compare the effects of the different HNF4α isoforms on gene expression in the liver. The analysis was done comparing the fed and fasted state at ZT3.5, a time when P2-HNF4α levels are low in the WT mice. The α7HMZ males had fewer DEGs compared to WT males between the fed and 12-hour fasted state from ZT 15.5 to ZT3.5 (Figure 2.6A), suggesting the α7HMZ mice were closer to a fasted state when they are normally fed as fewer genes change in response to the fast. When examining *Pck1*, the key gluconeogenic gene, the wildtype mice significantly increased expression levels in response to a fast, while the α7HMZ do not (Figure 2.6B). This suggests that the α7HMZ mice are less inclined to activate gluconeogenesis 12-hours into a fast. The key ketogenic gene, *Hmgcs2*, was significantly elevated in both the fed and fasted states in α7HMZ mice (Figure 2.6B). Moreover, the metabolite analysis showed that the α7HMZ had lower levels of glucose metabolites and elevated βHB, the key ketone body

(Figure 2.6C). Taken together, α7HMZ seem to favor fatty acid metabolism in response to a fast more so than WT mice.

Effect of prolonged and intermittent fasting on exon swap mice

During the analysis of the RNAseq data, the α7HMZ mice were noted to have an upregulation of genes associated with hibernation (data not shown). Taking into account the fact that fatty acid metabolism is favored over glucose metabolism in a fasted state, we hypothesized that the α7HMZ would fare better during a prolonged fast compared to α1HMZ mice. Interestingly, although all three genotypes tested had their glucose levels fluctuate throughout the fast, presumably due to an increase in gluconeogenesis, half of the α7HMZ mice died 60-hours into the fast. Upon investigating the βHB levels of the surviving α7HMZ mice, their levels were significantly higher than the other two genotypes (Figure 2.7). Based on the levels, the α7HMZ mice that did not survive could have had slightly higher βHB levels, pushing them over the ketoacidosis threshold leading to their death.

It is well established in the literature that males and females metabolize lipids differently and that females have higher circulating ketone body levels compared to males (Halkes et al., 2003). To examine the differences in lipid metabolism in response to time-restricted feeding, male and female mice were entrained for two weeks. During this time their food intake was restricted between ZT0 and ZT12, or during the day time. When comparing the fed state, ZT23, and the fasted state, ZT11, female mice had significantly lower βHB levels in the fed state in all three genotypes, with the α7HMZ mice having significantly higher βHB compared to the other two groups. The fasted state was more

intriguing, as the α7HMZ and the WT mice, both of which express P2-HNF4α, had significantly elevated βHB compared to the α1HMZ mice (Figure 2.8A). This suggests that in females P2-HNF4α is necessary for significant βHB elevation in response to fasting. With regards to the males, only the WT males had significantly higher βHB levels in the fasted state. That being said, in the fasted state the α7HMZ still had higher βHB levels compared to the other two genotypes further suggesting they favor ketogenesis even in a fed state (Figure 2.8B).

Taken together these data suggest that P1-HNF4α favors glucose metabolism and gluconeogenesis, as evident in the significant increase in glucose during the prolonged fast in the α1HMZ mice (Figure 2.7A). Moreover, P2-HNF4α favors lipid metabolism and ketogenesis, as evident with the consistently elevated βHB in the α7HMZ mice and the significantly elevated βHB in both the WT and α7HMZ females in response to the time-restricted feeding (Figures 2.7D and 2.8).

Previous results from our collaborators showed that the levels of the P2-HNF4α protein in the liver fluctuates during the day, with expression undetectable in the morning but becoming apparent at ZT9, dipping at ZT15 and then increasing again at ZT21 (Deans et al. 2021). In contrast, levels of P1-HNF4α do not fluctuate noticeably during the day. Given the elevated levels of glucose in α1HMZ and ketone bodies in α7HMZ (Figures 2.7 and 2.8) and the differential levels of *Pck1* and *Hmgcs2* and metabolites in the TCA cycle in WT and α7HMZ mice (Figure 2.6) we hypothesized that P1-HNF4α is the driver of gluconeogenesis, while P2-HNF4α is the driver of ketogenesis (Figure 2.16). Notably, the

ZT9 time point (red arrow) is around the time when glucose levels wane and ketone body levels rise in mice (Figure 2.16).

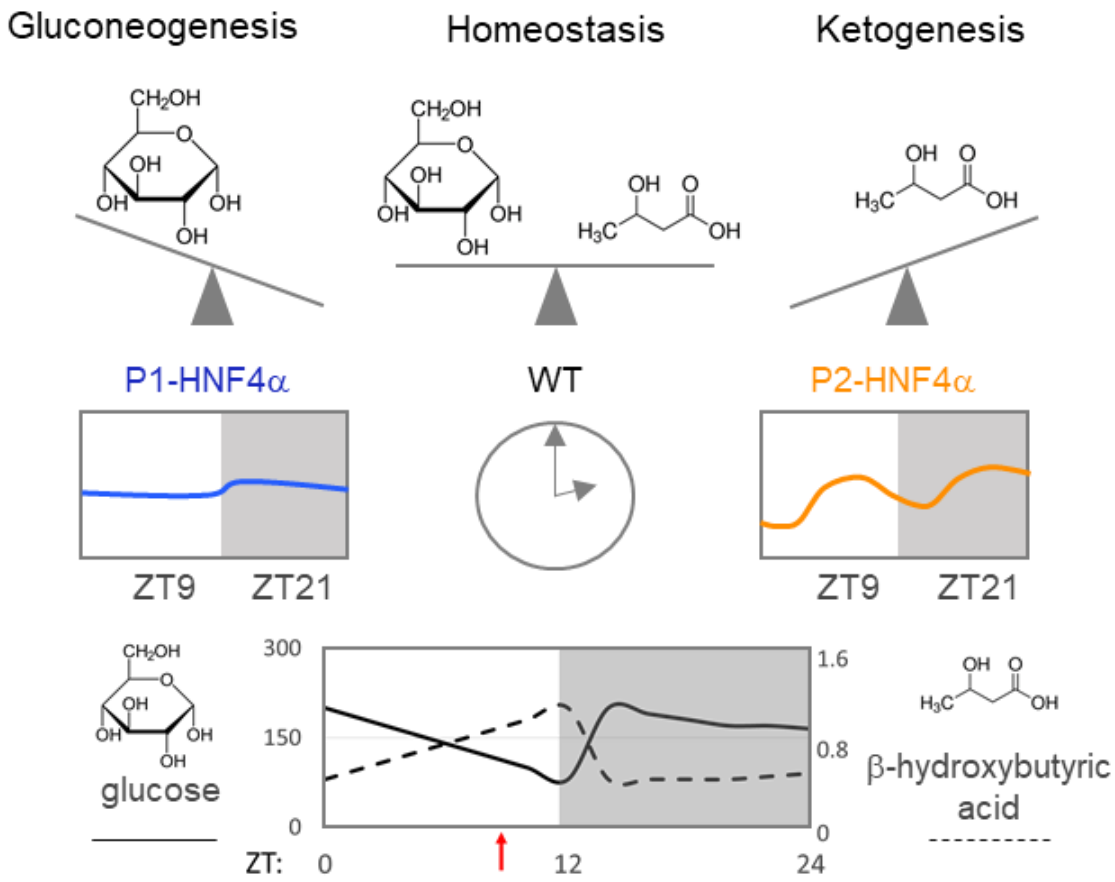

Figure 2. 16 HNF4α1 and HNF4α7-mediated switch between gluconeogenesis and ketogenesis.

Middle panels represent HNF4α protein levels at different times of the day, based on immunoblot data. Bottom graph shows glucose and beta-hydroxybutyrate levels throughout the day. Grey shading indicates lights out. Red arrow is ZT9, where HNF4α7 is increased. Figure by S. Radi, (Deans et al. 2021).

The increase in P2-HNF4α expression at ZT9 noted in Deans et al. 2021. could be in anticipation for the elevation of βHB towards the end of the normal daily fast (Figure 2.16). Additionally, there is a balance between the two isoforms in WT mice that allow them to maintain appropriate βHB levels in both fed and fasted state.

Females also exhibit a decrease in overall levels of circulating glucose in response to a fast, and as anticipated the βHB levels negatively correlate. In both males and females as glucose decreases, βHB levels increase and vice versa (Figure 2.9A, B, C). Moreover, females reach higher βHB levels than males which is consistent with the literature (Halkes et al 2003). The lipid metabolism profile in fasted α7HMZ male mice shows elevation of lipid metabolism genes in comparison to fasted WT mice (Figure 2.9D). This again suggests that the α7HMZ mice favor lipid metabolism presumably due to the sole expression of P2-HNF4α in the HNF4α expressing tissues.

Effect of AICAR on exon swap mice and P1-HNF4α

One of the energy-sensing kinases that is not only essential to metabolic control during the fasted state, but is also known to phosphorylate HNF4α, is AMPK (Figure 2.10). Based on the literature, it is clear that AMPK phosphorylates P1-HNF4α, but P2-HNF4α phosphorylation was never investigated. We hypothesize that AMPK differentially phosphorylates the HNF4α isoforms and began investigating this by treating exon swap mice with the AMPK activator, AICAR. The most interesting aspect of the AICAR treatments was that βHB levels were elevated in the α7HMZ mice as we had seen many times before (Figure 2.11). Although this was not necessarily due to the AICAR injection as the level does not increase throughout the experiment and the saline controls had similar

ketone body levels (data not shown). Additionally, the female α7HTZ mice, which express both isoforms of HNF4α, had significantly elevated glucose compared to the exon swap mice. This suggests that the expression of both isoforms creates a balance that is needed to maintain glucose levels in response to AICAR treatment. This balance also seems essential to ensure survival post-AICAR treatment, as only the α7HTZ mice have a 100% survival rate in either the males or females (Figure 2.12). The α7HTZ mice also did not seize when treated with AICAR (Figure 2.13).

Taken together, the balance between the HNF4α isoforms seems essential to ensuring proper levels of both glucose and βHB, especially in stressful states such as the prolonged fast and AICAR treatment. Interestingly, the seizing seems to correlate with elevated βHB levels and not low glucose levels, and when mice were given a glucose gavage at the end of the AICAR experiment, they did not survive as well as those given a saline gavage along (Figure 2.14). That being said, the AICAR injection does not significantly increase ketone body levels and thus the ketone bodies are not likely to be the cause of the seizures. Moreover, when given a saline gavage 20-minutes after the AICAR injection, most seizure frequency improved and any mice that did seize did so at a much later time (T>55 min). This is most notable because it suggests a role for other HNF4α expressing organs such as the kidneys and intestines. The kidneys and intestines play an important role in solute balance; solute imbalance is associated with seizures (Nardone et al., 2016). The kidneys are intriguing as they have been found to only express P1-HNF4α in WT mice (Ko et al., 2019) in the proximal tubules; the α7HMZ mice would express only P2-HNF4α. This switch could potentially play a role in solute resorption as the main

function of the proximal tubules, where P1-HNF4α is expressed(Marable et al., 2018, 2020) are to recapture water, NaCl, glucose, amino acids, and anions (Curthoys & Moe, 2014). Also, the kidney expresses sodium-glucose transporters that are activated by AMPK (Packer 2020): these transporters could play a role in maintaining sodium concentrations in the blood in response to AICAR treatment and could be altered in the exon swap mice, though this requires further investigation.

P2-HNF4α is expressed in the normal adult liver and drives ketogenesis in both males and females. α7HMZ mice do not survive a prolonged fast as well as α1HMZ and WT mice, likely due to dangerously high levels of ketone bodies. When exon swap mice are treated with AICAR the blood glucose levels decrease and the exon swap mice expressing only one form of HNF4α seize. The female α1 and α7HMZ mice seize more than the males and the α7HMZ mice more-so than the α1HMZ. Additionally, the seizures were ameliorated by saline gavage, likely indicating a role for the kidneys in the results. Lastly, the AICAR treatment in α1HMZ mice decreases P1-HNF4α levels in liver nuclear extract. Subsequent experiments are needed to determine if the AICAR also decreases P2-HNF4α levels in α7HMZ mice and whether the kidneys in fact play a role in the seizure phenotype.

REFERENCES

Briançon, N. (2005). *Hepatocyte Nuclear Factor 4α᾽ : régulation transcriptionnelle du promoteur distal et étude fonctionnelle des isoformes par "knock-in" réciproques chez la souris* [Paris 6]. http://www.theses.fr/2005PA066003

Briançon, N., & Weiss, M. C. (2006). In vivo role of the HNF4alpha AF-1 activation domain revealed by exon swapping. *The EMBO Journal*, *25*(6), 1253–1262.

Bumpus, N.N., and Johnson, E.F. (2011). 5-Aminoimidazole-4-carboxyamide-ribonucleoside (AICAR)-stimulated hepatic expression of Cyp4a10, Cyp4a14, Cyp4a31, and other peroxisome proliferator-activated receptor α-responsive mouse genes is AICAR 5'-monophosphate-dependent and AMP-activated protein kinase-independent. J. Pharmacol. Exp. Ther. 339, 886–895.

Cherif, A., Roelands, B., Meeusen, R., & Chamari, K. (2016). Effects of Intermittent Fasting, Caloric Restriction, and Ramadan Intermittent Fasting on Cognitive Performance at Rest and During Exercise in Adults. *Sports Medicine* , *46*(1), 35–47.

Curthoys, N. P., & Moe, O. W. (2014). Proximal tubule function and response to acidosis. *Clinical Journal of the American Society of Nephrology: CJASN*, *9*(9), 1627–1638.

Deans, J. R., Deol, P., Titova, N., Radi, S. H., Vuong, L. M., Evans, J. R., Pan, S., Fahrmann, J., Yang, J., Hammock, B. D., Fiehn, O., Fekry, B., Eckel-Mahan, K., Sladek, F. M. (2019). Alternative HNF4α isoform regulates the sex-specific diurnal balance between carbohydrate and lipid metabolism in the liver. *In Review, Nature Communications*.

Fulco, M., & Sartorelli, V. (2008). Comparing and contrasting the roles of AMPK and SIRT1 in metabolic tissues. *Cell Cycle* , *7*(23), 3669–3679.

Grajower, M. M., & Horne, B. D. (2019). Clinical Management of Intermittent Fasting in Patients with Diabetes Mellitus. *Nutrients*, *11*(4). https://doi.org/10.3390/nu11040873

Halkes, C. J. M., van Dijk, H., Verseyden, C., de Jaegere, P. P. T., Plokker, H. W. M., Meijssen, S., Erkelens, D. W., & Cabezas, M. C. (2003). Gender differences in postprandial ketone bodies in normolipidemic subjects and in untreated patients with familial combined hyperlipidemia. *Arteriosclerosis, Thrombosis, and Vascular Biology*, *23*(10), 1875–1880.

Halseth, A.E., Ensor, N.J., White, T.A., Ross, S.A., and Gulve, E.A. (2002). Acute and chronic treatment of ob/ob and db/db mice with AICAR decreases blood glucose concentrations. Biochem. Biophys. Res. Commun. 294, 798–805.

Herzig, S., & Shaw, R. J. (2018). AMPK: guardian of metabolism and mitochondrial homeostasis. *Nature Reviews. Molecular Cell Biology*, *19*(2), 121–135.

Holloway, M. G., Miles, G. D., Dombkowski, A. A., & Waxman, D. J. (2008). Liver-specific hepatocyte nuclear factor-4alpha deficiency: greater impact on gene expression in male than in female mouse liver. *Molecular Endocrinology* , *22*(5), 1274–1286.

Hong, Y. H., Varanasi, U. S., Yang, W., & Leff, T. (2003). AMP-activated protein kinase regulates HNF4alpha transcriptional activity by inhibiting dimer formation and decreasing protein stability. *The Journal of Biological Chemistry*, *278*(30), 27495–27501.

Jiang, G., Nepomuceno, L., Hopkins, K., & Sladek, F. M. (1995). Exclusive homodimerization of the orphan receptor hepatocyte nuclear factor 4 defines a new subclass of nuclear receptors. *Molecular and Cellular Biology*, *15*(9), 5131–5143.

Ko, H. L., Zhuo, Z., & Ren, E. C. (2019). HNF4α Combinatorial Isoform Heterodimers Activate Distinct Gene Targets that Differ from Their Corresponding Homodimers. *Cell Reports*, *26*(10), 2549–2557.e3.

Lessan, N., & Ali, T. (2019). Energy Metabolism and Intermittent Fasting: The Ramadan Perspective. *Nutrients*, *11*(5). https://doi.org/10.3390/nu11051192

Lipovka, Y., & Konhilas, J. P. (2014). Estradiol activates AMPK through interaction with extrogen receptor beta (15.4). *The FASEB Journal*, *28*(1_supplement), 15.4.

Maeda, Y., Seidel, S. D., Wei, G., Liu, X., & Sladek, F. M. (2002). Repression of hepatocyte nuclear factor 4alpha tumor suppressor p53: involvement of the ligand-binding domain and histone deacetylase activity. *Molecular Endocrinology* , *16*(2), 402–410.

Marable, S. S., Chung, E., Adam, M., Potter, S. S., & Park, J.-S. (2018). Hnf4a deletion in the mouse kidney phenocopies Fanconi renotubular syndrome. *JCI Insight*, *3*(14). https://doi.org/10.1172/jci.insight.97497

Marable, S. S., Chung, E., & Park, J.-S. (2020). Hnf4a Is Required for the Development of Cdh6-Expressing Progenitors into Proximal Tubules in the Mouse Kidney. *Journal of the American Society of Nephrology: JASN*, *31*(11), 2543–2558.

Maughan, R. J., Fallah, J., & Coyle, E. F. (2010). The effects of fasting on metabolism

and performance. *British Journal of Sports Medicine*, *44*(7), 490–494.

Mittendorfer, B. (2005). Sexual dimorphism in human lipid metabolism. *The Journal of Nutrition*, *135*(4), 681–686.

Nardone, R., Brigo, F., & Trinka, E. (2016). Acute Symptomatic Seizures Caused by Electrolyte Disturbances. *Journal of Clinical Neurology* , *12*(1), 21–33.

O'Neill, B., & Raggi, P. (2020). The ketogenic diet: Pros and cons. *Atherosclerosis*, *292*, 119–126.

Packer, M. (2020). Interplay of adenosine monophosphate-activated protein kinase/sirtuin-1 activation and sodium influx inhibition mediates the renal benefits of sodium-glucose co-transporter-2 inhibitors in type 2 diabetes: A novel conceptual framework. Diabetes, Obesity & Metabolism, 22(5), 734–742.

Palmer, B. F., & Clegg, D. J. (2015). The sexual dimorphism of obesity. *Molecular and Cellular Endocrinology*, *402*, 113–119.

Sampaio, L. P. de B. (2016). Ketogenic diet for epilepsy treatment. *Arquivos de Neuro-Psiquiatria*, *74*(10), 842–848.

Sladek, F. M. (1993). Orphan receptor HNF-4 and liver-specific gene expression. *Receptor*, *3*(3), 223–232.

Sladek, F. M., Dallas-Yang, Q., & Nepomuceno, L. (1998). MODY1 mutation Q268X in hepatocyte nuclear factor 4alpha allows for dimerization in solution but causes abnormal subcellular localization. *Diabetes*, *47*(6), 985–990.

Sladek, F. M., & Darnell, J. E. (1992). Mechanisms of liver-specific gene expression. *Current Opinion in Genetics & Development*, *2*(2), 256–259.

von Geijer, L., & Ekelund, M. (2015). Ketoacidosis associated with low-carbohydrate diet in a non-diabetic lactating woman: a case report. *Journal of Medical Case Reports*, *9*, 224.

V, R. A., & Zargar, A. H. (2017). Diabetes control during Ramadan fasting. *Cleveland Clinic Journal of Medicine*, *84*(5), 352–356.

Wheless, J. W. (2008). History of the ketogenic diet. *Epilepsia*, *49 Suppl 8*, 3–5.

Zhang, Y., Klein, K., Sugathan, A., Nassery, N., Dombkowski, A., Zanger, U. M., & Waxman, D. J. (2011). Transcriptional profiling of human liver identifies sex-biased genes associated with polygenic dyslipidemia and coronary artery disease. *PloS One*, *6*(8), e23506.

Zubrzycki, A., Cierpka-Kmiec, K., Kmiec, Z., & Wronska, A. (2018). The role of low-calorie diets and intermittent fasting in the treatment of obesity and type-2 diabetes. *Journal of Physiology and Pharmacology: An Official Journal of the Polish Physiological Society*, *69*(5). https://doi.org/10.26402/jpp.2018.5.02

CHAPTER 3: Effects of Aging on HNF4α Exon Swap Mice

INTRODUCTION

Aging and metabolism

A major focus of aging research is cellular aging. The cell consists of a very well-orchestrated series of signal transduction pathways that not only maintain normal cell function, but also work to prevent cellular dysfunction which can be detrimental to the organism. Total cellular metabolism is the sum of all of the catabolic and anabolic pathways in the cell, and normal cellular metabolism plays an important role in the aging process. The mitochondria are the main metabolic organelle, responsible for the majority of ATP production in the cell. Normal metabolic processes in the mitochondria produce reactive oxygen species (ROS), which are the most widely investigated aspect of cellular aging (Catic, 2018; Kudryavtseva et al., 2016). The electron transport chain in the mitochondria involves a series of redox reactions that produce a proton gradient in the inter-mitochondrial membrane space, which is utilized to drive ATP synthesis. Complexes I and III produce superoxide radicals as a byproduct of their reactions (Catic, 2018). Three stepwise enzymatic reactions are used to scavenge these free radicals; superoxide dismutase, catalase, and glutathione peroxidase (Catic, 2018). First, superoxide dismutase converts the superoxide (O_2^-) into hydrogen peroxide (H_2O_2), which can cause very reactive hydroxyl radicals. Both catalase and glutathione peroxidase are used to convert hydrogen peroxide into water. It has been shown that increased expression of superoxide dismutase alone can be harmful, as it leads to an accumulation of hydrogen peroxide, while an increase in glutathione peroxidase can have beneficial effects as it scavenges the

hydrogen peroxide molecules (Catic, 2018). It has been hypothesized that the accumulation of ROS in the mitochondria can lead to alterations in the mitochondrial genome and mitochondrial proteins and that could lead to accelerated aging. Nonetheless, there has yet to be a correlation with decreased ROS in the mitochondria and increased life span (Catic, 2018).

Mitochondrial function in general has been linked to aging. The mitochondria replicate independently of the cell cycle and are able to adapt to nutrient availability (Catic, 2018). As the cell ages, the mitochondria begin to lose their ability to replicate properly, which prevents overall metabolic flexibility in the cell. This could be due to damage to the mitochondrial genome, due to adducts, spontaneous damage which can lead to mutations as well as adducts on mitochondrial proteins that negatively affect their function (Catic, 2018). Elevated acetyl-CoA and succinyl-CoA in combination with increased pH promotes non-enzymatic acetylation of the ε-amino group of lysine residues. Sirtuins, SIRT3, 4, and 5, are protein deacetylases which are highly enriched in the mitochondria; the elevation of these enzymes has been shown to decrease detrimental acetylation and contribute to healthy aging. The SIRT proteins are dependent on NAD+ levels (Catic, 2018; Verdin, 2015). Although SIRT proteins are important for healthy aging, their effect on increased lifespan is controversial (Catic, 2018; Verdin, 2015).

Aging and cancer

Cancer is thought of as a "disease of old age" as it is most prevalent in the elderly and typically takes a long time to develop. There are many factors that contribute to cancer development, including DNA damage, oxidative stress, and a compromised immune

system. DNA can be damaged from outside agents such as x-rays, radiation, and chemical agents; as well as spontaneous damage from error-prone enzymes and spontaneous oxidative damage from the cell (Hoeijmakers, 2009). The DNA in a cell can accumulate lesions over time and if those lesions are not repaired, a mutation can occur in the DNA sequence (Hoeijmakers, 2009). Mutations can lead to the inactivation of tumor suppressor genes and the improper activation of oncogenes which will lead to the hallmark of cancer: uncontrolled cellular proliferation (Hoeijmakers, 2009). DNA can undergo spontaneous hydrolysis leading to abasic sites and deamination, spontaneous oxidation reactions from normal metabolism leading to lipid peroxidation and various alkylating agents (Hoeijmakers, 2009). Reactive oxidative and nitrogen species lead to single-stranded breads and various oxidized base and sugar lesions in DNA (Hoeijmakers, 2009). DNA damage, regardless of source, can lead to mutations that cause cancer, cell death, or senescence which contributes to aging. Luckily, the cell has an elaborate array of DNA repair mechanisms. There are many distinct DNA repair pathways that repair specific types of lesions and control various cell-cycle and signal-transduction pathways to ensure sufficient time to repair the genome, or induce apoptosis if the damage is too great to repair (Hoeijmakers, 2009). Moreover, DNA damage not only leads to carcinogenesis, but also to malignant progression from benign tumors by allowing the accumulation of mutations in the genome as well as epigenetic alterations which can impact gene expression.

Progeria (early aging) mouse models of defective nucleotide-excision repair, a specific type of DNA repair pathway, have a life span of three to eight weeks and have overall decreased growth, energy expenditure, and antioxidant defenses. Moreover, these

mice have expression profiles similar to those in wildtype (WT) mice that are 2.5 years of age (Hoeijmakers, 2009), linking DNA repair inhibition with premature aging. Additionally, in most cells, every round of DNA replication causes a shortening of the protective telomeres at the ends of the chromosomes. Thus, outgrowth of cancerous cells without the expression of the telomerase gene (hTERT) would lead to damage similar to double stranded breaks which would activate DNA repair mechanism and could lead to cell cycle arrest and apoptosis. Therefore, over 90% of all cancers express the telomerase gene (Hoeijmakers, 2009).

The immune system also plays a major role in cancer development as one ages, and aging is usually accompanied by an increase in inflammation. As a body ages, the immune function tends to decline, referred to as immunosenescence, and there is an increase in inflammatory cytokines such as Interleukin-1β and Interleukin-6 (Jackaman et al., 2017). The decrease in immune function and increased inflammatory state have not only been linked to many age-related diseases such as osteoporosis, Alzheimer's disease, diabetes and atherosclerosis, but also to many different types of cancer (Jackaman et al., 2017).

Aging and hearing loss

One of the most common associations with aging is hearing loss. Age-related hearing loss has been associated with cognitive decline and dementia (Uchida et al., 2019). In fact, the Lancet Commission on Dementia Prevention, Intervention, and Care posits that if mid-life hearing loss were eliminated, there would be a decline in dementia by nine percent (Uchida et al., 2019). Age-related hearing loss is usually characterized as the bilateral, symmetrical, sensorineural hearing loss that is caused by the degeneration of the

inner ear structures as a person ages (Chern & Golub, 2019). This type of hearing loss affects the perception of higher frequency sounds first, due to decreased sensitivity and impaired perception. The World Health Organization defines age-related hearing loss to be greater than 40 decibels (db) averaged over the frequencies of 0.5, 1, 2, and 4kHz, in the better-hearing ear (Davis et al., 2016).

There are many hypotheses as to the mechanism behind the connection between age-related hearing loss and dementia. One hypothesis is that the individual with hearing loss uses much of their cognitive reserve to focus on hearing such that they do not have sufficient brain capacity to dedicate to other tasks. Another hypothesis is that there are detectable changes in brain structure that are associated with hearing loss and these may be associated with dementia (Chern & Golub, 2019). Moreover, there is a well-supported hypothesis that the vascular degeneration that occurs with aging could play a role in both age-related hearing loss and dementia. The decrease in blood supply can contribute to a loss of cognitive function in different parts of the brain (Chern & Golub, 2019). Additionally, there are theories that indicate ketone bodies could play a role in decreasing the aging process and this could help prevent age-related hearing loss. Therefore, we chose to investigate how elevated ketone bodies in the HNF4α exon swap mice could contribute to better age-related hearing loss. Although many associate hearing loss with a normal part of the aging process, the intervention or even prevention of hearing loss can have a lasting effect on the mental, physical, and social well-being of the elderly.

Aging and the gut

The intestines are full of bacteria, referred to as the gut microbiota, which play a role in maintenance of the intestinal barrier function; produce short chain fatty acids, which are essential for mucus production; and are involved in innate immune system priming by contributing to the maturation of gut-associated lymphoid tissue which is important for local and systemic immunity (Mangiola et al., 2018). The gut microbiota helps to constantly stimulate the immune system by creating an environment of low-grade inflammation which effectively defends the body against pathogens. Changes in the gut microbiota have been associated with physiological changes including aging (Mangiola et al., 2018).

During the aging process, the enteric nervous system in the gastrointestinal tract degenerates which could be due to changes in the gut microbiota, which in turn causes a decrease in intestinal motility and barrier function which leads to development of intestinal diseases (Mangiola et al., 2018). During the aging process, the intestines may have an environment of excess inflammation, characterized by the expression of proinflammatory factors such as IL-6 and TNF-α which leads to the activation of the transcription factor NF-κB (Mangiola et al., 2018). This inflammatory response has been associated with Alzheimer's disease, Parkinson's disease, type-2 diabetes, osteoporosis, and a variety of cancers. The excess inflammation leads to an increase in cortisol levels and aids in the development of insulin resistance (Mangiola et al., 2018).

The gut microbiota changes throughout life and the aging process, decreasing in diversity in aged individuals which leads to a decrease in the abundance of butyrate

producing species. Butyrate not only alters the pH of the intestines and decreases *Escherichia coli* levels; it has been shown to drive differentiation and gene expression in the gut which is an important anti-cancer process (Mangiola et al., 2018).

One of the most impactful environmental factors on the gut microbiota is diet. High fat or carbohydrate diets have been shown to negatively impact the gut microbiota and important signal transduction pathways. For example, caloric restriction has been shown to delay the aging process. It is thought that the insulin signaling pathway leads to an increase in AKT which inactivates FOXO, an essential transcription factor that plays a role in cell metabolism, autophagy, and the stress-response. During caloric restriction, AKT is not activated, leading to an increase in FOXO expression and a decrease in aging (Kim & Jazwinski, 2018).

Interestingly, through gut microbiota transplantation, it was observed that addition of gut microbiota from Parkinson's or Alzheimer's disease patients to germ-free mice lead to an exacerbation of the corresponding disease, indicating a link between the gut microbiota and the development of the disease (Kim & Jazwinski, 2018). Gut dysbiosis is associated with normal chronological aging, the prevention of which has been associated with enhanced longevity (Kim & Jazwinski, 2018). The bacterial composition as well as abundance leads to differences in gene expression and inflammation that affect not only the intestines but the entire body.

The HNF4α gene is driven by two promoters and gives rise to two sets of isoforms, the P1-driven and P2-driven HNF4α or P1-HNF4α and P2-HNF4α respectively. P1-HNF4α is the main isoform in the adult liver and has long been thought of as the solely

expressed form of HNF4α. Previous research has shown an increase in P2-HNF4α in the adult liver in hepatocellular carcinoma (HCC) and colorectal cancers (Chellappa et al., 2012, 2016; Fekry et al., 2018; Tanaka et al., 2006).

In order to examine the role of gut health and basic metabolism on various aspects of the aging phenotype, including cancer, intestinal barrier dysfunction and hearing loss, I examined HNF4α exon swap that express either only P1-driven or P2-driven HNF4α isoforms. The Sladek lab has shown that α7HMZ mice, which express only P2-HNF4α, are highly sensitive to colitis induced by dextran sulfate sodium (DSS) and have impaired intestinal barrier function (Chellappa et al., 2016) which could be an indication of gut dysbiosis and hence a poor prognosis for aging. At the same time, young adult α7HMZ mice tend to have higher levels of ketone bodies than WT or α1HMZ mice (Chapter 2) and there are several reports of ketone bodies being protective against dementia as well as hearing loss (Broom et al., 2018; Henderson, 2008; Newman & Verdin, 2014; Puchalska & Crawford, 2017). Finally, others have shown that P1-HNF4α expression is greatly reduced in liver and colon cancer while P2-HNF4α expression is increased, suggesting that P2-HNF4α may help drive the cancer phenotype. In order to examine the impact of the HNF4α isoforms on various aspects of aging -- cancer, ketone body production, hearing loss and intestinal barrier function-- I compared tumor development, ketone body levels in response to fasting, auditory brain responses and FITC-dextran assays in aged WT, α1HMZ and α7HMZ mice.

MATERIALS AND METHODS

Tumor Analysis in Aging Mice

Mice were housed in non-specific pathogen free (SPF) facilities and were given food and water *ad libitum* with a 12-hour light/dark cycle. All experimental procedures were approved by UCR IACUC. The blood glucose and ketone bodies of WT, α7HMZ, and α1HMZ male and female mice over 18 months of age were collected and the mice were sacrificed using a CO_2 gas and a cervical dislocation. The abdominal cavity was opened and their organs were analyzed for gross abnormalities and obvious tumors. Any obvious macroscopic tumor or abnormality was noted and organized in Table 3-1. None of the organs or tumors were collected for further analysis.

Mouse entrainment and ketone body analysis

Both young (3 months of age) and old (over 9 months of age) WT, α7HMZ, and α1HMZ male and female mice were entrained for up to two weeks. During this process, mice were restricted to feeding between ZT12 (8 PM) and ZT0 (8 AM). To accomplish this, food (vivarium chow, Purina Test Diet 5001, Newco Distributors, Rancho Cucamonga, CA) was removed from the cage at ZT0 and fresh food was added at ZT12, this continued daily for up to two weeks including weekends. Throughout the experiment, the mice were placed on woodchip bedding. On the day of the ketone body analysis, food was removed as usual at ZT0, however mice were not given food until ZT14. Ketone bodies levels were analyzed from a tail bleed using a ketone body meter, as described in Chapter 2. AT ZT14, mice were given food after the ketone body levels were quantified. The last

ZT16 time point is two hours after being given food. Mice were allowed to recover for two weeks given food *ad libitum* before any entrainment was repeated.

Auditory Brain Response Analysis

Auditory analysis was done in collaboration with Dr. Khaleel Abdul-Razak's lab with the help of his graduate student Jamiela Kokash. Auditory brainstem response (ABR): Animals were anesthetized with ketamine (65 mg/kg), xylazine (13 mg/kg), and acepromazine (1.5 mg/kg) (KXA) in 0.9% sterile saline via intraperitoneal injection. Once mice were anesthetized, three platinum coated electrodes were placed under the dermis of the head: the recording electrode was on the vertex; the ground electrode was in the left cheek and the reference electrode was in the right cheek. The auditory experiments took place in a sound-proof room. The sound stimuli were delivered via a free field speaker (MR1 Multi-Field Magnetic Speakers, Tucker-Davis Technologies) that was placed 10 cm away from the left ear at 45º. Clicks of alternating±1.4 V (duration 0.1 ms) were generated and delivered using RZ6 hardware (Tucker-Davis Technologies, FL). Intensity of the clicks ranged from 10 to 90 dB in 10 dB steps. The ABRs were filtered and amplified (Grass Technologies) and averaged (BioSigRZ, Tucker-Davis Technologies).

FITC Dextran Barrier Function Analysis

WT, α7HMZ, and α1HMZ male and female mice over 1year of age were fasted overnight (15-hours) on wood chip bedding (Newco Specialty, catalog # 91100). The morning of the experiment, mice were weighed and gavaged, under yellow lights, with FITC-Dextran (FD-4, Sigma) diluted in water at a dose of 600 µg/g body weight. Four hours later, mice were sacrificed via CO_2 inhalation and cervical dislocation and blood was

collected via inferior vena cava bleed. Samples were incubated on ice for 45 minutes and then spun at 9.3 rcf for 15 minutes to separate the serum. The serum was diluted 1:5 in water and was loaded into black 96-well plates (Corning, catalog no.3991) in triplicate. Serum FITC-Dextran concentration was determined on a Veritas Microplate Luminometer (Turner Biosystems), GloMax software (Promega), using excitation/emission wavelengths of 490/520 nm. The relative fluorescence units obtained for the samples were compared to the values obtained from a standard curve generated by diluting the fluorophore stock in water.

RESULTS

Tumor development

I examined spontaneous tumor development in aged mice to determine whether the convention that P1-HNF4α is tumor suppressive and promotes differentiation, while P2-HNF4α is permissive of proliferation and thus cancer promoting. Using exon swap mice which express either P1-driven or P2-driven HNF4α, we investigated whether these mice would spontaneously develop more tumors compared to WT mice over 18 months of age. Contrary to the notion that P2-driven HNF4α is cancer promoting, there was no significant increase in macroscopic tumor development in the exon-swap mice only expressing P2-HNF4α (α7HMZ) (Table 3-1). Tumors were observed in all three genotypes -- WT, α7HMZ, and α1HMZ (P1-driven HNF4α expressing) mice -- but there was no significant enrichment in tumor incidence in any of the groups. Many of the mice (30-60%) had enlarged seminal vesicles which can be indicative of prostate cancer (Soylu et al., 2013) and which is common as males age. Normally, HNF4α is not thought to be expressed in

any part of the male reproductive tract, but there is one report of HNF4α being expressed in the epididymis and GTEX data shows HNF4α RNA expression in the testes (Tanaka et al., 2006). α1HMZ females did not have any noticeable tumors or polyps in their colons, although this could be due to a low number of mice. In contrast, a third of the WT and α7HMZ females had some abnormal growths in their colons (Table 3.1).

Genotype and sex	n	# of Liver Tumors	Intestinal Polyps/colon tumor	Seminal Vesicles Enlarged	Other?
WT Males	5	2	0	3	
WT Females	6	1	2	n/a	
α7HMZ Males	15	0	0	5	1 case of Spleen tumors and cyst on liver
α7HMZ Females	12	0	4	n/a	
α1HMZ Males	8	1	2	4	
α1HMZ Females	3	0	0	n/a	

Table 3. 1 No significant differences in tumor development in exon swap mice over 15 months of age compared to wildtype.

Quantification of obvious, gross tumor growth, or seminal vesicle enlargement in aged mice over 15 months of age. Statistics done using Student's T-test.

Metabolic changes

Metabolic changes are well documented in aging individuals, and responses to fasting could be altered with age. Young (four to five months) and old (more than 12 months), male and female mice were fasted from ZT0 (8 AM) to ZT14 (10 PM), and their blood β-hydroxybutyrate (βHB) levels were monitored at ZT10, ZT12, ZT14, and ZT16 (two hours after being given food). βHB is the major ketone body which becomes elevated in response to a fast. Interestingly, at ZT10 and ZT12, the young females have significantly higher βHB levels compared to all three other groups (Figure 3.1A), and at ZT14, the older females have elevated βHB levels similar to that of the young females, both of which are significantly higher than the other two male groups. Two hours after feeding at ZT16, all four groups have reduced βHB levels (Figure 3.1A).

To examine the effect of intermittent fasting on ketone body levels, young and old WT male and female mice were entrained for 1-2 weeks where they were restricted from feeding between ZT0 and ZT12 (when they are normally inactive and not eating) and given food from ZT12 to ZT24 (during their active hours). When comparing the entrained and not entrained males (Figure 3.1B), the young entrained males had significantly decreased βHB levels compared to all other groups at ZT14. Similarly, the young, entrained females had significantly lower βHB levels compared to the mice that were not entrained at ZT14 (Figure 3.1C). Next, we examined the entrainment in young and old exon swap mice. With regards to the young mice, at ZT10 and ZT14, male and female α7HMZ had significantly elevated βHB levels compared to α1HMZ males. At ZT14, the α7HMZ females had βHB levels significantly higher than the α7HMZ males. After feeding, at ZT16, the α7HMZ

females had significantly higher βHB levels compared to the α1HMZ females (Figure 3.1D). The old mice did not have the same profile as the young mice (Figure 3.1E). At ZT10, the α7HMZ males and females had significantly higher βHB levels compared to the α1HMZ males. At ZT12 and ZT16, the α7HMZ females had significantly elevated βHB compared to both the α1HMZ males and females. At ZT14, only the α7HMZ females and males had significantly different βHB levels with the females being higher than the males (Figure 3.1E).

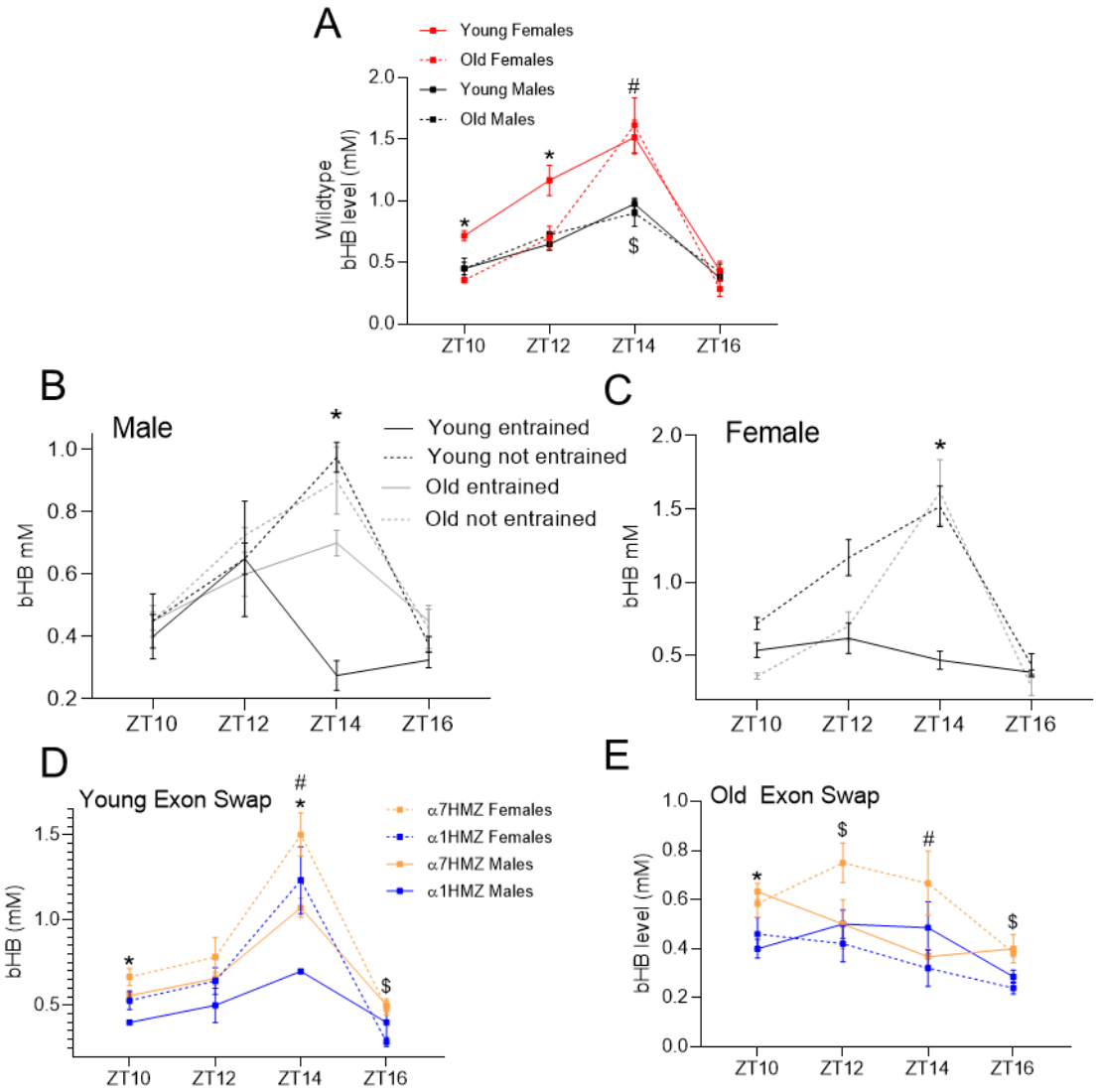
A
Young Females
Old Females
Young Males
Old Males
Wildtype
bHB level (mM)
2.0
1.5
1.0
0.5
0.0
ZT10
ZT12
ZT14
ZT16
*
*
#
$
B
Male
Young entrained
Young not entrained
Old entrained
Old not entrained
bHB mM
1.0
0.8
0.6
0.4
0.2
ZT10
ZT12
ZT14
ZT16
*
C
Female
bHB mM
2.0
1.5
1.0
0.5
ZT10
ZT12
ZT14
ZT16
*
D
Young Exon Swap
α7HMZ Females
α1HMZ Females
α7HMZ Males
α1HMZ Males
bHB (mM)
1.5
1.0
0.5
ZT10
ZT12
ZT14
ZT16
*
*
#
$
E
Old Exon Swap
bHB level (mM)
1.0
0.8
0.6
0.4
0.2
0.0
ZT10
ZT12
ZT14
ZT16
*
$
#
$

Figure 3. 1 Restricted feeding experiments reveal sex -specific effects on ketone body levels that are enhanced in the HNF4α exon-swap mice.

All mice fasted from ZT0-14 on day of measurement (n=4-10); females not synchronized for estrous cycle. A) βHB levels in young (4-5 mo) and old (>1yr) male & female mice, no entrainment, * $p<0.05$ vs all other groups, # $p<0.05$ young females vs both male groups, $ $p<0.05$ old females vs old males. B and C) Comparison of wildtype young and old, male and female mice (n=4-7) with and without entrainment. * $p<0.05$ young entrained vs. all other groups. D) βHB levels of young exon swap mice after 1-2 weeks entrainment, * $p<0.05$ α7HMZ male and female vs α1HMZ males, # $p<0.05$ α7HMZ females vs α7HMZ males, $ $p<0.05$ α7HMZ females vs α1HMZ females. E) βHB levels of old (>1yr) exon swap mice after 1-2 weeks entrainment, * $p<0.05$ α7HMZ males and females vs α1HMZ males, $ $p<0.05$ α7HMZ females vs α1HMZ females and α1HMZ males. # $p<0.05$ α7HMZ females vs α1HMZ females. All statistics done using Student's T-test.

Hearing loss

To examine the extent of the age-related hearing loss in our mice, we used auditory brain response curves to compare mice more than 18 months old from two different backgrounds, C57Bl6/N and a mixed background line with SV129, and three different genotypes, WT, α7HMZ, and α1HMZ. Comparing the males from a C57Bl6/N background at 18 months old, the WT had significantly worse hearing compared to the other two genotypes (Figure 3.2A). Whereas, the females were not significantly different at most of the frequencies tested (Figure 3.2B). Upon repeating the experiment two months later, the WT males no longer exhibited hearing loss as in the initial experiment and hence there was no significant difference in hearing capacity in any of the genotypes (Figure 3.2C).

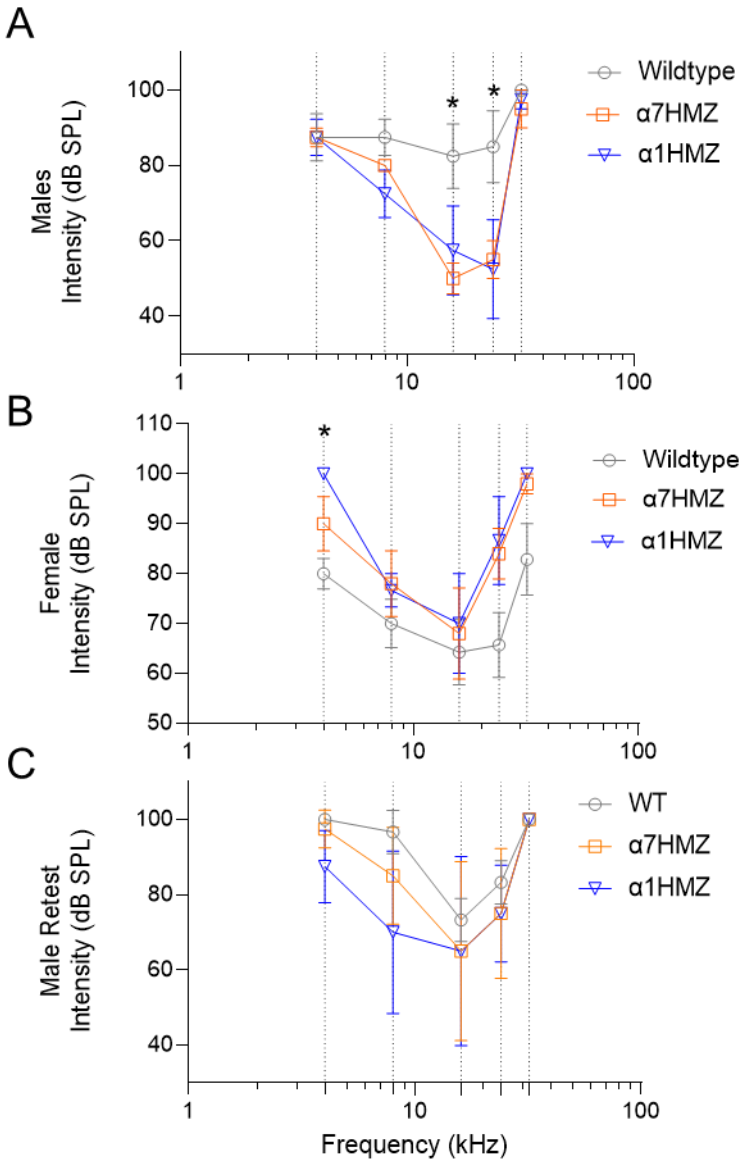

Figure 3. 2 Comparison of hearing profiles of old male and female wildtype and exon swap mice.

Auditory Brain Response curves 15 month or older A) C57Bl6/N wildtype male (n=4), C57Bl6/N α7HMZ male (n= 4), C57Bl6/N α1HMZ male (n=4). * $p<0.05$ wildtype vs α7HMZ. B) Mixed background wildtype female (n=7), C57Bl6/N α7HMZ female (n= 5), and C57Bl6/N α1HMZ male(n=3) * $p<0.05$ wildtype vs α1HMZ. C) Re-evaluation of male mice in A, 2 months later, all over 20 months old. All statistics done using Student's T-test.

Since it is well established that males tend to have more age-related hearing loss than females, we compared the results of the hearing test between the males and females within a given genotype. The WT males had significantly worse hearing at 8 kHz (Figure 3.3A), whereas the female α7HMZ mice had significantly worse hearing at another frequency (Figure 3.3B) In contrast, the α1HMZ males and females did not have any significant difference in hearing response (Figure 3.3C). Lastly, there was no significant difference in WT and α7HMZ male and female mice from the mixed background lines (Figure 3.4).

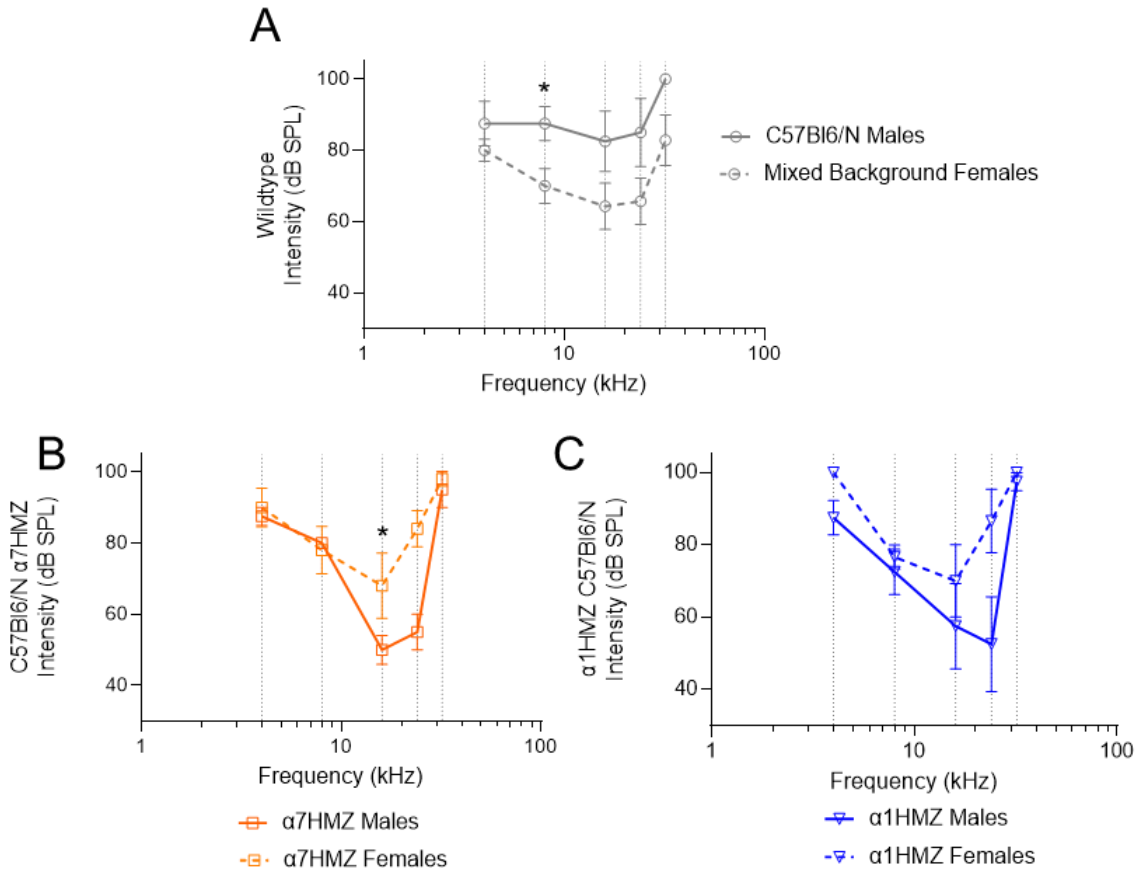

Figure 3. 3 Some significant differences in wildtype and exon swap male and female mouse hearing capacity over 15 months of age

Auditory brain response curves for A) C57Bl6/N wildtype male (n=4) and Mixed background wildtype female (n=7), B) C57Bl6/N α7HMZ male (n= 4) and C57Bl6/N α7HMZ female (n= 5), C) C57Bl6/N α1HMZ male (n=4) and C57Bl6/N α1HMZ female (n= 3). * $p<0.05$ Student's T-test.

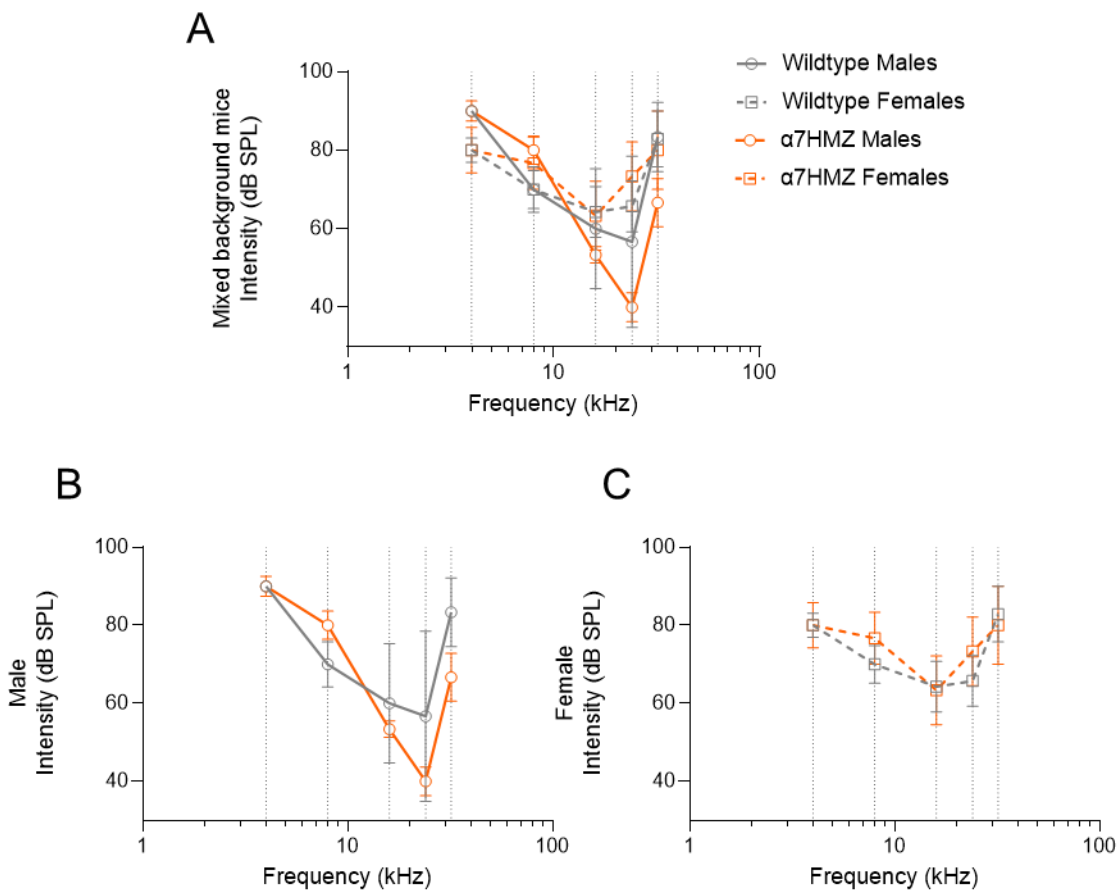

Figure 3. 4 No significant differences between male and female mixed background wildtype and α7HMZ mice over 15 months of age.

Auditory brain response curves for A) mixed background wildtype male (n=3), mixed background α7HMZ male (n=6) mice, mixed background wildtype female (n=7) and mixed background α7HMZ female (n=3) mice. B) male data from A., C) female data from A.

Comparing the body weights of all of the mice over 18 months old from the groups tested for auditory brain response, the only significant difference was between the α1HMZ and WT females (Figure 3.5).

Intestinal Barrier Function

Lastly, we examined intestinal barrier function in male and female mice from all three genotypes over 12 months old. Again, the only significant difference was between the α1HMZ and WT females, though there were no significant differences in age, with the α1HMZ females having significantly lower barrier function as noted by the increased levels of FITC in the serum (Figure 3.6).

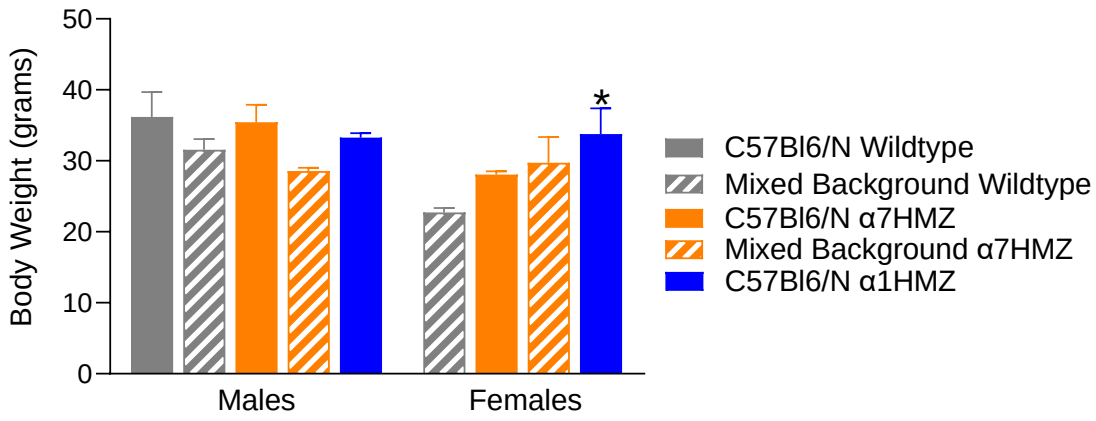

Figure 3. 5 No significant differences in body weight for most exon swap mice over 15 months of age.

Body weights of C57Bl6/N wildtype male (n=4, 19-22mos), Mixed background wildtype male (n=3, 15mos), C57Bl6/N α7HMZ male (n= 4, 18mos), Mixed background α7HMZ male (n=6, 19mos), C57Bl6/N α1HMZ male (n=4, 23mos). Mixed background wildtype female (n=7, 15mos), C57Bl6/N α7HMZ female (n=5, 18-23mos), Mixed background α7HMZ female (n=3, 19mos), and C57Bl6/N α1HMZ male (n=3, 23mos) mice all over 18 months of age. *$p<0.05$ α1HMZ females vs mixed background wildtype females, One-way ANOVA.

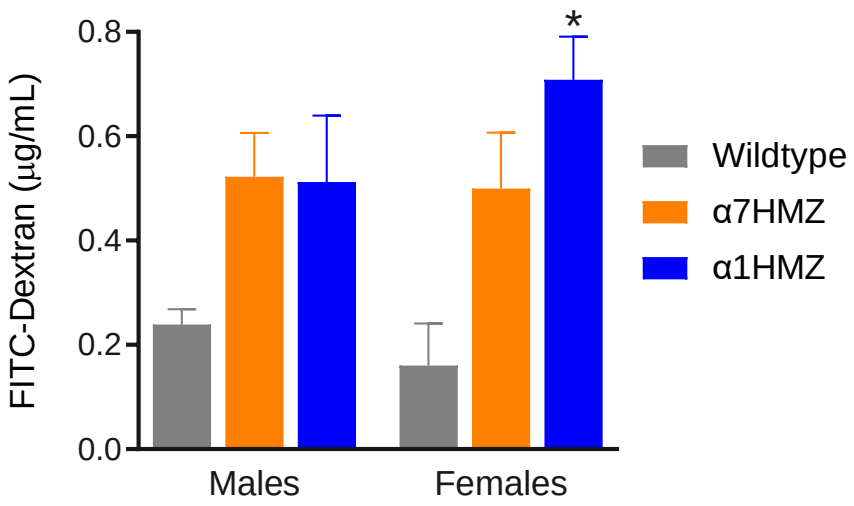

Figure 3. 6 Altered barrier function analysis in aged mice.

FITC dextran assay was used to determine barrier function in wildtype, α7HMZ, and α1HMZ male and female mice over 18 months old. Wildtype males (n=4), wildtype females (n=4), α7HMZ males (n=7), α7HMZ females (n=5), α1HMZ males (n=7), and α1HMZ females (n=5), *p<0.05 vs wildtype, One-way ANOVA. Completed with help from P. Deol.

DISCUSSION

There are many aspects to the aging process that have yet to be investigated. In this chapter, we examined potential effects of the liver and the intestines on several aspects of aging by looking at the impact of one of the most abundant transcription factors in those tissues -- namely, the nuclear receptor HNF4α. Since even tissue-specific HNF4α KO mice are lethal, we used the exon swap mouse model and examined the role of the different HNF4α isoforms. Specifically, we examined the effects of the HNF4α isoforms on spontaneous tumor development, fasting, age-related hearing loss, and barrier function.

P2-driven HNF4α, previously thought to only be expressed in the adult liver in a cancerous state, has recently been discovered to be expressed in the healthy adult liver (Chapter 2 data). Moreover, it has been observed that P2-HNF4α levels increase in colorectal cancer (Chellappa et al., 2016), and that overall P2-driven HNF4α is permissive of proliferation compared to P1-driven HNF4α which promotes differentiation and is tumor suppressive (Vuong et al., 2015). Using 18 month or older exon swap mice that express either P1- or P2-driven HNF4α in their HNF4α expressing tissues, we observed no significant differences in tumor development compared to WT mice in either the males or females. The only notable difference was the α1HMZ females did not exhibit any notable colon growths, while one third of both the WT and the α7HMZ females had some sort of abnormality. This could be due to the fact that the number of α1HMZ females was much lower than the number of six and 12 for the WT and α7HMZ examined (three for α1HMZ versus six and 12 for WT and α7HMZ, respectively). This will need to be further examined in more α1HMZ mice before any conclusions are made. That being said, if the N number

is not considered, this would be consistent with the notion that P1-HNF4α is tumor suppressive and having only P1-HNF4α in the colon could prevent polyp development. Interestingly, this would only be the case in the females, as the α1HMZ males were the only ones that had noticeable polyps in their colons (Table 3.1). This could be due to the fact that makes have a higher incidence of colon cancer compared to females, likely due to the protective properties of estrogens with regards to cancer (McCashland et al. 2001, Potter 1996)

Metabolic changes have been implicated in many aspects of aging, and there is a plethora of literature examining the effects of different diets on aging. The most well-supported hypothesis relating diet and longevity is that caloric restriction has been linked to increased life span (Hwangbo et al., 2020; Pifferi et al., 2018). Given the well-established role of HNF4α in metabolic pathways in the liver, we examined the effect of fasting on young and old male and female mice in WT and HNF4α exon swap mice. We found that in wildtype mice, young females are significantly different than males of any age and older females, suggesting that estrogen levels may play a role in the fasting response. However, as the fast progressed, the older females had similar ketone body levels to the younger females and they both had significantly higher βHB levels compared to the males (Figure 3.1A). This could suggest a role for the estrogen receptor in more prolonged fasts as both the young and old females would presumably have elevated estrogen receptor expression compared to the male mice.

We also looked at the effect of entrainment in young and old WT mice, it is evident that the entrainment affected the young male and female mice more than the older mice.

The young, entrained males and females both had decreased βHB levels at ZT14 even though they had been fasting for 14 hours. The older mice, either with or without entrainment, all continued to have elevated βHB levels until they were fed at ZT14 (Figure 3.1B, C). The younger mice may be more sensitive to changes in light compared to the older mice, as the lights were turned off at ZT12. Moreover, the younger mice may have grown accustomed to decreasing βHB at that time and did so despite not being fed. This could be due to a preemptive release of insulin which is known to decrease ketone body levels even without the introduction of food (Alberti et al., 1978). When examining the young and old exon swap mice, the profiles of the βHB levels differ drastically. In the younger mice both α1HMZ and α7HMZ and males and females have increasing βHB levels until they are fed after ZT14 (Figure 3.1D). In contrast, the older exon swap mice do not have the same increase and decrease in βHB levels during the fast and re-feedings as the younger mice, and there was no difference between the α1HMZ and α7HMZ genotypes (Figure 3.1E). Nonetheless, both the young and old α7HMZ females have the highest levels of ketone bodies. This further supports the notion that estrogen and the estrogen receptor play a role in ketone body formation, as the two female groups are the highest and second highest and the α7HMZ males, who have elevated estrogen receptor around ZT12.5 (Deans et al 2021), are close to the female α1HMZ levels.

We also examined the effect of the exon swap on age-related hearing loss to see if HNF4α could potentially play a role. Our hypothesis was that since P2-driven HNF4α causes an elevation in ketone bodies which has been linked to decreased dementia (Henderson 2008, Hertz et al. 2015), the α7HMZ mice, especially the females, would have

better hearing than the WT or α1HMZ mice, especially the males. Elevated ketone bodies could also be one reason why caloric restriction increases longevity, as it is essentially a prolonged fasted state (Veech et al., 2017). Initially, in the first experiment the 18-month-old male WT mice had decreased hearing capacity compared to both of the exon swap mice (Figure 3.2A). However, upon repeating the experiment two months later, no significant hearing loss was detected using the ABR assay between the WT mice and exon swap mice (Figure 3.2C). Comparing males and females of each genotype, the WT males had worse hearing compared to females (Figure 3.3A) which is well-established in the literature (Nolan, 2020), while the α7HMZ female mice had worse hearing at one frequency compared to the males, and the α1HMZ males and females were not significantly different (Figure 3.3B, C). Lastly, comparing the WT and α7HMZ male and female mice from a mixed background, as opposed to the pure C57Bl6/N background, there was no significant hearing loss in the male WT mice and hence no significant difference with WT females or either male or female α7HMZ exon swap mice (Figure 3.4). This suggests that the background of the WT mice plays an important role in aging and the role that the HNF4α isoforms play in aging is complex and not necessarily related to ketone body levels.

Body weight is known to increase with age, so we investigated whether any of the genotypes would have a significantly different body weight compared to the WT when the mice were over 18 months old. Interestingly, the only significant difference is between the α1HMZ females and the WT females -- the α1HMZ females were significantly heavier than the WT females (Figure 3.5). This could be due to the α1HMZ mice having lower ketone body levels in general compared to the WT and α7HMZ (Chapter 2), suggesting

that they may be less able to mobilize fat than the WT or α7HMZ mice. This will need to be further investigated.

Intestinal barrier function is known to decline with age and there are many theories behind this phenomenon. That being said, although HNF4α is known to play an important role in barrier function in the colon (Chellappa et al., 2016), the only significant difference in barrier function in the groups tested was between the α1HMZ females and the WT females (Figure 3.6). Again, this could be due to the α1HMZ mice having significantly heavier body weight, as obesity is known to decrease barrier function (Wilbrink et al., 2020).

The aging process is quite complex and although HNF4α plays a significant role in metabolism, cancer, and intestinal barrier function, it does not appear to play a significant role in the macroscopic aging process, although we have not examined how long the different exon swap mice live. That being said, HNF4α is known to interact with proteins that have heavily been implicated in aging, such as AMPK, SIRTs, mTOR, FOXO, AKT, and such could still play a significant role in cellular metabolism (Fulco & Sartorelli, 2008).

REFERENCES

Alberti, K. G., Johnston, D. G., Gill, A., Barnes, A. J., & Orskov, H. (1978). Hormonal regulation of ketone-body metabolism in man. *Biochemical Society Symposium*, *43*, 163–182.

Broom, G. M., Shaw, I. C., & Rucklidge, J. J. (2018). The ketogenic diet as a potential treatment and prevention strategy for Alzheimer's disease. *Nutrition* , *60*, 118–121.

Catic, A. (2018). Cellular Metabolism and Aging. *Progress in Molecular Biology and Translational Science*, *155*, 85–107.

Chellappa, K., Deol, P., Evans, J. R., Vuong, L. M., Chen, G., Briançon, N., Bolotin, E., Lytle, C., Nair, M. G., & Sladek, F. M. (2016). Opposing roles of nuclear receptor HNF4α isoforms in colitis and colitis-associated colon cancer. *eLife*, *5*. https://doi.org/10.7554/eLife.10903

Chellappa, K., Jankova, L., Schnabl, J. M., Pan, S., Brelivet, Y., Fung, C. L.-S., Chan, C., Dent, O. F., Clarke, S. J., Robertson, G. R., & Sladek, F. M. (2012). Src tyrosine kinase phosphorylation of nuclear receptor HNF4α correlates with isoform-specific loss of HNF4α in human colon cancer. *Proceedings of the National Academy of Sciences of the United States of America*, *109*(7), 2302–2307.

Chern, A., & Golub, J. S. (2019). Age-related Hearing Loss and Dementia. *Alzheimer Disease and Associated Disorders*, *33*(3), 285–290.

Davis, A., McMahon, C. M., Pichora-Fuller, K. M., Russ, S., Lin, F., Olusanya, B. O., Chadha, S., & Tremblay, K. L. (2016). Aging and Hearing Health: The Life-course Approach. *The Gerontologist*, *56 Suppl 2*, S256–S267.

Deans, J. R., Deol, P., Titova, N., Radi, S. H., Vuong, L. M., Evans, J. R., Pan, S., Fahrmann, J., Yang, J., Hammock, B. D., Fiehn, O., Fekry, B., Eckel-Mahan, K., Sladek, F. M. (2019). Alternative HNF4α isoform regulates the sex-specific diurnal balance between carbohydrate and lipid metabolism in the liver. *In Review, Nature Communications*.

Fekry, B., Ribas-Latre, A., Baumgartner, C., Deans, J. R., Kwok, C., Patel, P., Fu, L., Berdeaux, R., Sun, K., Kolonin, M. G., Wang, S. H., Yoo, S.-H., Sladek, F. M., & Eckel-Mahan, K. (2018). Incompatibility of the circadian protein BMAL1 and HNF4α in hepatocellular carcinoma. *Nature Communications*, *9*(1), 4349.

Fulco, M., & Sartorelli, V. (2008). Comparing and contrasting the roles of AMPK and SIRT1 in metabolic tissues. *Cell Cycle* , *7*(23), 3669–3679.

Henderson, S. T. (2008). Ketone bodies as a therapeutic for Alzheimer's disease. *Neurotherapeutics: The Journal of the American Society for Experimental NeuroTherapeutics*, *5*(3), 470–480.

Hertz, L., Chen, Y., & Waagepetersen, H. S. (2015). Effects of ketone bodies in Alzheimer's disease in relation to neural hypometabolism, β-amyloid toxicity, and astrocyte function. Journal of Neurochemistry, 134(1), 7–20.

Hoeijmakers, J. H. J. (2009). DNA damage, aging, and cancer. *The New England Journal of Medicine*, *361*(15), 1475–1485.

Hwangbo, D.-S., Lee, H.-Y., Abozaid, L. S., & Min, K.-J. (2020). Mechanisms of Lifespan Regulation by Calorie Restriction and Intermittent Fasting in Model Organisms. *Nutrients*, *12*(4). https://doi.org/10.3390/nu12041194

Jackaman, C., Tomay, F., Duong, L., Abdol Razak, N. B., Pixley, F. J., Metharom, P., & Nelson, D. J. (2017). Aging and cancer: The role of macrophages and neutrophils. *Ageing Research Reviews*, *36*, 105–116.

Kim, S., & Jazwinski, S. M. (2018). The Gut Microbiota and Healthy Aging: A Mini-Review. *Gerontology*, *64*(6), 513–520.

Kudryavtseva, A. V., Krasnov, G. S., Dmitriev, A. A., Alekseev, B. Y., Kardymon, O. L., Sadritdinova, A. F., Fedorova, M. S., Pokrovsky, A. V., Melnikova, N. V., Kaprin, A. D., Moskalev, A. A., & Snezhkina, A. V. (2016). Mitochondrial dysfunction and oxidative stress in aging and cancer. *Oncotarget*, *7*(29), 44879–44905.

Mangiola, F., Nicoletti, A., Gasbarrini, A., & Ponziani, F. R. (2018). Gut microbiota and aging. *European Review for Medical and Pharmacological Sciences*, *22*(21), 7404–7413.

McCashland, T. M., Brand, R., Lyden, E., de Garmo, P., & CORI Research Project. (2001). Gender differences in colorectal polyps and tumors. The American Journal of Gastroenterology, 96(3), 882–886.Newman, J. C., & Verdin, E. (2014). Ketone bodies as signaling metabolites. *Trends in Endocrinology and Metabolism: TEM*, *25*(1), 42–52.

Nolan, L. S. (2020). Age-related hearing loss: Why we need to think about sex as a biological variable. *Journal of Neuroscience Research*, *98*(9), 1705–1720.

Pifferi, F., Terrien, J., Marchal, J., Dal-Pan, A., Djelti, F., Hardy, I., Chahory, S., Cordonnier, N., Desquilbet, L., Hurion, M., Zahariev, A., Chery, I., Zizzari, P., Perret, M., Epelbaum, J., Blanc, S., Picq, J.-L., Dhenain, M., & Aujard, F. (2018). Caloric restriction increases lifespan but affects brain integrity in grey mouse lemur primates. *Communications Biology*, *1*(1), 1–8.

Potter, J. D., Bostick, R. M., Grandits, G. A., Fosdick, L., Elmer, P., Wood, J., Grambsch, P., & Louis, T. A. (1996). Hormone replacement therapy is associated with lower risk of adenomatous polyps of the large bowel: the Minnesota Cancer Prevention Research Unit Case-Control Study. Cancer Epidemiology, Biomarkers & Prevention: A Publication of the American Association for Cancer Research, Cosponsored by the American Society of Preventive Oncology, 5(10), 779–784.

Puchalska, P., & Crawford, P. A. (2017). Multi-dimensional Roles of Ketone Bodies in Fuel Metabolism, Signaling, and Therapeutics. *Cell Metabolism*, *25*(2), 262–284.

Soylu, F. N., Peng, Y., Jiang, Y., Wang, S., Schmid-Tannwald, C., Sethi, I., Eggener, S., Antic, T., & Oto, A. (2013). Seminal vesicle invasion in prostate cancer: evaluation by using multiparametric endorectal MR imaging. *Radiology*, *267*(3), 797–806.

Tanaka, T., Jiang, S., Hotta, H., Takano, K., Iwanari, H., Sumi, K., Daigo, K., Ohashi, R., Sugai, M., Ikegame, C., Umezu, H., Hirayama, Y., Midorikawa, Y., Hippo, Y., Watanabe, A., Uchiyama, Y., Hasegawa, G., Reid, P., Aburatani, H., … Kodama, T. (2006). Dysregulated expression of P1 and P2 promoter-driven hepatocyte nuclear factor-4alpha in the pathogenesis of human cancer. *The Journal of Pathology*, *208*(5), 662–672.

Uchida, Y., Sugiura, S., Nishita, Y., Saji, N., Sone, M., & Ueda, H. (2019). Age-related hearing loss and cognitive decline - The potential mechanisms linking the two. *Auris, Nasus, Larynx*, *46*(1), 1–9.

Veech, R. L., Bradshaw, P. C., Clarke, K., Curtis, W., Pawlosky, R., & King, M. T. (2017). Ketone bodies mimic the life span extending properties of caloric restriction. *IUBMB Life*, *69*(5), 305–314.

Verdin, E. (2015). NAD^+ in aging, metabolism, and neurodegeneration. *Science*, *350*(6265), 1208–1213.

Vuong, L. M., Chellappa, K., Dhahbi, J. M., Deans, J. R., Fang, B., Bolotin, E., Titova, N. V., Hoverter, N. P., Spindler, S. R., Waterman, M. L., & Sladek, F. M. (2015). Differential Effects of Hepatocyte Nuclear Factor 4α Isoforms on Tumor Growth and T-Cell Factor 4/AP-1 Interactions in Human Colorectal Cancer Cells. *Molecular and Cellular Biology*, *35*(20), 3471–3490.

Wilbrink, J., Bernards, N., Mujagic, Z., van Avesaat, M., Pijls, K., Klaassen, T., van Eijk, H., Nienhuijs, S., Stronkhorst, A., Wilms, E., Troost, F., & Masclee, A. (2020). Intestinal barrier function in morbid obesity: results of a prospective study on the effect of sleeve gastrectomy. *International Journal of Obesity* , *44*(2), 368–376.

CHAPTER 4: CONCLUSION

The liver is the main metabolic organ and is responsible for the majority of the body's gluconeogenesis and ketogenesis. In response to a fast, the liver begins producing glucose to supply the body with energy. After prolonged gluconeogenesis, oxaloacetate levels are depleted, triggering the switch to ketogenesis. Ketogenesis occurs in the liver mitochondria and converts acetyl-CoA from fatty acid breakdown into ketone bodies. The main ketone body, β-hydroxybutyrate (βHB), is released into the blood to be used in other tissues such as the muscle and the brain.

The master regulator of liver-specific gene expression is HNF4α. HNF4α is driven by two promoters, the P1- and P2-promoter. The difference between the isoforms driven by the two promoters is only the first exon, which results in a sixteen amino acid difference in the N-terminus of the proteins. Though this difference is small, the P1-isoform appears to be tumor suppressive and to promote differentiation, while the P2-isoform appears to be more permissive of proliferation; the differences are likely due to altered protein interactions between the isoforms[1].

HNF4α has been implicated in many aspects of metabolism and disease. HNF4α is expressed in a few organs including the liver, kidney, stomach, intestines, and pancreas. It has been shown to play a role in glucose and lipid metabolism, as well as lipid mobilization through apolipoproteins. Moreover, it is mutated in maturity onset diabetes of the young 1 (MODY1), a rare form of type-2 diabetes, which is interesting as it is implicated in the

[1] The majority of the references for the statements in this chapter can be found in Chapter 1 and introductory sections of chapters 2 and 3.

insulin release from pancreatic β-cells. HNF4α has also been shown to play a potential role in gastric, liver, and colorectal cancers although the differential roles of the isoforms remains to be elucidated.

This dissertation explores the differential role of the HNF4α isoforms in glucose and lipid metabolism and proposes a potential mechanism for the switch between P1- and P2-HNF4α via AMP-activated protein kinase (AMPK). In the adult liver, it was previously thought that only P1-HNF4α was expressed in normal conditions, while P2-HNF4α became expressed under cancerous conditions and in normal fetal livers. Interestingly, it was found that P2-HNF4α is in fact expressed in the normal adult liver, though only at specific times of the day; most notably ZT9. Others have also seen P2-HNF4α in conditions of fasting and alcoholic liver disease (Argemi et al., 2019; Da Li et al., 2020). To elucidate the role of P2-HNF4α in the adult liver, we utilized an exon-swap mouse model that expressed either P1-HNF4α, denoted α1HMZ, or P2-HNF4α, denoted α7HMZ, in the HNF4α expressing tissues. Beginning with RNAseq and metabolomics data, it was evident that the α7HMZ mice seemed to favor lipid metabolism compared to the wildtype mice, even in a fed state. With that in mind, we attempted a prolonged fast on all three genotypes, α7HMZ, α1HMZ, and wildtype, under the assumption that the α7HMZ would survive better as they are more accustomed to a fasted state. Half of the α7HMZ mice died; the remaining mice had very high levels of ketone bodies (>4 mmol) suggesting that the mice died of ketoacidosis. Moreover, α7HMZ have elevated levels of ketone bodies both in the fed and fasted state compared to the other two genotypes. They also have elevated

levels of *Hmgcs2*, the key ketogenic gene compared to wildtype, which could explain the elevated ketone bodies.

HNF4α has been shown to be phosphorylated by AMPK, an energy-sensing kinase that is essential in the fasting response. Interestingly, only P1-HNF4α has been shown to be phosphorylated by AMPK. We hypothesized that AMPK would differentially phosphorylate the isoforms leading to a decrease in P1-HNF4α and an increase in P2-HNF4α. To begin exploring this, we treated exon-swap mice with AICAR, an AMPK activator, and measured their glucose and βHB levels. As expected, the AICAR injection caused a decrease in glucose in both male and female mice. Although it did not seem to affect ketone bodies, it did cause a decrease in P1-HNF4α protein levels in α1HMZ male mice. The most notable results from the AICAR experiments were the seizures. Only the α7HMZ and α1HMZ mice seized, the α7HMZ more-so than the α1HMZ and the females in both genotypes more-so than the males. There was no indication in the literature that AICAR could cause seizures, and it was very interesting that this occurred in both of the exon-swap mice. This was one of the first indications that both HNF4α isoforms are essential for normal function. It is important to elucidate the underlying mechanism causing the seizures because it has been shown that different diets could affect levels of HNF4α (Deol et al. 2015) and thus if someone were taking a drug that activates AMPK, such as type-2 diabetes medications, this could potentially lead to seizures. The seizure result is something we will be exploring further to see what the potential cause is, and potentially creating a reliable model for acute seizures.

One of the most prescribed drugs in the United States is Metformin. This is another AMPK activator, similar to AICAR, although the mechanism of action is different. Metformin acts on the electron transport chain in the mitochondria to decrease energy output and increase AMP, while AICAR binds directly to AMPK. We performed a pilot experiment to determine whether Metformin causes seizures in the α7HMZ and α1HMZ female mice, as AICAR did, and interestingly it does not (data not shown). Out of the 13 mice tested, none of them seized; although one died presumably due to an improper injection. The cause of the seizures following the AICAR injection remains unknown and will require further experimentation and collaboration with researchers with expertise in the brain to elucidate. We will next determine whether Metformin has the same effect of glucose and βHB levels as AICAR has and whether Metformin decreases the P1-HNF4α isoform as does AICAR. Metformin is the most prescribed type-2 diabetes medication and thus understanding its effect on the master regulator of liver specific gene expressed, HNF4α, is essential in minimizing side effects. Interestingly, Metformin has been shown to help ameliorate seizures not cause them (Yimer et al. 2019).

One of the most robust results we observed is that females have elevated levels of βHB compared to males, a phenomenon that is well-established in the literature in both rodents and humans. We collected and processed liver tissue for RNA-seq from male and female, α7HMZ and wildtype, fed and fasted (12 hours) mice, N of three each, to compare the expression profiles of these mice. All of the groups had increased levels of *Hmgcs2*, the key ketogenic gene, upon fasting, with the α7HMZ males and females having significantly higher levels than the wildtype in the fasted condition (Figure 4). The elevated

ketone bodies (Figure 2.8) in these conditions directly correlate with the *Hmgcs2* levels. In contrast, *Ppara,* another nuclear receptor known to be involved in driving ketogenesis (Grabacka et al., 2016), was decreased in the α7HMZ males and females compared to wildtype in the fasted conditions, and was significantly decreased in the α7HMZ males in the fed state compared to the wildtype males (Figure 4). *Pparg* was significantly reduced in the fed state in females compared to males for both the wildtype and α7HMZ mice. It was also significantly reduced in the fasted wildtype males compared to the fed state (Figure 4). The increase in *Hmgcs2* expression does not correlate with the PPAR expression, nor do ketone body levels, suggesting that in our system the PPARs are not the major drivers of ketogenesis. Lastly, *Hnf4a*, which is has been shown to repress PPAR expression (Martinez-Jimenez et al. 2010), was significantly elevated in the α7HMZ females compared to the wild type in the fed and fasted state, and was elevated in the α7HMZ males compared to the wildtype males in the fasted state. α7HMZ males had significantly lower *Hnf4a* levels in the fed state compared to females. Moreover, both α7HMZ and wildtype males had elevated *Hnf4a* levels in the fasted state compared to the fed state (Figure 4). In contrast, the alterations in *Hnf4a* levels between the sexes is quite interesting and could play a role in the differences in their metabolic profiles. There is an enormous amount of data that is yet to be processed from the RNAseq, including glucose metabolism genes, tricarboxylic acid cycle genes, lipid metabolism genes, cholesterol metabolism genes, the insulin pathway, and different transport proteins for glucose and lipids. We will continue to mine these data to better elucidate differences between the male and female exon swap mice, something that has not been done in the literature previously.

A

	Fed				Fasted			
Gene	WT male	WT female	α7 Male	α7female	WT male	WT female	α7 Male	α7female
Hmgcs2	1.00	0.83	1.37	1.56	1.65	2.02	2.71	2.82
PPARa	1.00	0.78	0.45	0.50	1.41	1.21	0.74	0.66
PPARg	1.00	0.42	0.90	0.47	0.61	0.69	0.80	0.75
PGC1a	1.00	1.73	0.91	1.75	1.97	2.00	1.18	2.18
HNF4a	1.00	1.27	1.36	1.82	1.47	1.38	1.89	2.18

B

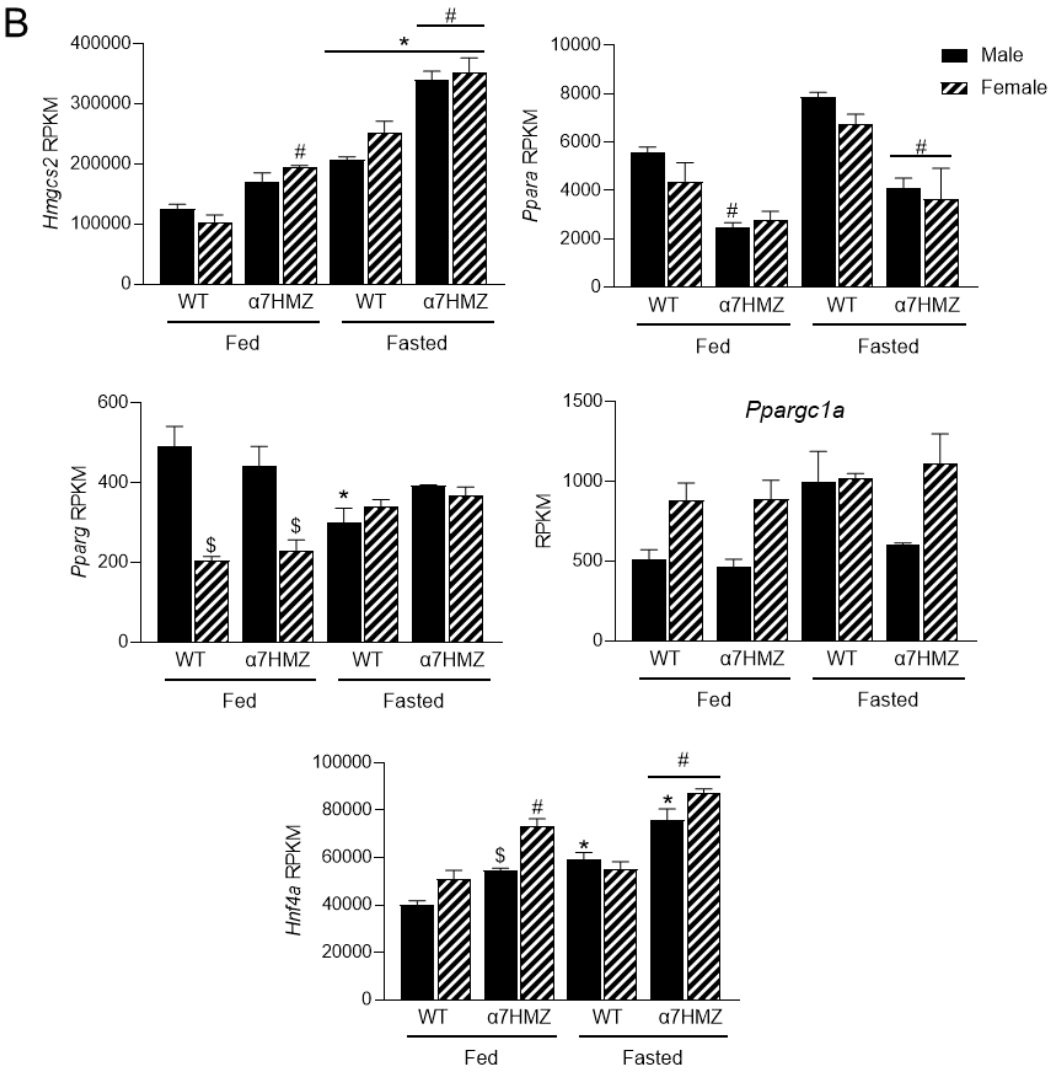

Figure 4. 1 Females and males have altered genes upon fasting

Liver RNAseq data from wildtype and α7HMZ, male and female mice, 16-20 weeks old. RPKM graphed for each gene. * $p<0.05$ fed vs fasted, # $p<0.05$ wildtype vs α7HMZ, $ $p<0.05$ male vs female, One-Way ANOVA.

Another small project looked at the effect of HNF4α isoforms on aging. Although at first it seemed like there could be an interesting result regarding the auditory profiles of the exon-swap mice it did not hold up to repeated experiments. Overall, it does not seem like HNF4α plays a large role in aging, nor does having exclusively one isoform or the other increase the susceptibility of the mice to cancer development. The literature that linked HNF4α to cancer showed an increase in expression in cancer cells but did not explore if HNF4α expression was involved in the cancer development or was a result of the cancerous state of the cells. These preliminary results do not necessarily exclude HNF4α from playing a role in cancer development or progression on the cellular or metabolic level, nor does it exclude HNF4α from playing a role in cellular aging. Although they do indicate that additional studies would be needed to come to a definitive conclusion.

HNF4α is an essential protein for many aspects of normal metabolism and liver function. It plays an important role in glucose and lipid metabolism in the liver, which are essential functions for the organism. In the literature, more groups are differentiating between the two HNF4α isoforms and are exploring their distinct roles in the liver. There is much more to explore, and any discoveries could give insights into metabolic diseases, obesity, diabetes, and cancer. Finally, the molecular mechanism underlying the switch between the HNF4α isoforms, via AMPK or another player, remains to be elucidated.

MATERIALS AND METHODS

Liver RNA isolation and library prep

Wildtype and α7HMZ male and female mice were either fasted for 12 hours from 10:30pm (ZT15.5) to 10:30am (ZT3.5) or given food *ad libitum*. Each group had an n of 3. On the day of harvest, mice were euthanized by CO_2 inhalation followed by cervical dislocation. The skin was soaked with 95% ethanol and the skin was cut followed by the peritoneal membrane. The inferior vena cava between the liver and diaphragm was cut and the liver was gripped with forceps and removed from the cavity. The liver was put on ice, and three 30 mg triangular pieces from the center of the large lobe were removed and put in 500 mL of RNAlater®. The rest of the liver was split and frozen in liquid nitrogen for protein extraction. The RNA pieces were kept at room temperature for one hour, and then placed at 4ºC overnight. The next day, the pieces were frozen at 80ºC.

On the day of the RNA extraction, the samples were thawed on ice and weighed. Using the Monarch® Total RNA extraction kit from New England BioLabs (cat# T2010S) total RNA was extracted from each sample following the manufacturer's protocol. The RNA integrity and concentration were analyzed the same day using a Nanodrop in the UCR Genomics Core, followed by analysis using a BioAnalyzer for RNA integrity and concentration. Once the Bioanalyzer results were acceptable (>7.6), the samples were submitted to the UCR Genomics Core for library prep and submission to UC Berkeley for sequencing.

RNA Analysis:

Libraries were submitted for 150-bp paired-end sequencing at the UC Berkeley Genomics Core. A total of 24 libraries (2 genotypes, 2 genders, 1 fed time point, 1 fasted time point, 3 replicates) were multiplexed and sequenced in two separate runs, each of which yielded ~1249 M reads, averaging ~52 M reads per sample. Reads were aligned to the mouse reference genome (GRCm39) with STAR v2.5.0a using default parameters. Raw read counts were also calculated with STAR using the GeneCounts option of the quantMode parameter since the libraries were unstranded. Library normalization was performed with EDASeq (Risso et al., 2011); within-lane normalization on GC content was performed with the LOESS method and between-lane normalization was performed with non-linear full quantile method. Normalization factors from EDASeq were used for differential expression analysis with DESeq2. Normalized read counts, FPKM (fragments per kilobase per million), and rlog (regularized log transformation) results were generated for downstream analysis.

REFERENCES

Argemi, J., Latasa, M. U., Atkinson, S. R., Blokhin, I. O., Massey, V., Gue, J. P., Cabezas, J., Lozano, J. J., Van Booven, D., Bell, A., Cao, S., Vernetti, L. A., Arab, J. P., Ventura-Cots, M., Edmunds, L. R., Fondevilla, C., Stärkel, P., Dubuquoy, L., Louvet, A., … Bataller, R. (2019). Defective HNF4alpha-dependent gene expression as a driver of hepatocellular failure in alcoholic hepatitis. *Nature Communications*, *10*(1), 3126.

Da Li, Cao, T., Sun, X., Jin, S., Di Xie, Huang, X., Yang, X., Carmichael, G. G., Taylor, H. S., Diano, S., & Huang, Y. (2020). Hepatic TET3 contributes to type-2 diabetes by inducing the HNF4α fetal isoform. *Nature Communications*, *11*(1), 342.

Deol, P., Evans, J. R., Dhahbi, J., Chellappa, K., Han, D. S., Spindler, S., & Sladek, F. M. (2015). Soybean Oil Is More Obesogenic and Diabetogenic than Coconut Oil and Fructose in Mouse: Potential Role for the Liver. PloS One, 10(7), e0132672.

Grabacka, M., Pierzchalska, M., Dean, M., & Reiss, K. (2016). Regulation of Ketone Body Metabolism and the Role of PPARα. *International Journal of Molecular Sciences*, *17*(12). https://doi.org/10.3390/ijms17122093

Martinez-Jimenez, C. P., Kyrmizi, I., Cardot, P., Gonzalez, F. J., & Talianidis, I. (2010). Hepatocyte nuclear factor 4alpha coordinates a transcription factor network regulating hepatic fatty acid metabolism. Molecular and Cellular Biology, 30(3), 565–577.

Risso, D., Schwartz, K., Sherlock, G., & Dudoit, S. (2011). GC-content normalization for RNA-Seq data. *BMC Bioinformatics*, *12*, 480.

Yimer, E. M., Surur, A., Wondafrash, D. Z., & Gebre, A. K. (2019). The Effect of Metformin in Experimentally Induced Animal Models of Epileptic Seizure. Behavioural Neurology, 2019. https://doi.org/10.1155/2019/6234758

APPENDIX

Fatty acid metabolism from heatmap in Figure 2.6D

Gene Symbol	Enzyme name	Rationale
Acadsb	short/branched chain acyl-CoA dehydrogenase	Beta oxidation gene
Acat2	Acetyl-CoA Acetyltransferase 2	Beta oxidation gene
Acat1	Acetyl-CoA Acetyltransferase 1	Beta oxidation gene
Hmgcl	3-Hydroxy-3-Methylglutaryl-CoA Lyase	Ketogenesis gene
Ech1	Enoyl-CoA Hydratase 1	Beta oxidation gene
Acads	short-chain acyl-CoA dehydrogenase	Beta oxidation gene
Acad11	Acyl-CoA Dehydrogenase Family Member 11	Beta oxidation gene
Acadm	medium-chain acyl-CoA dehydrogenase	Beta oxidation gene
Acadl	long-chain acyl-CoA dehydrogenase	Beta oxidation gene
Hmgcs2	3-Hydroxy-3-Methylglutaryl-CoA Synthase 2	Ketogenesis gene
Acaa1a	acetyl-Coenzyme A acyltransferase 1	Beta oxidation gene
Acaa1b	acetyl-Coenzyme A acyltransferase 1b	Beta oxidation gene
Hadha	Hydroxyacyl-CoA Dehydrogenase	Beta oxidation gene
Bdh1	3-Hydroxybutyrate Dehydrogenase 1	Ketogenesis gene
Cpt1a	Carnitine Palmitoyltransferase 1A	Beta oxidation gene